DOCTORAL THESIS

Sensitivity and Individual Temporal Stability of Electroencephalography-Based Measures

Tuuli Uudeberg

TALLINNA TEHNIKAÜLIKOOL
TALLINN UNIVERSITY OF TECHNOLOGY
TALLINN 2026

TALLINN UNIVERSITY OF TECHNOLOGY
DOCTORAL THESIS
14/2026

Sensitivity and Individual Temporal Stability of Electroencephalography-Based Measures

TUULI UUDEBERG

TAL TECH PRESS

TALLINN UNIVERSITY OF TECHNOLOGY
School of Information Technologies, Department of Health Technologies
Curriculum: School of Science
This dissertation was accepted for the defence of the degree of Doctor of Philosophy in Biomedicine and Health Technologies 16/02/2026

Supervisor: Assoc. Prof. Maie Bachmann, PhD
School of Information Technologies
Tallinn University of Technology
Tallinn, Estonia

Co-supervisor: Assoc. Prof. Juri Belikov, PhD
School of Information Technologies
Tallinn University of Technology
Tallinn, Estonia

Opponents: Prof. Tarmo Lipping, PhD
Faculty of Information Technology and Communication Sciences
Tampere University
Tampere, Finland

Dr. Dr. med. Florian Raabe
Max Planck Institute of Psychiatry and
Department of Psychiatry and Psychotherapy, LMU University Hospital Munich, Germany

Defence of the thesis: 10/03/2026, Tallinn

Declaration:
Hereby I declare that this doctoral thesis, my original investigation and achievement, submitted for the doctoral degree at Tallinn University of Technology has not been submitted for doctoral or equivalent academic degree.

Tuuli Uudeberg

Signature

European Union
European Regional Development Fund

Investing in your future

ISSN 2585-6898 (publication)
ISBN 978-9916-80-466-7 (publication)
ISSN 2585-6901 (PDF)
ISBN 978-9916-80-467-4 (PDF)
DOI https://doi.org/10.23658/taltech.14/2026

Uudeberg, T. (2026). Sensitivity and Individual Temporal Stability of Electroencephalography-Based Measures [TalTech Press]. https://doi.org/10.23658/taltech.14/2026

TALLINNA TEHNIKAÜLIKOOL
DOKTORITÖÖ
14/2026

Elektroentsefalograafial põhinevate mõõdikute tundlikkus ja individuaalne ajaline stabiilsus

TUULI UUDEBERG

TAL TECH
KIRJASTUS

Contents

List of Publications

The list of the author's publications, based on which the thesis has been prepared:

I Päeske, L., **Uudeberg, T**., Hinrikus, H., Lass, J., & Bachmann, M. (2023). Correlation between electroencephalographic markers in the healthy brain. *Scientific Reports*, 13, 6307. https://doi.org/10.1038/s41598-023-33364-z

II **Uudeberg, T**., Belikov, J., Päeske, L., Hinrikus, H., Liiv, I., & Bachmann, M. (2024). In-phase matrix profile: A novel method for the detection of major depressive disorder. *Biomedical Signal Processing and Control*, 88, 105378. https://doi.org/10.1016/j.bspc.2023.105378

III **Uudeberg, T**., Päeske, L., Hinrikus, H., Lass, J., Põld, T., & Bachmann, M. (2025). Individual stability of single-channel EEG measures over one year in healthy adults. *Scientific Reports*, 15, 28426. https://doi.org/10.1038/s41598-025-13614-y

IV **Uudeberg, T**., Hinrikus, H., Päeske, L., Lass, J., & Bachmann, M. (2022). Changes in EEG measures of a recipient of the mRNA COVID-19 vaccine—A case study. In *2022 44th Annual International Conference of the IEEE Engineering in Medicine and Biology Society (EMBC)*, 3702–3705. IEEE. https://doi.org/10.1109/EMBC48229.2022.9871524

Author's Contribution to the Publications

Contribution to the publications in this thesis is the following:

I The author developed and implemented the MATLAB scripts that produced the figures, performed the statistical computations supporting the reported correlations, and proofread the manuscript to ensure clear wording and consistent formatting throughout.

II The author partially conceptualized and fully designed the study, processed all data, performed all statistical analyses and visualizations in MATLAB, took a major role in analyzing and interpreting the results, and wrote the entire manuscript.

III The author contributed to the study's design, carried out most EEG recordings, performed all data processing, statistical analyses, and visualizations in MATLAB, interpreted the results, and wrote the entire manuscript.

IV The author contributed to the study's design, carried out all EEG recordings, performed all data processing, statistical analyses, and visualizations using MATLAB, interpreted the results, and wrote the entire manuscript.

Other Related Publications

1. **Uudeberg, T**., Päeske, L., Hinrikus, H., Lass, J., & Bachmann, M. (2020). Reliability of electroencephalogram-based individual markers: Case study. In *2020 42nd Annual International Conference of the IEEE Engineering in Medicine and Biology Society* (EMBC), 276–279. IEEE. https://doi.org/10.1109/EMBC44109.2020.9175274.
2. **Uudeberg, T**., Päeske, L., Põld, T., Lass, J., Hinrikus, H., & Bachmann, M. (2020). Long-term stability of EEG spectral asymmetry index: Preliminary study. In P. Henriques, P. de Carvalho, & H. P. de Oliveira (Eds.), *XV Mediterranean Conference on Medical and Biological Engineering and Computing – MEDICON 2019, Coimbra, Portugal, September 26–28, 2019* (IFMBE Proceedings, 76), 276–281. Springer. https://doi.org/10.1007/978-3-030-31635-8_33.
3. Pilt, K., Karai, D., Bachmann, M., Gavriljuk, M., Allik, A., **Uudeberg, T**., Tarnov, K., & Fridolin, I. (2022). Influence of mental stress on the arterial stiffness parameters detected from photoplethysmographic signal waveform. In *18th Biennial Baltic Electronics Conference* (BEC 2022), Tallinn, Estonia, 4–6 October 2022. IEEE Computer Society. https://doi.org/10.1109/BEC56180.2022.9935609.
4. **Uudeberg, T**., Päeske, L., Hinrikus, H., Lass, J., & Bachmann, M. (in press). Correlation between EEG spectral asymmetry index and depression questionnaire – longitudinal case study. In *IUPESM World Congress on Medical Physics and Biomedical Engineering* (IUPESM WC2022), Singapore, 12–17 June 2022.
5. Gavriljuk, M., **Uudeberg, T**., Pilt, K., Karai, D., Fridolin, I., & Bachmann, M. (2023). Electroencephalography as an objective indicator of stress. In *19th Nordic-Baltic Conference on Biomedical Engineering and Medical Physics* (NBC 2023), Liepaja, Latvia, 12–14 June 2023 (IFMBE Proceedings, 89), 221–226. Springer. https://doi.org/10.1007/978-3-031-37132-5_28.

Introduction

Mental health disorders are widespread and impose a substantial societal burden. Recent assessments estimate that more than a billion individuals are affected globally, with anxiety and depressive disorders among the most prevalent conditions, and with additional increases linked to the COVID-19 pandemic (Ettman et al., 2025; WHO, 2025). Diagnosis and follow-up still rely primarily on clinical interviews and self-report questionnaires, which generate variable outcomes and can contribute to misclassification and treatment gaps in routine care (Patel et al., 2018). These realities motivate the use of measures derived from electroencephalographic signals, providing an objective complement to traditional clinical evaluations.

Electroencephalography (EEG) offers an objective window into brain dynamics, characterized by high temporal resolution, relatively low cost, and portability. EEG is an electrophysiological technique that records the brain's electrical activity using electrodes placed on the scalp (Buzsáki, 2006). Small but substantial alterations in resting-state EEG have been linked at the group level to several psychiatric conditions, e.g., major depressive disorder (MDD), generalized anxiety disorder (GAD), attention-deficit/hyperactivity disorder (ADHD), schizophrenia, and stress-related disorders (Hinrikus et al., 2009; Ahmadlou et al., 2012; Arns et al., 2013; Bachmann et al., 2013, 2018; Mumtaz et al., 2015; Kesić & Spasić, 2016; Moran et al., 2019; Newson & Thiagarajan, 2019; Wang et al., 2025). Despite success in research settings, EEG measures have not transitioned into routine clinical practice for detecting or monitoring common psychiatric disorders because the evidence base is limited to group-level findings (and not always fully consistent across studies).

Two practical obstacles hinder transition. First, the wide selection of EEG measures is unorganized: diverse measures are selected and parameterized in ad hoc ways, such that similar clinical questions are addressed with different feature sets that yield variable results. The mutual relationships between these measures—how much complementary versus overlapping information they express—are unknown, which compromises comparability of findings, complicates interpretation, and slows clinical transition. To ensure consistent findings across studies and to enable progress toward clinical implementation, complementary, cross-site, and comparable measures are required. Although multimeasure combinations have been demonstrated to improve classification (Hosseinifard et al., 2013; Bachmann et al., 2018; Čukić, Stokić, Simić, et al., 2020), a systematic assessment of inter-measure correlations—and, by extension, the informational independence across measures—has not been previously performed.

As a second obstacle, there is dispersion across individuals, characterized by substantial inter-individual (between-person) differences in EEG measure values that can overshadow intra-individual (within-person) changes. Crucially, strong group-level effects do not automatically yield individual-level utility; a measure can successfully separate clinical and healthy groups yet fail to assign an individual to either the clinical or control group with sufficient accuracy because of individual-level differences in EEG (Lopez et al., 2023). However, this dispersion has rarely been examined directly; instead, most available evidence comes from test–retest reliability studies of specific measures. Prior literature emphasizes the group-level reliability of EEG band powers (Gasser et al., 1985; Kondacs & Szabó, 1999; Ip et al., 2018; Tenke et al., 2018) and provides mixed evidence for nonlinear measures (Gudmundsson et al., 2007; Põld et al., 2021). Higher reliability is evidenced when an individual's test–retest measurements are more similar

to their own subsequent recordings than to those of others, indicating inter-individual differentiation alongside temporal stability. Although many factors are known to affect EEG (Hoffman & Polich, 1998; Brötzner et al., 2014; Höller et al., 2022), the extent of its individual-level stability remains unclear, as the temporal stability of EEG measures at the individual level has been scarcely examined (Põld et al., 2023). It is therefore essential to quantify intra-individual EEG stability by characterizing the expected fluctuation ranges of EEG measures through a dedicated longitudinal design, which enables individualized, baseline-referenced decisions.

As the temporal stability of EEG measures at the individual level (normative intra-individual range) and their inter-measure relationships (e.g., correlation structure) have not been systematically characterized, the baseline variability against which to judge individual change and the degree of overlap or complementarity among measures remain unknown. For individualized monitoring, measures must be stable under steady conditions yet responsive to clinically meaningful physiological perturbations across time scales. Although numerous group-level studies demonstrate case–control differences in EEG under altered brain states, there is little and, to date, no systematic evidence assessing whether a single individual's state changes register as deviations from that person's own baseline. This motivates the search for EEG-based brain-state measures that are stable over time, sensitive to clinically relevant change, and robust in practical deployment for individualized monitoring. Accordingly, the central goal of this thesis is to guide the selection of EEG measures for individualized monitoring.

The thesis is based on four publications, which together support the thesis goal. **Publication I** addresses the diversity of measures by systematically mapping inter-relationships among widely used measures in healthy adults to assess overlap and guide the selection of complementary measures. More broadly, commonly used EEG measures in psychiatric research primarily index spectral power, generic nonlinear complexity, or connectivity, and thus do not directly capture the temporal self-similarity of waveform patterns. Yet converging evidence suggests that psychiatric disorders are characterized by abnormalities in neural synchrony and the temporal organization of oscillatory activity, particularly in alpha and gamma bands (Uhlhaas & Singer, 2006; Başar & Güntekin, 2013; Tsai et al., 2023; Han et al., 2025), indicating that the stability of ongoing rhythms may be clinically relevant. Therefore, **Publication II** introduces the in-phase matrix profile (pMP) as such a temporal self-similarity measure with reduced amplitude dependence and benchmarks it against a widely used nonlinear measure in MDD to test whether waveform stability better captures case–control differences than generic complexity. **Publication III** evaluates temporal stability at the individual level over one year by quantifying intra-individual variability in linear and nonlinear single-channel measures, while providing insight into inter-individual dispersion by describing personal baselines. **Publication IV** demonstrates intra-individual sensitivity to a controlled perturbation using a dense single-participant design around mRNA vaccination to test whether selected measures register transient deviations against a well-characterized personal baseline. This provides an explicit stress-test of sensitivity, grounded in prior evidence that stressors modulate EEG rhythms (Al-Shargie et al., 2016; Minguillon et al., 2016; Schlink et al., 2017; Põld et al., 2018).

Aim of the Thesis

The overall aim of this thesis is to guide the selection of EEG measures for individualized longitudinal monitoring. This overall aim is pursued through four specific aims:

1. Describe interrelationships among common resting-state EEG measures to assess complementarity and guide compact, informative measure selection (**Publication I**).
2. Develop and evaluate a new single-channel EEG measure of waveform stability and compare its performance with an established reference measure in distinguishing depression-related differences (**Publication II**).
3. Characterize long-term intra-individual temporal variability and inter-individual differences in single-channel EEG measures, to determine whether they can provide stable baselines for monitoring (**Publication III**).
4. Verify whether EEG measures are sensitive to controlled perturbations in brain physiology within an individual, thereby testing their suitability for detecting meaningful intra-individual neurophysiological changes captured by EEG measures over time (**Publication IV**).

Abbreviations

Explanations of abbreviations used in the thesis.

ABP	alpha band power
ADHD	attention-deficit/hyperactivity disorder
BBP	beta band power
CI	confidence interval
DFA	detrended fluctuation analysis
DP	distance profile
E	effectiveness index
EC	eyes closed (recording condition)
EEG	electroencephalography
EST-Q	Emotional State Questionnaire
GAD	generalized anxiety disorder
GBP	gamma band power
HAM-D	Hamilton Depression Rating Scale
HFD	Higuchi's fractal dimension
ImC	imaginary coherence
ICC	intraclass correlation coefficient
LZC	Lempel-Ziv complexity
LB	lower bound (of CI)
MDD	major depressive disorder
MI	mutual information
MP	matrix profile
MSC	magnitude-squared coherence
OCD	obsessive-compulsive disorder
pMP	in-phase matrix profile
PTSD	post-traumatic stress disorder
rDif	maximum relative difference from annual mean
REST	reference electrode standardization technique
SASI	spectral asymmetry index
SL	synchronization likelihood
TBP	theta band power

1 Toward Robust, Stable, and Sensitive Individualized Measures of Resting-State EEG

A mental disorder is a clinically significant disturbance in cognition, emotion regulation, or behavior that causes distress or impairs daily functioning. Mental disorders are highly prevalent and socially consequential: in 2021, an estimated 1.1 billion people worldwide, about one in seven, were living with a mental disorder, with anxiety and depressive disorders most common (WHO, 2025). During 2020, COVID-19 pandemic modeling indicated global increases of 28% in major depressive disorder and 26% in anxiety disorders (Santomauro et al., 2021; WHO, 2022). These conditions are leading causes of disability, accounting for 14.6% of all years lived with disability worldwide in 2019 (Ferrari et al., 2022). People with severe mental disorders also face substantial premature mortality, dying on average 10–20 years earlier than the general population (Walker et al., 2015). Beyond health, the societal burden is large and sustained: depression and anxiety alone are associated with 12 billion lost workdays annually, costing the global economy about US$1 trillion each year (WHO, 2024). Major treatment gaps persist, particularly in low-resource settings, with national surveys from India and China showing that over 80% of people with any mental or substance use disorder did not seek care, and with minimally adequate treatment for depression reaching about one in five in high-income countries but only one in 27 in low- and middle-income countries, aggravating impacts on education, employment, families, and community participation (Patel et al., 2018; WHO, 2025).

Key challenges persist in mental healthcare: limited availability of specialists and persistent social stigma, and the inherently subjective nature of diagnosis and treatment planning, which rely primarily on clinician judgment and self-report questionnaires. There is a need for objective, scalable methods that complement clinical evaluation by supporting the assessment of mental health status, identifying the need for intervention, and quantifying treatment effectiveness. Against this backdrop, electrophysiological methods that directly capture neuronal field activity are prospective tools for objective assessment and monitoring. Among these, EEG is often the most practical option for ongoing monitoring because it couples very high temporal resolution with affordability, portability, and feasibility for repeated, longitudinal assessments in clinics, research facilities, and naturalistic settings (Buzsáki et al., 2012). Compared with magnetoencephalography (MEG), which shares exquisite temporal resolution but requires costly, shielded environments, EEG is substantially easier to deploy (Baillet, 2017); invasive intracranial EEG offers exceptional spatiotemporal precision but is reserved for narrow clinical indications (Parvizi & Kastner, 2018).

Historically, EEG has been central to the study of human brain function for nearly a century, beginning with Hans Berger's recordings in the 1920s that revealed the alpha rhythm, an oscillation around 10 Hz prominent during relaxed wakefulness with eyes closed (Berger, 1929). Early EEG interpretation relied on visual inspection, with alpha suppression upon eye opening (alpha blocking) recognized as one of neuroscience's first robust physiological observations (Niedermeyer & Lopes da Silva, 2005). Since then, alpha activity has served both as a hallmark of typical brain function and as a clinical research target. However, several EEG measures have been introduced to date, each characterizing EEG from a different perspective.

1.1 Linear Measures

Traditional EEG analysis relies on spectral band power measures, which provide essential insights into brain dynamics by quantifying neural oscillations across different frequency bands. EEG frequency bands are linked to distinct cognitive and physiological processes, with delta (<4 Hz) associated with deep sleep, theta (4–8 Hz) with memory and drowsiness, alpha (8–13 Hz) with relaxation and attentional control, beta (13–30 Hz) with active thinking and motor planning, and gamma (>30 Hz) with higher-order cognitive functions such as perception and consciousness (Sörnmo & Laguna, 2005; Buzsáki, 2006).

Band power differences are frequently reported in psychiatric disorders. The review of 184 studies has demonstrated that differences in EEG frequency band powers are evident for many psychiatric disorders, including MDD, ADHD, autism, addiction, bipolar disorder, anxiety, panic disorder, post-traumatic stress disorder (PTSD), obsessive-compulsive disorder (OCD), and schizophrenia (Newson & Thiagarajan, 2019). Generally, a dominant pattern in MDD and alcohol addiction is an increase in absolute theta (TBP) and beta band power (BBP) (Knott et al., 2001; Newson & Thiagarajan, 2019) and a decrease in the alpha band power (ABP) in MDD (Wolff et al., 2019). In schizophrenia, OCD, and ADHD, a common finding is a slowing of the EEG: increased power in slow waves (delta, theta), accompanied by reduced power in the faster alpha band (Newson & Thiagarajan, 2019). In GAD, heightened beta band activity has been reported (Wang et al., 2025). As can be seen, power changes within specific frequency bands are not unique to one disorder but show overlap across disorders as well as variability within disorders, highlighting that spectral power shifts are a sensitive but not highly specific measure of psychopathology (Newson & Thiagarajan, 2019).

The alpha band is arguably the most intensively studied frequency band, owing to its prominent resting-state amplitude, ease of detection, and long research history. Beyond power, alpha has been examined for power-independent characteristics, most notably individual alpha peak frequency and spatial topography. Earlier reports supported the diagnostic value of frontal alpha asymmetry for depression (Knott et al., 2001; Thibodeau et al., 2006); however, its robustness has since been questioned by meta-analyses (van der Vinne et al., 2017; Kaiser et al., 2018). Earlier work reported a higher overall oscillatory frequency in depression, whereas peak frequency in a specific frequency band did not yield consistent group differences (Knott et al., 2001). More recent evidence indicates the opposite trend for the alpha band: Wolff et al. (2019) reported lower peak frequency in MDD. Taken together, the alpha band carries important information, but results have been somewhat contradictory, likely due to differences in methodological choices and analytic approaches across studies.

Combining band powers into ratios can sharpen group differences; for example, children with ADHD often show an elevated theta/beta power ratio; however, meta-analyses indicate only a moderate effect with substantial between-study heterogeneity and strong age dependence (Arns et al., 2013; Newson & Thiagarajan, 2019). An additional combining method is the spectral asymmetry index (SASI), which captures the balance between higher- and lower-frequency power excluding the alpha band. SASI has differentiated patients with MDD from controls (Hinrikus et al., 2009; Bachmann et al., 2013, 2018) and has been sensitive to diverse stressors (Suhhova et al., 2011; Saifudinova et al., 2015; Põld et al., 2018).

Given the limited specificity of linear measures, especially band powers, they are rarely sufficient for diagnosing or monitoring mental health on their own. Demonstrated group effects often coexist with cross-disorder overlap and pipeline sensitivity; therefore, linear measures are best used in conjunction with complementary measures, rather than as standalone decision variables.

1.2 Nonlinear Measures

EEG signals are complex, stochastic, nonstationary, and nonlinear; accordingly, the wide variety of measures for studying brain activity is diverse and extends well beyond linear spectral measures. Consequently, many nonlinear measures from dynamical systems, information theory, and fractal analysis have been adopted in EEG research. Complexity-oriented, nonlinear measures quantify self-similarity, irregularity, and long-range temporal dependencies, capturing aspects of EEG dynamics that linear approaches miss. Such measures often reveal subtler differences between healthy and psychiatric groups, providing complementary diagnostic information. These characteristics make nonlinear measures promising for sensitivity, but their translational value hinges on robustness to analysis choices.

Fractal dimension quantifies the scale-dependent irregularity (fractal complexity) of an EEG signal. Higuchi's fractal dimension (HFD) is among the most widely used estimators because it operates directly on the time series and is computationally efficient (Higuchi, 1988). In addition, across several psychiatric disorders, including MDD, schizophrenia, and autism spectrum disorder, HFD has demonstrated moderate discrimination between groups (Ahmadlou et al., 2012; Hosseinifard et al., 2013; Kesić & Spasić, 2016; Bachmann et al., 2018). In MDD, HFD is often elevated relative to healthy controls (Bachmann et al., 2013; Akar et al., 2015a; Čukić, Stokić, Radenković, et al., 2020). In schizophrenia, effects are regionally specific, with increases in HFD reported over temporal and occipital regions and reductions over frontal regions, and age- and symptom-nature-dependent (Fernández et al., 2013; Kesić & Spasić, 2016). While widely applied and promising for psychiatric evaluation, HFD is sensitive to noise and thus benefits from careful preprocessing (Accardo et al., 1997). This noise susceptibility raises the risk that preprocessing choices confound longitudinal comparisons, which must be controlled for individualized monitoring.

Detrended fluctuation analysis (DFA) is a nonlinear method for quantifying long-range temporal correlations in time series data. Initially developed for DNA sequences and heart-rate dynamics (Peng et al., 1994, 1995), DFA is now also used in neuroscience, especially in EEG, to estimate a scaling exponent (α) that indexes fractal-like temporal structure. DFA has shown successful discrimination between MDD and controls (Mumtaz et al., 2015; Bachmann et al., 2018) while showing higher α for MDD and a linear correlation with the severity (Lee et al., 2007). DFA has also distinguished individuals with schizophrenia from healthy controls in the beta band (Moran et al., 2019). However, choices such as scale ranges and detrending order introduce analyst degrees of freedom that complicate reproducibility and cross-site synthesis.

Lempel-Ziv complexity (LZC) quantifies the emergence of new patterns in a sequence (Lempel & Ziv, 1976). In EEG, LZC is now a staple complexity measure; it has been reported to decrease during mental arithmetic relative to rest and to be elevated in psychiatric cohorts, including MDD and schizophrenia (Y. Li et al., 2008). In MDD, higher LZC is observed particularly in frontal and parietal regions and can increase during music

listening, whereas in the healthy cohort, LZC tends to decline from baseline during music exposure, consistent with relaxation (Akar et al., 2015b). Binarization rules substantially affect LZC estimates, emphasizing the need for standardized pipelines when comparing individuals over time.

Collectively, nonlinear measures can provide complementary information and sometimes stronger group-level effects than linear measures, and show somewhat topographical specificity in some studies, depending on the measure. However, many nonlinear measures require user-set analysis choices (e.g., windowing, scales) that can influence results and complicate reproducibility and cross-site comparability. Though nonlinear measures enrich sensitivity, typical parameter dependence is a liability for robust deployment. This motivates the development of an easily deployable measure that does not require user-defined parameter tuning, enhancing reproducibility through robustness.

1.3 Connectivity Measures

Connectivity measures quantify coordinated activity across brain regions by estimating dependencies between channels (Fingelkurts et al., 2007; Leuchter et al., 2012; Olbrich et al., 2014; Y. Li et al., 2016). Within the functional connectivity family, different measures emphasize complementary facets: magnitude-squared coherence (MSC) summarizes linear frequency-specific coupling but can be inflated by zero-lag effects and reference choices (Srinivasan et al., 2007); imaginary coherence (ImC) retains only nonzero-phase-lag interactions, reducing volume conduction artifacts (Nolte et al., 2004); synchronization likelihood (SL) captures generalized (linear + nonlinear) synchronization (Stam & van Dijk, 2002); and mutual information (MI) indexes shared information irrespective of linearity, with symbolic/weighted variants improving robustness (Imperatori et al., 2019). These measures extend beyond local activity to capture network-level coordination implicated in psychopathology.

In MDD, many studies report altered connectivity, often increased alpha/theta coherence (Fingelkurts et al., 2007; Leuchter et al., 2012; Y. Li et al., 2016), while others show decreases in graph-level organization (Chen et al., 2024)—illustrating directional heterogeneity across pipelines and measures. Phase-sensitive/lagged measures (e.g., ImC, SL) demonstrate discriminative value and treatment sensitivity (Olbrich et al., 2014; Sun et al., 2019). Beyond MDD, convergent dysconnectivity has also been observed in schizophrenia (Na et al., 2002; Kam et al., 2013; A. Ibáñez-Molina et al., 2024; Domingos et al., 2025), bipolar disorder (Kam et al., 2013; Kim et al., 2013), ADHD (Furlong et al., 2021), anxiety disorders (Liu et al., 2024), OCD (Perera et al., 2024), and PTSD (Q. Li et al., 2022). However, the direction and locations vary by band and measure. Such heterogeneity indicates that connectivity effects are sensitive to band selection, referencing, and graph-building choices, thereby hindering reproducibility.

Crucially, choices of reference, montage, windowing, filtering, and artifact handling can shift estimates, with consequences for comparability across sites and settings (Bonita et al., 2014). Connectivity measures complement single-channel measures by indexing large-scale coordination. Still, their pipeline sensitivity suggests the need for careful complementarity mapping and prioritizing robust, tuning-minimal measures when aiming for individual-level monitoring.

The mixed and measure-dependent picture raises a key question: how do strong group-level results translate into decisions about individual cases? Beyond understanding which EEG measures can discriminate between clinical groups, it is equally important to

examine how consistent these measures remain within individuals over time and how sensitively they reflect dynamic brain-state changes. These aspects—stability and sensitivity—are reviewed in the following sections.

1.4 From Strong Group-Level Effects to Individual Decisions

Despite the wide range of EEG measures introduced above, only one measure has been approved for routine clinical use to detect or monitor a psychiatric disorder. The theta/beta power ratio was approved regionally in 2013 by the US Food and Drug Administration to be used as a complementary method to aid in diagnosing ADHD in children (U.S. FDA, 2013), but has received critical feedback for not adding value to clinical evaluation (Gloss et al., 2016). This narrow clinical uptake highlights a translational gap between promising research and measures that are robust and sensitive enough to meet reproducibility and clinical-utility demands.

At the group level, however, several feature sets differentiate patients from controls with high accuracy. For example, a combination of nonlinear measures—HFD, DFA, correlation dimension, and the Lyapunov exponent—achieved 90% accuracy for MDD, exceeding the 76.6% reported for linear band-power measures (Hosseinifard et al., 2013). Likewise, different combinations of linear (SASI, alpha power variability, relative gamma power) and nonlinear (HFD, DFA, LZC) measures yielded closely similar accuracies (88% for linear vs 85% for nonlinear) in another study (Bachmann et al., 2018). More broadly, band power, HFD, LZC, SASI, and related measures have delivered comparable performance in evaluating MDD (Hosseinifard et al., 2013; Bachmann et al., 2018; Mahato & Paul, 2019). Two interpretations follow. First, the disorder may induce multiple physiological alterations that are differentially captured by distinct EEG measures, such that each measure probes a partially unique facet of brain dynamics. Second, several measures may index largely the same underlying deviations in neural function, yielding convergent or overfitting performance. However, reported accuracies can be inflated by feature selection choices, cross-validation leakage, and site effects; thus, notable outcomes can overestimate real-world utility.

These considerations argue for deliberate, hypothesis-driven measure selection to maximize complementary information. In practice, classification accuracy tends to depend more on the choice of features than on the specific learning algorithm applied (Čukić, Stokić, Simić, et al., 2020). The chosen measures serve as input data that govern classification performance. Yet only a few studies have directly examined how combining different EEG measures affects classification accuracy (Hosseinifard et al., 2013; Bachmann et al., 2018; Čukić, Stokić, Simić, et al., 2020).

Crucially, strong group-level separation does not imply reliable individual-level discrimination: EEG exhibits substantial inter-individual variability (Zhang et al., 2021; Lopez et al., 2023; Tatar, 2023), many measures are not disorder-specific, and patient–control distributions often overlap. Consequently, promising group averages can fail to identify where a particular person lies within the relevant distribution, limiting clinical decision-making. To bridge this gap, reliability and temporal stability must be established explicitly—especially within individuals over time.

1.5 Reliability and Temporal Stability

While the previous section outlined why strong group-level effects may not translate to individual decisions, this section reviews quantitative evidence on the reliability and temporal stability of EEG measures over time.

For EEG measures to be clinically useful, they must be reliable and temporally stable. Reliability is commonly quantified with the intraclass correlation coefficient (ICC), which expresses the proportion of total variance attributable to inter-individual differences relative to intra-individual variability (and residual error) in a given measurement design (Shrout & Fleiss, 1979; McGraw & Wong, 1996; Koo & Li, 2016). Values approaching 1 indicate high consistency across raters or sessions, whereas values near 0 indicate poor reliability. According to Koo & Li (2016), reliability should be evaluated from the 95% confidence interval (CI) of the ICC estimate, not the point estimate alone. As a general guideline, a CI lower bound (LB) < 0.50 indicates poor reliability, 0.50–0.75 moderate, 0.75–0.90 good, and > 0.90 excellent reliability. Because EEG is sensitive to day-to-day influences (e.g., nutrition, time of day, seasonality, hormonal cycles), some variability is expected even in healthy individuals (Hoffman & Polich, 1998; Brötzner et al., 2014; Höller et al., 2022). Critically, reliability is not equivalent to temporal stability (intra-individual consistency) required for longitudinal monitoring.

At the group level, ICC quantifies the proportion of total variance attributable to stable inter-individual differences. A high ICC, therefore, indicates that inter-individual variance substantially exceeds intra-individual variance: individuals are distinguishable from one another, and the measure separates people well, but this does not by itself demonstrate strong temporal stability within any given individual. Conversely, a low ICC implies that intra-individual variability (and/or measurement error) is large relative to inter-individual differences, or that individuals differ little, yielding weak discrimination at the group level. In short, group-level ICCs conflate intra-individual stability with the magnitude of between-person differences and should not be interpreted as a pure index of individual test–retest stability.

The reliability of linear EEG measures, especially spectral power in classical frequency bands, has been documented extensively. Early studies reported that band powers show test–retest reliability (Gasser et al., 1985; Salinsky et al., 1991; Kondacs & Szabó, 1999), and subsequent work confirmed and extended these findings to additional linear parameters (Cannon et al., 2012; Gevins et al., 2012; Ip et al., 2018; Tenke et al., 2018). By contrast, the reliability of nonlinear measures has been less frequently examined, with only a handful of studies including them (Dünki et al., 2000; Gudmundsson et al., 2007; Põld et al., 2021; Lord & Allen, 2023). This scarcity represents a key evidence gap for nonlinear measures intended for longitudinal use.

Across studies, mid-spectrum bands (theta, alpha, beta) tend to exhibit higher reliability than delta or gamma band power (GBP) (Gudmundsson et al., 2007; Ip et al., 2018; Põld et al., 2021). Nonlinear measures show mixed results, ranging from somewhat lower (Gudmundsson et al., 2007) to comparable reliability relative to band power measures (Põld et al., 2021). Developmental factors also play a role: the reliability of linear measures is generally stronger in adults than in children or adolescents, likely reflecting maturational changes, whereas sex differences in reliability appear minimal (Tenke et al., 2018). These patterns suggest prioritizing mid-band measures for stable baselines while cautiously interpreting delta/gamma unless temporal stability is demonstrated within the intended pipeline.

Temporal stability has been far less studied than reliability. At the group level, temporal stability is typically assessed as the relative difference between group means across recording sessions. In a three-year test–retest study with 17 participants (two sessions per person), spectral band powers showed the smallest group-level change in the alpha band (0.72%) and the largest in the gamma band (2.28%) (Põld et al., 2021). Among single-channel linear measures, SASI exhibited the greatest change (11.89%), whereas interhemispheric asymmetry showed very poor stability over three years (236%). By contrast, nonlinear measures demonstrated higher temporal stability at the group level than linear measures, with HFD and DFA changing by only 0.18% and 0.49%, respectively. This suggests that, in nonlinear measures, individuals may show less difference in baselines and possibly higher intra-individual stability than in linear measures.

In a follow-up study (Põld et al., 2023), both linear and nonlinear measures showed strong between-session correlations (Pearson $r \geq 0.88$). Nevertheless, average individual relative changes were larger for linear measures (21%–36%) than for nonlinear measures (3%–10%). By comparison, depression questionnaire scores for the Hamilton Depression Rating Scale (HAM-D) (Hamilton, 1960) and Emotional State Questionnaire (EST-Q) (Aluoja et al., 1999) were much less temporally stable (52.8%–69.3%; $r = 0.52$ and $r = 0.61$), indicating the subjective nature of not only self-report questionnaires (EST-Q) but also questionnaires filled in by a health specialist (HAM-D). The comparative instability of questionnaires underscores the value of objective measures; however, individual-level change thresholds must still be predefined to avoid post hoc interpretation errors.

However, small group-mean changes can conceal substantial individual-level fluctuations, cautioning against overreliance on generalized statistics. Even under tightly controlled recording conditions in healthy individuals, distinct EEG profiles can be observed. Aggregating to means or medians smooths extreme values, making the group appear more stable than most individuals. To evaluate whether an EEG measure can be clinically useful for longitudinal monitoring, temporal stability must therefore be demonstrated at the individual level, not only at the group level. Accordingly, stability should be formalized as individualized reference intervals with explicit exceedance criteria. With baselines in place, the remaining question is whether candidate measures show adequate intra-individual sensitivity when the brain state truly changes.

1.6 Individual-Level Sensitivity

Having selected complementary, less redundant measures and established not only their reliability but also their temporal stability at the individual level, the next task is to determine whether they are also sensitive at the individual level. As discussed previously, numerous EEG measures, especially when combined, differentiate healthy controls from cohorts with psychiatric disorders in group studies; however, because EEG is highly person-specific, such group-level evidence offers limited insight into whether the same individual would show detectable change when moving from a healthy state to the onset of a psychiatric condition. Accordingly, beyond choosing stable, information-rich measures, it is essential to assess their individual-level sensitivity: given a well-characterized personal normative range for each measure across relevant conditions, do deviations beyond that range emerge when brain function becomes perturbed?

Taken together, the reviewed evidence suggests that EEG measures vary in both their temporal stability and their responsiveness to brain-state changes. Measures showing high stability may reflect trait-like properties of brain function, whereas those with

greater variability may index state-dependent processes. The optimal biomarker for individualized monitoring should therefore balance stability and sensitivity—remaining relatively stable under comparable conditions yet responsive to meaningful neurophysiological change. The current thesis addresses this balance by systematically quantifying both aspects in multiple EEG measure families.

2 Methods

2.1 Subjects and Prerecording Conditions

In **Publication I**, 80 neurologically and psychiatrically healthy volunteers (38 women, 42 men; age mean ± SD 37 ± 15, range 19–75 years) were recruited for the cross-sectional study. In **Publication II**, 66 right-handed participants formed two groups: 33 medication-free outpatients with MDD (12 men, 21 women) and 33 age- and sex-matched healthy controls. Mean age was 34.5 ± 14.9 years in the MDD group and 34.7 ± 15.0 years in controls (overall range 18–75 years). In **Publication III**, nine healthy, right-handed male participants (mean age 37.2 ± 8.1 years; range 26–49) each completed twelve monthly recordings. **Publication IV** followed a single healthy, right-handed male aged 49 years, with twelve monthly reference recordings and two post-stressor recordings.

In **Publications I**, **III**, and **IV**, all participants self-reported as healthy and denied a history of concussions with loss of consciousness, epilepsy, brain injury, use of narcotic or psychotropic substances, or other neurological or psychiatric conditions. In **Publication II**, MDD was confirmed during a clinical interview, and participants were diagnosed with MDD by a psychiatrist according to ICD-10 criteria. Participants in the control group were enrolled if they scored below the EST-Q thresholds referring to probable depressive or anxiety disorder.

Pre-recording conditions were standardized across studies: in **Publications I–II**, participants were instructed to avoid alcohol for 24 h and caffeine for at least 2 h; in **Publications III–IV**, they maintained their usual routines and abstained from both alcohol and caffeinated beverages for 24 h before each EEG session. Additionally, in the longitudinal protocols (**Publications III–IV**), the weekday and time of the recording were held constant within participants across sessions to minimize confounding influences.

All studies were conducted in accordance with the Declaration of Helsinki and were approved by the Tallinn Medical Research Ethics Committee and/or the Estonian Institute for Health Development Human Research Ethics Committee. Written informed consent was obtained from every participant before enrolment.

2.2 EEG Recordings and Preprocessing

EEG was acquired with a Neuroscan Synamps2 amplifier and 32-channel cap (QuikCap) (Compumedics, NC, USA). The EEG data were obtained in 30 channels and the electrodes were positioned according to the extended international 10–20 system at positions Fp1, Fp2, F7, F3, Fz, F4, F8, FT7, FC3, FCz, FC4, FT8, T7, C3, Cz, C4, T8, TP7, CP3, CPz, CP4, TP8, P7, P3, Pz, P4, P8, O1, Oz, and O2 (Figure 1) referenced to linked mastoids. Electrooculograms (horizontal and vertical) were recorded concurrently in two channels to monitor eye movements. The impedance of EEG electrodes was kept below ten kΩ to achieve good conductivity between the skin and the electrode.

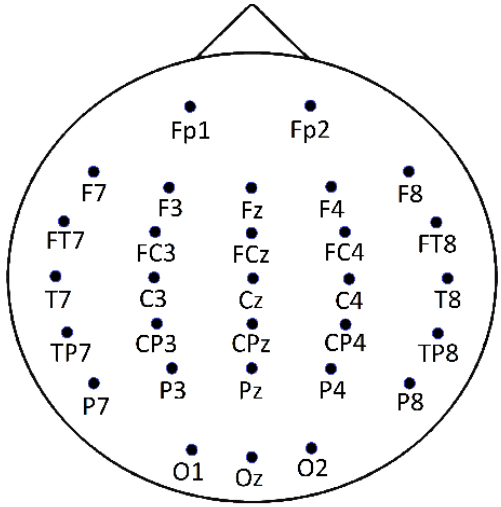

Figure 1. Locations of the 30 EEG electrodes corresponding to the channels used in this thesis, positioned according to the extended international 10–20 system.

Eyes-closed (EC) resting-state EEG was recorded in a dimly lit shielded room for 6 min in **Publication I** and for 10 min in **Publications II–IV**; in the longitudinal protocols (**Publications III–IV**), the EC block was followed by a 5-minute eyes-open period, which was not analyzed in this thesis. Pre-processing was performed in MATLAB (MathWorks, MA, USA). Initially, EC EEG recordings were segmented into 20.48-s epochs, and artifact-containing epochs were visually identified and flagged. The EC EEG data were re-referenced with the reference electrode standardization technique (REST). REST approximates a neutral "infinite" reference to minimize dependence on the original reference, making EEG more physiologically interpretable and comparable across recordings (Yao, 2001; Hu et al., 2018; Yao et al., 2019). Digital filtering was applied to remove baseline drift and high-frequency noise, leaving 1-45 Hz band in **Publication I** and 2-47 Hz band in **Publications II–IV**. All data were acquired at 1000 Hz; data were down-sampled to 200 Hz in **Publications I–II** and, in **Publications III–IV**, for nonlinear measures (power band measures were computed at the original rate). EC EEG recordings were segmented into 20.48-s epochs again, and 10 visually clean epochs per subject were retained in **Publications I–II**, 12 segments in **Publication III**, and the first 9 segments in **Publication IV**.

2.3 Calculated Measures and Statistics

The thesis employs a broad range of quantitative EEG measures, all of which are collated in Table 1.

Table 1. EEG measures used in the thesis.

	Measure	Abbreviation	Usage in publications	Quantifies
Linear measures	Theta band power	TBP	I, III, IV	Absolute power in the theta band
	Alpha band power	ABP	I, III, IV	Absolute power in the alpha band
	Beta band power	BBP	I, III, IV	Absolute power in the beta band
	Gamma band power	GBP	I, III, IV	Absolute power in the gamma band
	Spectral asymmetry index	SASI	I, IV	Balance between higher and lower band powers
	Magnitude-squared coherence	MSC	I	Inter-channel coupling
	Imaginary coherence	ImC	I	Phase-lagged inter-channel coupling
Nonlinear measures	Mutual information	MI	I	Inter-channel dependence
	Synchronization likelihood	SL	I	Inter-channel synchronization
	Higuchi's fractal dimension	HFD	I, II, III, IV	Fractal complexity
	Detrended fluctuation analysis	DFA	I, III	Long-range correlations
	Lempel-Ziv complexity	LZC	I, III	Sequence complexity
	in-phase matrix profile	pMP	II, III	Waveform stability

2.3.1 Publication I

Publication I extracted 12 EEG measures—band powers in the theta, alpha, beta, and gamma ranges; four single-channel dynamics measures (HFD, DFA, LZC, SASI); and four functional connectivity measures (SL, MI, MSC, ImC). Power was computed within the bands TBP (4–7 Hz), ABP (8–12 Hz), BBP (13–30 Hz), and GBP (31–45 Hz). HFD was computed according to the original algorithm (Higuchi, 1988), with kmax = 8, as in Bachmann et al. (2018) and Päeske et al. (2018). DFA followed Peng et al. (1995) with the EEG adaptation of Bachmann et al. (2018). LZC was calculated as in Lempel & Ziv (1976) with the adjustment in Bachmann et al. (2018). SASI summarized lower versus higher EEG-band power while excluding the central alpha band (Hinrikus et al., 2009). SL was implemented as described by Stam & van Dijk (2002), with parameters set as in Päeske et al. (2018) to capture time–frequency structure. MI was estimated with the Fraser & Swinney (1986) algorithm, following the EEG procedure of A. J. Ibáñez-Molina et al. (2020). MSC and ImC were computed in the frequency domain as in Päeske et al. (2020).

Band power and dynamics measures were computed for each of the 30 channels, and connectivity measures were computed for every channel pair (30×29/2 = 435) within

each EEG segment; segment-wise values were first averaged within channel/pair and then averaged across channels/pairs to obtain the subject-level value. Pairwise differences among the 12 measures ((12×12–12)/2 = 66 comparisons) were tested with the Wilcoxon rank-sum test (Bonferroni-corrected to $\alpha = 0.00076$). Correlations between measures were quantified with Spearman coefficients; at n = 80, $|r| > 0.37$ met the same corrected significance level via t-testing ($\alpha = 0.00076$).

Publication I introduced an effectiveness index *E* that reflects both the reach and the strength of a measure's associations with others. For measure *i*, the effectiveness E_i was defined as

$$E_i = N_i \times R_i, \quad (1)$$

where N_i is the number of measures significantly correlated with *i* and R_i is the average of those correlation coefficients. This quantitative index helps assess how broadly a measure reflects EEG patterns and, in turn, its potential to reveal the varied symptom profiles seen in mental disorders.

2.3.2 Publication II

A parameter-independent, time-domain measure of EEG waveform stability was introduced in **Publication II**. The proposed pMP builds on the classic matrix profile (MP) (Yeh et al., 2016), a threshold-free data-mining algorithm for large-scale time series to identify motifs and discords. MP has been used modestly on physiological signals and can perform well on quasi-periodic data, where recurring motifs enable anomaly detection (Wankhedkar & Jain, 2021; Seoni et al., 2022). Resting-state EEG lacks stable motifs—eyes-closed alpha rhythm shows apparent periodicity without true recurrence; therefore, classic MP, which targets changes in motif, misses subtle global alterations (e.g., in MDD) and is better suited to pronounced temporal shifts such as seizures or blinks. The pMP method thereby indexes the consistency of waveform shape across short, phase-aligned segments. The signal is scanned with 1-s windows (Figure 2); for each window (query with the length *m*), the algorithm compares its z-normalized waveform to all other same-length z-normalized windows of the segment (with the length *n*) by calculating Euclidean distance between them, producing a distance profile (DP) using the MASS_V2 algorithm (Mueen et al., 2022; Zhong & Mueen, 2024). The acquired DP plummets whenever the query is aligned in phase with the comparable window (Figure 3).

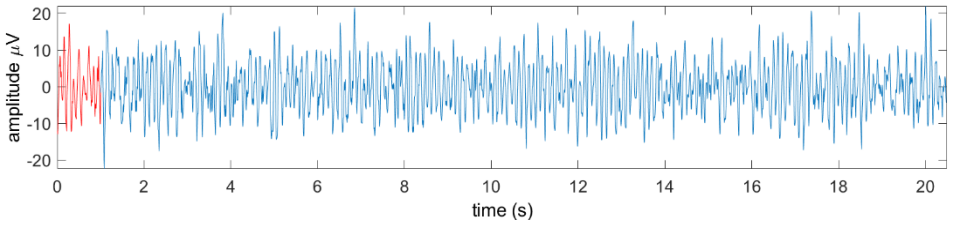

Figure 2. Example EEG signal segment (channel FCz, 20.48 s; 4096 samples). The red segment marks the first 1-s query used to compute the distance profile (Publication II).

Each possible window of the signal is treated as a query in a sliding window manner. For each query q_i, pMP retains only the local minimum values of the DP (the in-phase matches marked with red circles in Figure 3) and computes the median across these local

minimums, $M(q_i)$, for the query. The $M(q_i)$ values corresponding to each query are averaged to yield a single score, as in

$$pMP = \frac{1}{n-m+1} \times \sum_{i=1}^{n-m+1} M(q_i), \quad (2)$$

Because each comparison is z-normalized, the measure is largely insensitive to absolute amplitude. Instead, it reflects the timing regularity of rhythms: lower pMP indicates more regular, phase-aligned recurrence, whereas higher pMP indicates more irregular timing. It is thus a parameter-independent, single-channel measure of in-phase self-similarity.

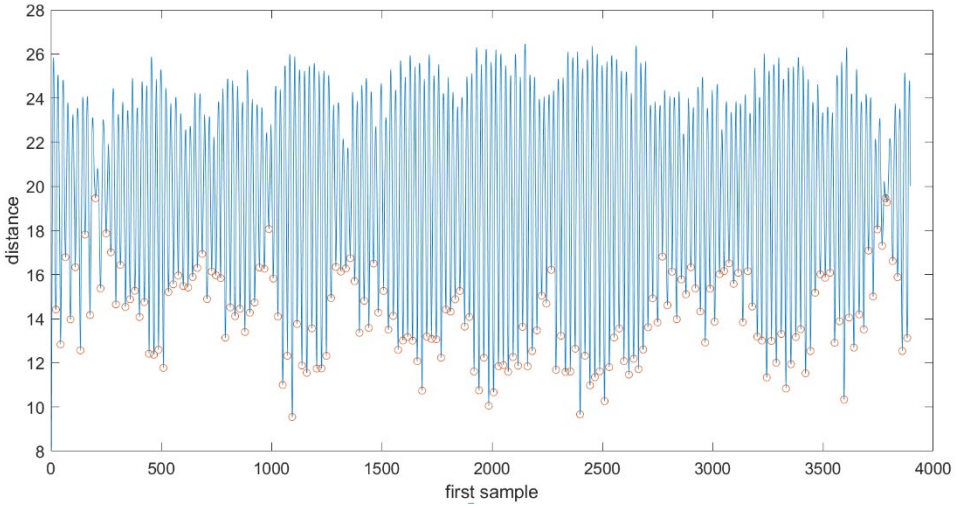

Figure 3. Distance profile for the query in Figure 2. Local minimums (circled) correspond to subsegments most in phase with the query. These minimums form the inputs to pMP (Publication II).

The reference measure, HFD, was calculated as in **Publication I**. Per subject, HFD and pMP were computed for 10 segments at each of 30 channels, and segment-level values were summarized per channel using the median. Group differences were tested with the Mann–Whitney U test (nonparametric test of median differences) ($\alpha = 0.05$), and *p* values were adjusted with a modified Bonferroni correction for multiple comparisons. Classification performance was then assessed using a support vector machine with leave-one-out cross-validation on single-channel features.

2.3.3 Publication III

Absolute powers were calculated for the theta (4–8 Hz), alpha (8–13 Hz), beta (13–30 Hz), and gamma (30–47 Hz) frequency bands. HFD, LZC, DFA, and pMP were calculated for the whole band as in **Publications I** and **II**. For each monthly recording, measures were computed for each channel across 12 clean segments, and the segment-level values were summarized using the median, yielding one value per channel, per subject, per month.

With 12 monthly sessions per participant (n = 9), ICC was used to assess the reliability of repeated EEG measurements. A two-way mixed-effects model (average measures, absolute agreement (McGraw & Wong, 1996; Koo & Li, 2016) for all 30 channels was employed. Reliability was considered excellent when ICC 95% CI LB > 0.9.

Inter-individual differences in channel P3 were analyzed with the global Kruskal–Wallis test ($\alpha = 0.05$) (Kruskal & Wallis, 1952), a nonparametric ANOVA alternative for multiple

groups that does not assume normality and is relatively insensitive to unequal variances. If a significant difference is detected in the global test, a post hoc test can be conducted to identify which subjects differ. In this study, the Dunn test (α = 0.05) was employed to determine how many subject pairs differed statistically (Dunn, 1964). Given nine subjects, 9(9 − 1)/2 = 36 unique pairwise comparisons were performed, and *p* values were adjusted using the Šidák correction (Šidák, 1967).

For each participant, the annual mean and standard deviation for each measure were calculated in channel P3, as well as the maximum relative difference (rDif, intra-individual stability), which indicates the largest deviation from the annual mean, as in

$$rDif = \left|\frac{v_{max} - \bar{v}}{\bar{v}}\right| \times 100, \quad (3)$$

where v_{max} is the most extreme monthly measurement across the year for a given subject, and $\overline{v}$ is that subject's annual mean.

2.3.4 Publication IV

Two BNT162b2 (an mRNA vaccine encoding the SARS-CoV-2 spike protein marketed under the name Comirnaty, Pfizer–BioNTech) doses were administered to the participant three weeks apart. After the first dose, adverse effects were limited to pain at the injection site and in the ipsilateral upper limb for several days; after the second dose, adverse effects included ipsilateral upper-limb pain, headache, myalgia, fatigue, fever, and fogginess (fogginess lasted up to one week; the others resolved by day 4). In **Publication IV**, 12 monthly baseline EEG recordings served as references (r1–r12). Two post-vaccination sessions (p1, p2) were acquired 5 and 12 days after the second dose, scheduled on the same weekday and at the same start time as the reference recordings. Because the first dose preceded the next EEG session by 19 days and no recordings were obtained immediately afterward, that session (r7) was treated as a reference, and first-dose effects were not analyzed.

Absolute power in the theta (4–8 Hz), alpha (8–12 Hz), beta (12–30 Hz), and gamma (30–47 Hz) bands, as well as SASI and HFD, were computed as in **Publication I** from the Fz channel signal. For each recording, each measure was calculated for nine segments, and the segment-level values were summarized by their median.

A two-sample t-test (α = 0.05) was used to test if post-vaccination EEG measures differed from reference recordings. Because six measures were analyzed, *p* values were adjusted for multiple testing using a modified Bonferroni correction.

3 Results

3.1 Interrelationship Between EEG Measures (Publication I)

Publication I investigated the interrelationships between 12 EEG measures in healthy participants to assess their complementarity. Of 66 pairwise comparisons, 37 (56%) were statistically significantly correlated according to Spearman's correlation after Bonferroni correction. The pairwise Spearman's correlations among the EEG measures are shown in the heatmap in Figure 4.

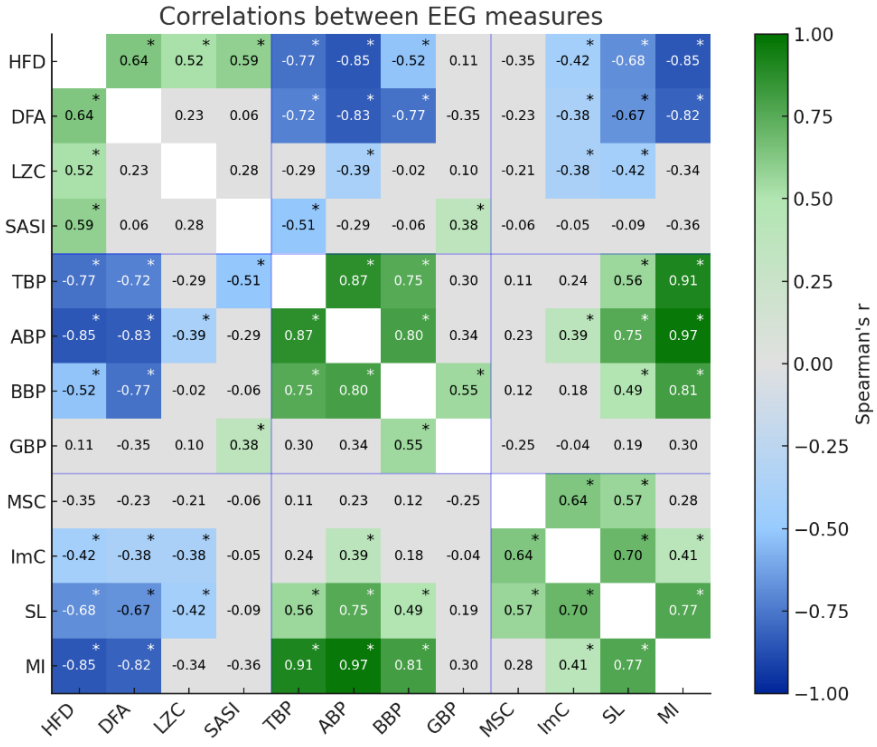

Figure 4. Spearman's correlation matrix across 12 EEG measures (n = 80). Each cell displays the correlation coefficient r, with an asterisk (*) indicating correlations that remain significant after the Bonferroni correction ($p < 0.00076$; $|r| \geq 0.37$). Significant positive correlations are shaded green and negative correlations blue. Gray denotes nonsignificant correlations, and blue separators delineate the three measure families (dynamics, band power, connectivity). Adapted from Publication I.

Band power measures. According to the Wilcoxon test, the calculated values of different band power measures were mutually significantly different ($p < 0.00076$) in all combinations except TBP and BBP ($p = 0.03$). Spearman's correlation revealed that four of six (66.7%) pairings were significant ($|r| > 0.37$). Correlations were highest between adjacent bands: TBP and ABP (r = 0.87), ABP and BBP (r = 0.80), but also between TBP and BBP (r = 0.75). Pairs involving the GBP had lower (GBP and BBP, r = 0.55) or insignificant correlations after correction (ABP and GBP, r = 0.34; TBP and GBP, r = 0.30).

Dynamics measures. The Wilcoxon test showed that all dynamics measures differed significantly in all combinations ($p < 0.00076$). Three of six (50%) correlations were significant: HFD and DFA (r = 0.64), HFD and SASI (r = 0.59), and HFD and LZC (r = 0.52); the remaining pairs among DFA, LZC, and SASI were not significant.

Functional connectivity measures. The Wilcoxon test indicated significant differences among connectivity measures in all pairings except SL and MI ($p = 0.297$). Spearman's analysis showed five of six (83.3%) significant correlations: SL and MI (r = 0.77), SL and ImC (r = 0.70), MSC and ImC (r = 0.64), SL and MSC (r = 0.57), and ImC and MI (r = 0.41).

Across categories. The strongest observed association was between ABP and MI (r = 0.97). The weakest significant associations included LZC and ImC, and GBP and SASI (r = 0.38). By the number of significant links (degree), the counts were: HFD 9, SL 9, MI 8, ABP 8, BBP 7, TBP 7, ImC 7, DFA 6, SASI 4, LZC 4, MSC 2, and GBP 2. Figure 5 summarizes the effectiveness (*E*) of these measures.

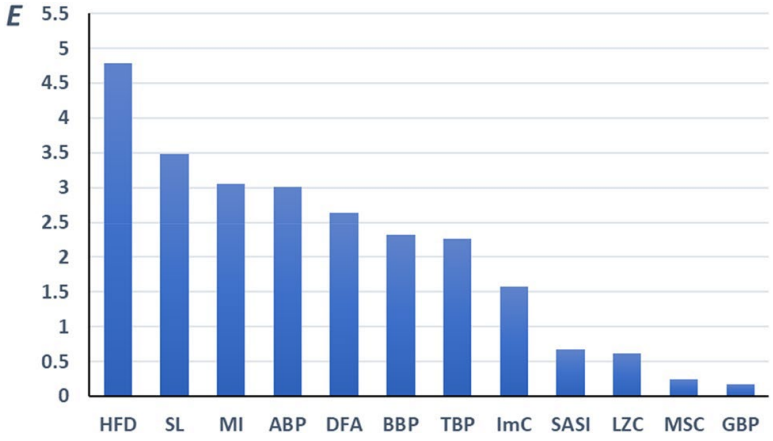

Figure 5. Effectiveness E for each EEG measure, indicating the reach and strength of its associations with other measures. E = NR, where N is the number of measures correlated with the indicated measure, and R is the average value of the corresponding correlation coefficients (Publication I).

3.2 Waveform Stability Measure to Detect MDD (Publication II)

Publication II introduced a waveform stability measure, pMP, and compared it with HFD for distinguishing patients with MDD from healthy controls. Across 66 subjects, both pMP and HFD values were higher in the MDD group than in controls. Group means and topographies for pMP and HFD, as well as the MDD and control group differences, are shown in Figure 6. For both measures, values were lowest in the occipital region and higher over lateral and prefrontal areas.

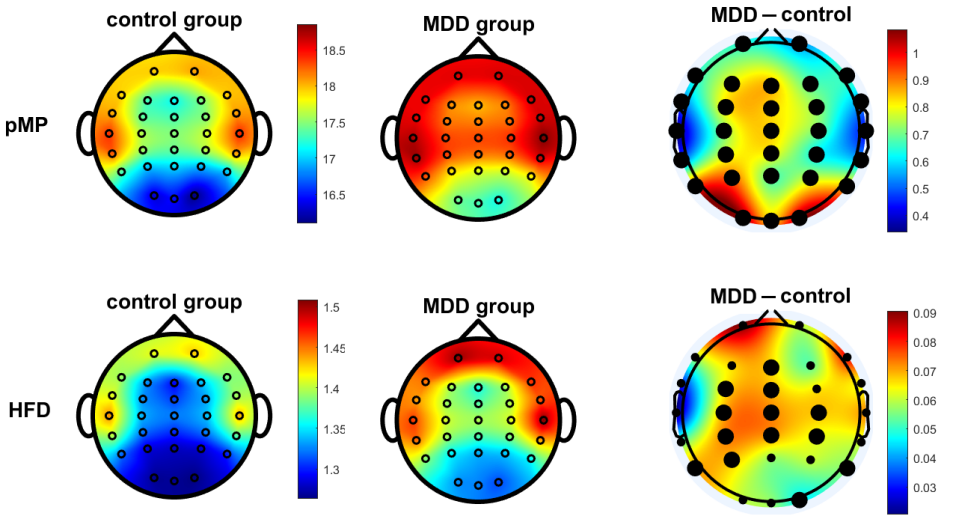

Figure 6. Topographies of group means for pMP (top) and HFD (bottom) across 30 EEG channels in controls and MDD (n = 66). The rightmost column shows group differences (MDD – Control); large black dots mark channels significant after Mann–Whitney U test with a modified Bonferroni adjustment to p values (α = 0.05) (Publication II).

Channel-wise testing (Mann–Whitney U test with modified Bonferroni correction) showed that pMP distinguished the MDD group from the control group in all 30 EEG channels ($p < 0.05$). In contrast, HFD was significant in 13 of 30 channels (43%). The significant channels in HFD were mainly central (CP4, C4, CP3, CPz, Cz, C3, FCz, Fz, FC3) with a few posterior sites (O2, P7, P8, P3). In pMP, the largest between-group difference appeared in the occipital region. Classification with support vector machines yielded the highest accuracy of 73% for pMP and 67% for HFD.

3.3 Intra-Individual Stability and Inter-Individual Differences (Publication III)

Across twelve monthly recordings in nine participants, band powers and nonlinear measures showed generally excellent long-term reliability (ICCs) in **Publication III**. TBP and ABP showed excellent reliability in all 30 channels (Table 2). BBP and GBP also demonstrated excellent reliability, but BBP showed slightly reduced reliability in three temporal channels (TP7, T8, TP8), with the lowest ICC in TP8 (0.908, 95% CI [0.786, 0.975]), which is still indicative of good reliability. GBP remained excellent centrally but fell below the excellent threshold in 13 peripheral (mostly prefrontal/frontal/temporal) channels, with the lowest ICC at FT8 (0.756, 95% CI [0.424, 0.935]). All nonlinear measures (HFD, LZC, DFA, pMP) exhibited excellent reliability across all channels.

Figure 7 shows the monthly values for all eight measures for each of the nine participants, illustrating distinct participant-specific ranges within which the monthly values fall. Across measures, participants showed clear inter-individual differentiation (Dunn test): for each measure, 14–16 of the 36 subject pair comparisons differed significantly (Table 2). Band powers exhibited comparable separation (TBP: 15 pairs; ABP: 16; BBP and GBP: 14), and nonlinear measures showed similarly strong differentiation (HFD and LZC: 14; DFA and pMP: 15).

Intra-individual temporal stability (rDif in the parietal channel P3) indicated substantially greater month-to-month fluctuation for band powers than for nonlinear measures. Mean annual deviations across participants were 66% (TBP), 64% (ABP), 32% (BBP), and 30% (GBP), compared with 23% (DFA), 10% (LZC), 6% (pMP), and 4% (HFD) (Table 2). Marked inter-individual heterogeneity was also apparent: across measures, participant-specific variability ranged from 17% to 53%.

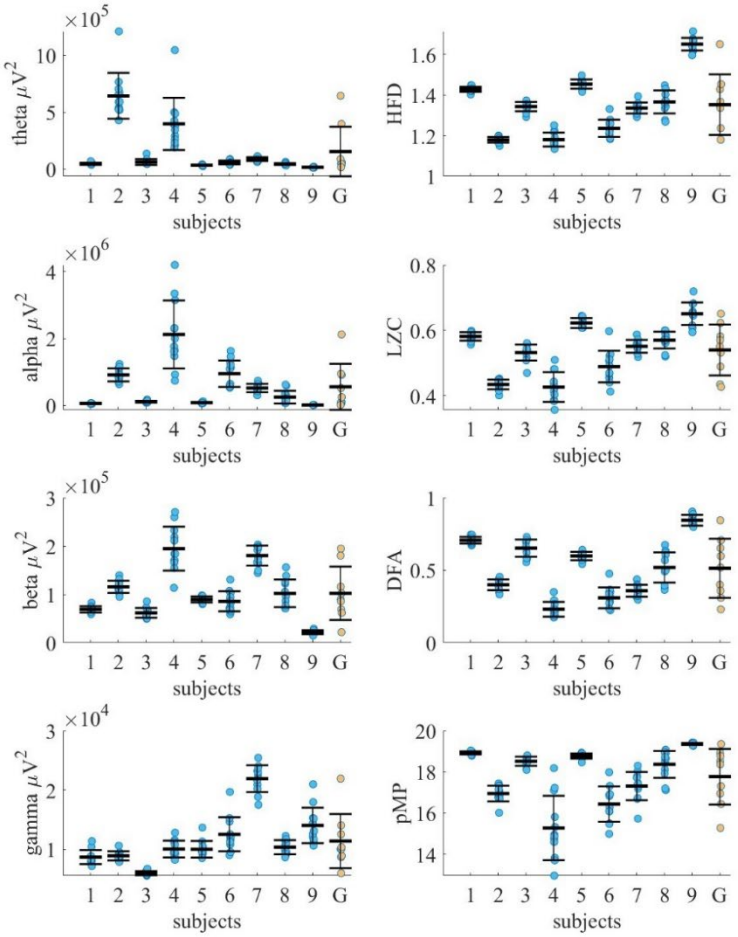

Figure 7. Inter-individual and intra-individual variability in EEG measures across one year for each subject 1–9 and the group G (n = 9). Blue dots represent twelve individual monthly values; black dashes show subject-specific annual means. Error bars for subjects 1–9 represent intra-individual standard deviations. For group G, the yellow dots represent the annual mean of each subject, the black dash indicates the group-level mean, and the error bars represent the standard deviation (Publication III).

Table 2. Reliability and temporal stability of EEG band power and nonlinear measures across 12 monthly recordings (n = 9). The table presents mean intraclass correlation coefficients (ICC) across 30 channels, the lowest ICC 95% confidence interval lower bound (CI LB) value across channels and corresponding channel, the count of significantly different subject pairs out of 36 pairwise comparisons according to Dunn test, and the mean value across subjects and the range of maximal relative difference from annual average across subjects in channel P3.

Measure	Mean ICC	Lowest ICC 95% CI LB	Dif. subject pairs (of 36)	Intra-individual deviation mean and range (%)
TBP	0.991	0.952 (P4)	15	66 (24–163)
ABP	0.984	0.917 (O2)	16	64 (27–152)
BBP	0.978	0.786 (TP8)	14	32 (11–53)
GBP	0.935	0.424 (FT8)	14	30 (12–57)
HFD	0.993	0.949 (T7)	14	4 (2–8)
LZC	0.985	0.922 (T7)	14	10 (4–22)
DFA	0.992	0.967 (O2)	15	23 (5–54)
pMP	0.977	0.908 (Oz)	15	6 (<1–19)

3.4 Sensitivity to Controlled Physiological Perturbation (Publication IV)

Publication IV assessed whether resting-state EEG exhibits short-term changes after a second dose of Comirnaty vaccine. The reference distribution and the two post-vaccination values in channel Fz are presented in Figure 8. Relative to this baseline, **Publication IV** showed that on day 5 after the second vaccine dose, the values of three measures lay outside the subject's usual fluctuation range after modified Bonferroni correction of the p values: GBP (10.81×10^3 μV^2; $p = 0.008$), SASI (0.214; $p = 0.013$), and HFD (1.288; $p = 0.01$). TBP and ABP were more than one standard deviation below the reference mean but were not significantly different after the correction, and BBP showed no change from the baseline. By day 12, no measure differed significantly from the reference distribution, and all values fell within the normal range.

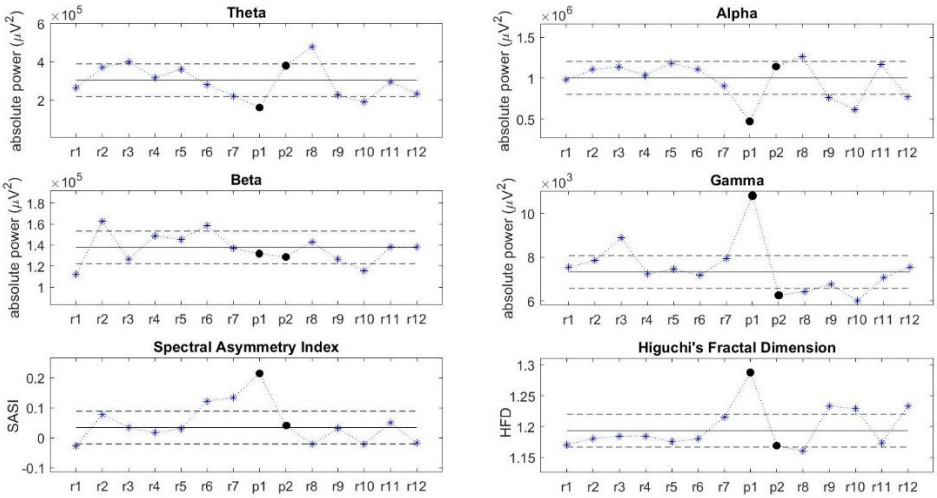

Figure 8. One-year longitudinal time courses of the powers in the theta, alpha, beta, and gamma frequency bands, and single-channel dynamics (SASI, HFD) showing the effect of a controlled physiological perturbation (Comirnaty vaccination) on these measures (n = 1). Asterisks indicate reference recordings (r1–r12) that were acquired four weeks apart regularly. The dots (p1, p2) show the values on the fifth and twelfth day after the vaccination. Straight and dashed lines represent the mean and standard deviation values of the twelve reference recordings (Publication IV).

4 Discussion

The overarching motivation of this thesis was the persistent gap between promising research findings and limited clinical uptake of resting-state EEG measures for common psychiatric disorders. Despite numerous reports of group-level EEG differences between clinical and control samples, these effects have not translated into robust tools for detecting or monitoring psychiatric health, as they have not been validated for individual-level use. In the Introduction, knowledge gaps in two main areas were highlighted that hinder the clinical adoption of EEG measures in evaluating psychiatric health: (1) the wide selection of diverse, unorganized EEG measures, whose mutual relationships and overlap are not well understood; and (2) substantial dispersion across individuals, which can obscure intra-individual change and limit individual-level interpretability.

To address these obstacles, the overall aim was to guide the selection of EEG measures for individualized monitoring. This aim was pursued in four steps: organizing the measure space (**Publication I**), introducing and testing a waveform stability measure in MDD (**Publication II**), characterizing long-term individual stability (**Publication III**), and demonstrating intra-individual sensitivity to a controlled perturbation (**Publication IV**). Across four studies aligned with the overall and specific aims of the thesis, converging evidence was obtained that common resting-state EEG measures share substantial information, that the new time-domain waveform stability measure provides added value for group separability in MDD, that selected nonlinear single-channel measures are temporally stable within individuals over one year, and that selected EEG measures remain sensitive to controlled physiological perturbation in brain physiology. Together, these findings guide the selection of EEG measures for individualized monitoring.

4.1 Complementarity in Resting-State EEG Measures (Publication I)

The first aim was to describe interrelationships among common resting-state EEG measures to assess complementarity and guide compact, informative measure selection. **Publication I** found that more than half of the pairwise relationships were significantly correlated, indicating substantial overlap in the information they capture and suggesting that several ostensibly distinct EEG measures capture partly the same information.

From a clinical perspective, this redundancy has clear implications. Combining many highly correlated measures can inflate apparent classifier performance in small samples without adding genuinely independent information, while increasing the risk of overfitting and hindering interpretability (Hosseinifard et al., 2013; Bachmann et al., 2018; Čukić, Stokić, Simić, et al., 2020; Wen et al., 2025). Therefore, the goal should be small but complementary panels rather than maximal feature sets.

Mental disorders can produce diverse EEG alterations across individuals; thus, clinically practical measures should be able to pick up a wide range of possible alterations. To compare measures on this criterion, the effectiveness index E was introduced in **Publication I**, which summarized the extent to which each measure was correlated with others (Figure 5). HFD, SL, MI, and ABP formed a high-effectiveness group that covered a wide range of other measures; GBP, MSC, LZC, and SASI contributed narrower, more specific information. Choosing one broad-coverage measure together with one or a few weakly correlated, more specific measures is a principled way to construct compact panels.

HFD emerged as an efficient core measure showing the highest effectiveness among all those compared. This aligns with numerous studies showing that HFD is a broadly sensitive measure of brain physiology, detecting subtle EEG changes related to depression (Ahmadlou et al., 2012; Bachmann et al., 2013, 2018; Hosseinifard et al., 2013; Akar et al., 2015b, 2015a; Čukić, Stokić, Radenković, et al., 2020; Greco et al., 2021) anxiety (Kawe et al., 2019), epilepsy (Khoa et al., 2012), sleep stages (Olejarczyk et al., 2022) and even gaming addiction (Hosseini et al., 2021). Its central position in the correlation structure makes it a strong reference against which to benchmark new measures.

At the same time, measures such as GBP and LZC, which demonstrated narrower specificity (lower effectiveness), carry relatively more independent information and can improve classification when paired with complementary features (Bachmann et al., 2018). GBP's low effectiveness largely reflects the small absolute contribution of gamma to the total EEG power spectrum, yet gamma-related changes have been linked to stress and cognitive demands (Minguillon et al., 2016; Schlink et al., 2017).

Overall, **Publication I** provides the first systematic map of inter-measure relationships in resting-state EEG and demonstrates that many widely used measures are mutually correlated rather than fully independent. This directly addresses the first obstacle identified in the Introduction—the wide selection of diverse, unorganized EEG measures, in which features are selected and parameterized ad hoc for similar clinical questions, yielding inconsistent results—and supports moving from large, redundant feature sets toward small, complementary panels.

4.2 Waveform Stability as a Measure to Detect MDD (Publication II)

The second aim was to develop and evaluate a new single-channel EEG measure of waveform stability and to test whether waveform stability carries clinically relevant information in MDD. Converging evidence indicates that psychiatric disorders, including MDD and schizophrenia, are characterized by abnormalities in neural synchrony and the temporal organization of oscillatory activity, particularly in alpha and gamma bands (Uhlhaas & Singer, 2006; Başar & Güntekin, 2013; Moran et al., 2019; Tsai et al., 2023; Han et al., 2025). In MDD, atypical alpha dynamics and altered rest–stimulus interactions have been reported (Fingelkurts et al., 2007; Newson & Thiagarajan, 2019; Wolff et al., 2019). These findings suggest that the stability and organization of ongoing rhythms are diagnostically relevant.

Existing single-channel measures, such as LZC, HFD, and DFA index sequence diversity, fractal complexity, or long-range correlations (Lempel & Ziv, 1976; Higuchi, 1988; Peng et al., 1995), but none explicitly quantify the temporal similarity of recurring waveform motifs. **Publication II** introduced the pMP method specifically to fill this gap by quantifying waveform-level temporal similarity (stability) independent of amplitude. Elevated pMP and HFD in the 66-subject resting-state sample showed increased waveform-level temporal irregularity and fractal complexity in MDD, aligning with prior reports of higher EEG complexity in depression (Lee et al., 2007; Y. Li et al., 2008; Bachmann et al., 2013, 2018; Akar et al., 2015b; Čukić, Stokić, Radenković, et al., 2020). For both measures, minima were observed over occipital sites (Figure 6), consistent with the strong, relatively regular alpha rhythm in eyes-closed rest. The fact that pMP was lowest where alpha is strongest and most stable supports its interpretation as a measure of timing regularity of oscillatory activity: more stable alpha frequency yields more frequent in-phase matches and lower pMP values. The higher pMP in MDD is compatible

with reports of greater variability in alpha peak frequency in depression (Wolff et al., 2019), suggesting more irregular timing of oscillatory bursts.

Regarding spatial extent, pMP showed broader group separation than HFD: pMP distinguished MDD from controls in all 30 channels, whereas HFD reached significance in 13 channels (43%), primarily in central and posterior regions. At the same time, HFD remains a strong benchmark, as prior work has reported considerable group-level discrimination in MDD (Ahmadlou et al., 2012; Bachmann et al., 2013, 2018; Hosseinifard et al., 2013; Akar et al., 2015b; Kesić & Spasić, 2016; Čukić, Stokić, Radenković, et al., 2020), and **Publication I** further showed its effectiveness in capturing a broad spectrum of disturbances in the brain. Additionally, single-channel classification accuracy reached 73% for pMP versus 67% for HFD in this sample—modest but notable given that HFD is a strong reference measure and that earlier work reporting slightly higher accuracies often used smaller cohorts and different classifiers (Hosseinifard et al., 2013; Bachmann et al., 2018; Greco et al., 2021).

Furthermore, the widespread and methodologically diverse selection of measures in EEG analysis is coupled with analyst-specified parameterization, which reduces comparability across sites and settings and complicates interpretability for practical use. In this regard, a key advantage of pMP is that it is parameter-independent in routine use: it does not require user-defined parameter tuning. It can be applied in a standardized form, thereby reducing analysts' degrees of freedom and improving cross-study and cross-site comparability.

Taken together, these findings support three conclusions. First, waveform stability, as quantified by pMP, is altered in resting state MDD and captures increased amplitude-invariant waveform instability and heightened dynamical lability, which are not fully reflected in power or generic complexity measures. Second, pMP offers a parameter-independent alternative to traditional complexity measures, reducing analysts' degrees of freedom and supporting cross-site comparability. Third, because pMP is z-normalized at the short segment level, it is less sensitive to absolute amplitude differences (e.g., skull thickness, electrode impedance) and also attenuates the influence of strong individual alpha amplitude, thereby reducing a key confound in cross-individual comparisons in psychiatric EEG. Thus, **Publication II** not only introduces a mechanistically motivated measure but also demonstrates that waveform stability provides added value over a widely used complexity measure, thereby directly addressing the second aim.

4.3 Temporal Stability and Person-Specific Baselines (Publication III)

For EEG measures to support individualized monitoring, they must show predictable intra-individual behaviour over time under stable conditions, enabling applicable baselines against which meaningful deviations can be detected. Accordingly, the third aim was to characterize long-term intra-individual temporal variability and inter-individual differences in single-channel EEG measures, to determine whether they can provide stable baselines for monitoring. In this context, **Publication III** supports baseline-referenced monitoring by demonstrating the long-term stability of several EEG measures, while also highlighting pronounced inter-individual differences that necessitate individualized baselines rather than group-derived norms.

The obtained ICCs indicate that commonly used band power and nonlinear measures can provide highly stable group-level estimates, while reliability can be somewhat reduced at peripheral temporal and frontotemporal sites, explained by residual tonic electromyographic (EMG) activity in muscle-prone regions (Whitham et al., 2007;

Urigüen & Garcia-Zapirain, 2015). This pattern is consistent with previous literature, which has also stated that the most reliable frequency bands are theta and alpha (Gudmundsson et al., 2007; Ip et al., 2018; Põld et al., 2021). However, ICCs reflect the combination of inter-individual and intra-individual variance and do not directly describe individual stability (Shrout & Fleiss, 1979; McGraw & Wong, 1996; Koo & Li, 2016). Therefore, **Publication III** complemented ICCs with inter-individual differentiation and intra-individual temporal stability. First, the pronounced inter-individual differentiation supports a central conclusion for individualized monitoring: even when a measure is generally stable, its baseline level can differ markedly across individuals. In practical terms, this means that group-level reference ranges are unlikely to be sufficiently specific for longitudinal interpretation at the individual level. Instead, the results support a personalized approach in which each person's EEG is treated as a distinct operating point, and deviations are evaluated relative to that person's own baseline rather than to population norms. This perspective also clarifies why measures can show excellent group-level reliability yet remain difficult to translate into universal decision thresholds, and it is consistent with the notion of EEG as a biometric-like fingerprint (Zhang et al., 2021; Lopez et al., 2023; Tatar, 2023). For deployment, this implies that monitoring pipelines must distinguish trait-like differences (inter-individual offsets) from state-like changes (intra-individual shifts). Without that separation, cross-sectional comparisons risk conflating normal individuality with clinically meaningful deviation.

Second, the analysis of intra-individual fluctuation ranges points to another requirement for individualized monitoring: a measure must not only have a person-specific baseline, but also a sufficiently predictable envelope of normal variation to support thresholding. From this perspective, stability is best understood as an individual tolerance range around the baseline—wide ranges reduce sensitivity to subtle change. In contrast, narrow, well-bounded ranges make deviations easier to interpret. **Publication III** highlights that these tolerance ranges differ substantially not only across measures but also across individuals, implying that a single, universal change criterion is unlikely to be appropriate. Instead, clinically usable alerting rules will need to be calibrated to each individual's expected fluctuation range. In practical terms, band-power measures—particularly TBP and ABP—are probably more responsive to clinically insignificant influences (e.g., arousal regulation, vigilance), leading to broader normal variability.

In contrast, several nonlinear measures appear to operate within narrower intra-individual ranges and may therefore be better suited as baseline-referenced indicators of change. This interpretation is compatible with prior work reporting comparatively greater long-term group-level stability for nonlinear measures than for band powers (Põld et al., 2021, 2023). In Põld et al. (2023), the relative changes for nonlinear measures were of similar magnitude to those observed here, whereas band power changes were larger in the present study, especially for TBP and ABP. Notably, Põld et al. (2023)directly contrasted two sessions three years apart, whereas the present analysis quantified the directly contrasted two sessions three years apart, whereas the present analysis quantified the maximal relative deviation from a participant's annual mean; in principle, such deviation-from-mean values should be smaller than two-point contrasts. However, with only two observations, the available information is too limited to characterize true intra-individual variability. By sampling monthly over a year, the current design captures a more realistic range of intra-individual fluctuations.

As previous literature has only scarcely described temporal stability and even then only at the group level, there was no knowledge of how stable EEG measures are at the

individual level. The results from **Publication III** highlighted inter-individual heterogeneity: substantial differences in absolute values and in individual ranges. However, most participants showed only modest oscillations around their personal mean, especially for the nonlinear measures, whereas their band-power values (especially in the lower-frequency bands) could vary more widely from month to month. A few individuals nevertheless exhibited year-scale fluctuation magnitudes in certain measures that matched or even exceeded the group's cross-sectional distribution (Figure 7), an effect more pronounced for band-power measures. This suggests that band power might be more susceptible to day-to-day physiological or psychological fluctuations, whereas nonlinear dynamics capture more invariant traits of the brain.

Even with careful control of recording conditions and electrode placement, intrinsic physiology and lifestyle still introduce variance: individual differences in hormones, neuroanatomy, and brain physiology, as well as sleep, diet, and activity, can modulate EEG stability over time (Hoffman & Polich, 1998). In this light, the wide ranges observed for subject 4, despite being healthy by self-report, may reflect transient mental-state fluctuations or prodromal changes not yet consciously perceived, as psychological states and disorders are known to alter EEG patterns, as demonstrated in prior group studies (Accardo et al., 1997; Hinrikus et al., 2009; Ahmadlou et al., 2012; Bachmann et al., 2013, 2018; Mumtaz et al., 2015; Newson & Thiagarajan, 2019). To clarify this, additional contextual data for subject 4 (e.g., sleep, stress, medication, and health status) should be analyzed to rule out or support reasonable explanations for the unusually high variability. Accordingly, identifying whether variability arises from intrinsic traits, temporary states, or early pathological processes is essential for tailoring analysis strategies and setting person-specific baselines.

Because EEG is highly individual, the ability to predict each person's normal variability range is essential. Establishing such ranges through numerous recordings at the population scale would be prohibitively costly and time-consuming. Although the wider adoption of wearable devices may soon provide suitable baseline data, interim approaches are needed to estimate the expected variability for EEG measures. This requires identifying the individual-level key factors that influence variability in the healthy state and using them to construct person-specific variability profiles that separate disorder-related change from normal neuropsychological fluctuation. Practical heuristics could be developed to flag high variability profiles without prolonged tracking, thereby improving efficiency.

Taken together, **Publication III** supports three key points. First, nonlinear resting-state EEG measures exhibit high trait-like stability, making them suitable to establish person-specific baselines. Second, nonlinear measures, particularly HFD and pMP, exhibit higher intra-individual temporal stability than band powers, reinforcing their suitability as anchors for longitudinal monitoring. Third, even when measures are stable on average, global thresholds are problematic because both baseline magnitudes and natural fluctuation ranges vary substantially between individuals; therefore, person-specific reference ranges are required. Notably, pMP combines strong intra-individual stability (**Publication III**) with demonstrated group-level sensitivity (**Publication II**), supporting its potential to be informative for individualized, baseline-referenced monitoring. The outcome of **Publication III** directly addresses the second obstacle identified in the Introduction—dispersion across individuals—by showing that, when quantified appropriately, intra-individual stability is robust enough to support baseline-referenced interpretation.

4.4 Sensitivity to Controlled Physiological Perturbation (Publication IV)

Temporal stability alone is not sufficient for a practical monitoring measure; it must also be sensitive to clinically meaningful change in brain state. Therefore, the fourth aim was to verify whether EEG measures are sensitive to controlled perturbations in brain physiology within an individual. The findings from **Publication IV** indicate that EEG measures that are stable under typical conditions can nevertheless show clear, intra-individual deviations when physiology is transiently perturbed by a mild systemic stressor, supporting their potential utility for individualized, baseline-referenced monitoring.

Importantly, most self-reported side effects had resolved by day 5, suggesting that at this stage the EEG deviations likely reflected physiological processes associated with the immune response rather than discomfort or fatigue due solely to side effects. The normalization of the EEG by day 12 further indicates that these changes were transient, physiologically meaningful perturbations, not random fluctuations. Consistent with **Publication I**, in which HFD demonstrated the capability to capture a wide range of disturbances in brain function, HFD also proved sensitive to immune response–related changes in this setting. The pattern—modestly reduced TBP and ABP, significantly increased higher-frequency content (GBP) and elevated complexity (HFD)—is consistent with earlier reports that acute stress and cognitive load are associated with suppressed low-frequency power and enhanced beta and gamma activity (Al-Shargie et al., 2016; Minguillon et al., 2016; Schlink et al., 2017), as well as increased complexity (Ahmadlou et al., 2012; Bachmann et al., 2013; Akar et al., 2015b; Kawe et al., 2019; Čukić, Stokić, Radenković, et al., 2020). Although SASI and GBP had narrower reach in terms of effectiveness, prior work indicates that theta, beta, and gamma band activity, which is combined in SASI, can be sensitive to various stressors (Suhhova et al., 2011; Saifudinova et al., 2015; Põld et al., 2018), supporting SASI and GBP as complementary measures for detecting stress-related spectral shifts toward higher frequencies. Within this framework, increased complexity and a shift toward higher frequencies constitute complementary signatures of a transiently perturbed state that normalizes as the immune response abates.

Therefore, the finding in **Publication IV** provides proof of principle that the same measures that are stable over long periods can detect short-lived, physiologically relevant changes in a single individual. It also illustrates the importance of contextual information: without knowledge of recent vaccination, such deviations could be misinterpreted as a clinically concerning change. Any clinical deployment will need to integrate EEG-derived measures with details about recent stressors, illnesses, sleep patterns, and medication use.

4.5 From Measure Selection to Baseline-Referenced Monitoring

Across the four aims, this thesis guides the selection of EEG measures for individualized monitoring. The first aim showed that commonly used measures are strongly interrelated and partly redundant, but that this structure can be exploited. By mapping correlations and defining an effectiveness index, it became possible to identify broadly informative anchor measures and more specific, weakly correlated measures that can be combined into small, complementary, easy-to-interpret panels instead of large, ad hoc feature sets that might be prone to overfitting.

The second aim added a mechanistically motivated measure (pMP), which quantifies waveform self-similarity with reduced dependence on amplitude. Benchmarking against HFD in MDD indicated that pMP can modestly exceed a well-established nonlinear reference and yield more spatially uniform group separation, and support the clinical relevance of waveform stability as an additional aspect of resting-state EEG alteration.

The third aim demonstrated that nonlinear single-channel measures—especially HFD and pMP—are highly stable within individuals over one year, while both measure values and fluctuation ranges differ substantially between individuals, supporting their use as anchors for person-specific baselines.

The fourth aim showed that selected measures remain sensitive to a controlled physiological perturbation (vaccination) and return to baseline thereafter, indicating that stability under steady conditions can coexist with responsiveness to meaningful change.

Taken together, these steps show how resting-state EEG measures can be organized, enriched, and characterized, enabling a small set of complementary measures to support individualized, baseline-referenced monitoring. Potential applications include early detection of change, tracking progression or recovery, and evaluating treatment effects at the individual level. Further research and validation in clinical populations are needed, but the principles and empirical findings laid out here provide a strong foundation for the continued development of personalized EEG biomarkers.

4.6 Limitations

Some limitations should be noted. First, sample sizes and designs constrain generalizability. The cross-sectional studies (n = 80 and n = 66) are adequate for mapping inter-measure relationships and demonstrating MDD–control differences, but do not support robust stratification by age or sex. The longitudinal study of nine healthy men illustrates overall stability trends but does not allow characterization of the population distribution of EEG stability profiles or analysis by age and sex. The controlled perturbation study examined a short-term perturbation after vaccination, suggesting possible sensitivity to change. Still, as a single-subject case study, it cannot establish how broadly sensitive these measures are.

Second, the set of EEG measures was limited and not fully consistent across the thesis. Only a subset of potentially informative measures was examined; therefore, the conclusions do not span the whole EEG feature space and may be biased toward the selected features. In addition, pMP was validated later in the project and is therefore absent from the inter-measure correlation and effectiveness mapping in healthy adults, as well as from the vaccination case study. Consequently, the position of pMP within the broader measure network—including its reach, complementarity, and sensitivity to controlled perturbations in brain physiology at the individual level—remains unresolved. Future work should therefore employ larger and more diverse samples spanning age (He et al., 2021) and sex (Langrová et al., 2012), explicitly model demographic effects, and include pMP. Longitudinal designs with controlled perturbations in larger cohorts will be needed to jointly characterize long-term stability in health and the generalizable sensitivity of these measures to meaningful change.

Conclusions

This thesis demonstrates that resting-state EEG can support individualized brain-state monitoring when measures are chosen for stability, complementarity, and sensitivity. It also develops and validates a parameter-independent waveform similarity measure that is reproducible through robustness and sensitive to MDD.

The main findings of the thesis are:

- Common resting-state EEG measures are strongly interrelated and partly redundant. Mapping correlations among measures showed substantial informational overlap, but also revealed a structure that allows the construction of small, complementary panels rather than large, redundant feature sets.
- Nonlinear single-channel measures, especially HFD and pMP, are strong core candidates for monitoring clinically relevant changes in brain physiology. HFD emerged as a broadly informative backbone measure, while the newly introduced pMP modestly exceeded HFD in MDD–control discrimination and provided more spatially uniform effects across the scalp.
- Nonlinear measures can anchor individualized EEG profiles, showing strong long-term intra-individual stability; however, both stability (fluctuation range) and baseline magnitude vary substantially across individuals, reinforcing the need for person-specific baselines and reference ranges rather than global thresholds.
- Measures that are stable under steady conditions can still be sensitive to changes in neurophysiology, showing transient, physiologically meaningful deviations in response to a controlled systemic stressor (vaccination) and a subsequent return toward baseline—supporting the principle of stable in health, responsive to perturbation.

Together, these findings outline a practical pathway to individual-level EEG monitoring: build small complementary feature sets that include robust, stable, and sensitive measures; establish person-specific baselines and interpret subsequent EEG measure values relative to the individual, not population averages.

References

Accardo, A., Affinito, M., Carrozzi, M., & Bouquet, F. (1997). Use of the fractal dimension for the analysis of electroencephalographic time series. *Biological Cybernetics*, *77*(5), 339–350. https://doi.org/10.1007/s004220050394

Ahmadlou, M., Adeli, H., & Adeli, A. (2012). Fractality analysis of frontal brain in major depressive disorder. *International Journal of Psychophysiology*, *85*(2), 206–211. https://doi.org/10.1016/j.ijpsycho.2012.05.001

Akar, S. A., Kara, S., Agambayev, S., & Bilgiç, V. (2015a). Nonlinear analysis of EEG in major depression with fractal dimensions. *In 2015 37th Annual International Conference of the IEEE Engineering in Medicine and Biology Society (EMBC)*, 7410–7413. https://doi.org/10.1109/EMBC.2015.7320104

Akar, S. A., Kara, S., Agambayev, S., & Bilgiç, V. (2015b). Nonlinear analysis of EEGs of patients with major depression during different emotional states. *Computers in Biology and Medicine*, *67*, 49–60. https://doi.org/10.1016/j.compbiomed.2015.09.019

Al-Shargie, F., Kiguchi, M., Badruddin, N., Dass, S. C., Hani, A. F. M., & Tang, T. B. (2016). Mental stress assessment using simultaneous measurement of EEG and fNIRS. *Biomedical Optics Express*, *7*(10), 3882–3898. https://doi.org/10.1364/BOE.7.003882

Aluoja, A., Shlik, J., Vasar, V., Luuk, K., & Leinsalu, M. (1999). Development and psychometric properties of the Emotional State Questionnaire, a self-report questionnaire for depression and anxiety. *Nordic Journal of Psychiatry*, *53*(6), 443–449. https://doi.org/10.1080/080394899427692

Arns, M., Conners, C. K., & Kraemer, H. C. (2013). A decade of EEG theta/beta ratio research in ADHD: A meta-analysis. *Journal of Attention Disorders*, *17*(5), 374–383. https://doi.org/10.1177/1087054712460087

Bachmann, M., Lass, J., Suhhova, A., & Hinrikus, H. (2013). Spectral asymmetry and Higuchi's fractal dimension measures of depression electroencephalogram. *Computational and Mathematical Methods in Medicine*, *2013*. https://doi.org/10.1155/2013/251638

Bachmann, M., Päeske, L., Kalev, K., Aarma, K., Lehtmets, A., Ööpik, P., Lass, J., & Hinrikus, H. (2018). Methods for classifying depression in single channel EEG using linear and nonlinear signal analysis. *Computer Methods and Programs in Biomedicine*, *155*, 11–17. https://doi.org/10.1016/j.cmpb.2017.11.023

Baillet, S. (2017). Magnetoencephalography for brain electrophysiology and imaging. *Nature Neuroscience*, *20*(3), 327–339. https://doi.org/10.1038/nn.4504

Başar, E., & Güntekin, B. (2013). Review of delta, theta, alpha, beta, and gamma response oscillations in neuropsychiatric disorders. In E. Başar, C. Başar-Eroĝlu, A. Özerdem, P. M. Rossini, & G. G. Yener (Eds.), *Supplements to Clinical Neurophysiology* (Vol. 62, pp. 303–341). Elsevier. https://doi.org/10.1016/B978-0-7020-5307-8.00019-3

Berger, H. (1929). Über das elektrenkephalogramm des menschen. *Archiv Für Psychiatrie Und Nervenkrankheiten*, *87*(1), 527–570. https://doi.org/10.1007/BF01797193

Bonita, J. D., Ambolode, L. C. C., Rosenberg, B. M., Cellucci, C. J., Watanabe, T. A. A., Rapp, P. E., & Albano, A. M. (2014). Time domain measures of inter-channel EEG correlations: a comparison of linear, nonparametric and nonlinear measures. *Cognitive Neurodynamics*, *8*(1), 1–15. https://doi.org/10.1007/s11571-013-9267-8

Brötzner, C. P., Klimesch, W., Doppelmayr, M., Zauner, A., & Kerschbaum, H. H. (2014). Resting state alpha frequency is associated with menstrual cycle phase, estradiol and use of oral contraceptives. *Brain Research*, *1577*, 36–44. https://doi.org/10.1016/j.brainres.2014.06.034

Buzsáki, G. (2006). *Rhythms of the brain*. Oxford University Press. https://doi.org/10.1093/acprof:oso/9780195301069.001.0001

Buzsáki, G., Anastassiou, C. A., & Koch, C. (2012). The origin of extracellular fields and currents — EEG, ECoG, LFP and spikes. *Nature Reviews Neuroscience*, *13*(6), 407–420. https://doi.org/10.1038/nrn3241

Cannon, R. L., Baldwin, D. R., Shaw, T. L., Diloreto, D. J., Phillips, S. M., Scruggs, A. M., & Riehl, T. C. (2012). Reliability of quantitative EEG (qEEG) measures and LORETA current source density at 30 days. *Neuroscience Letters*, *518*(1), 27–31. https://doi.org/10.1016/j.neulet.2012.04.035

Chen, W., Cai, Y., Li, A., Jiang, K., & Su, Y. (2024). MDD brain network analysis based on EEG functional connectivity and graph theory. *Heliyon*, *10*(17), e36991. https://doi.org/10.1016/j.heliyon.2024.e36991

Čukić, M., Stokić, M., Radenković, S., Ljubisavljević, M., Simić, S., & Savić, D. (2020). Nonlinear analysis of EEG complexity in episode and remission phase of recurrent depression. *International Journal of Methods in Psychiatric Research*, *29*(2), e1816. https://doi.org/10.1002/mpr.1816

Čukić, M., Stokić, M., Simić, S., & Pokrajac, D. (2020). The successful discrimination of depression from EEG could be attributed to proper feature extraction and not to a particular classification method. *Cognitive Neurodynamics*, *14*(4), 443–455. https://doi.org/10.1007/s11571-020-09581-x

Domingos, C., Więcławski, W., Frycz, S., Wojcik, M., Jáni, M., Dudzińska, O., Adamczyk, P., & Ros, T. (2025). Functional connectivity in chronic schizophrenia: An EEG resting-state study with corrected imaginary phase-locking. *Brain and Behavior*, *15*(3), e70370. https://doi.org/10.1002/brb3.70370

Dünki, R. M., Schmid, G. B., & Stassen, H. H. (2000). Intraindividual specificity and stability of human EEG: Comparing a linear vs a nonlinear approach. *Methods of Information in Medicine*, *39*(1), 78–82. https://doi.org/10.1055/s-0038-1634249

Dunn, O. J. (1964). Multiple comparisons using rank sums. *Technometrics*, *6*(3), 241–252. https://doi.org/10.1080/00401706.1964.10490181

Ettman, C. K., Abdalla, S. M., Wang, R., Rosenberg, S. B., & Galea, S. (2025). Generalized anxiety disorder in low-resourced adults: a nationally representative, longitudinal cohort study across the COVID-19 pandemic. *American Journal of Epidemiology*, *194*(3), 755–765. https://doi.org/10.1093/aje/kwae270

Fernández, A., Gómez, C., Hornero, R., & López-Ibor, J. J. (2013). Complexity and schizophrenia. *Progress in Neuro-Psychopharmacology and Biological Psychiatry*, *45*, 267–276. https://doi.org/10.1016/j.pnpbp.2012.03.015

Ferrari, A. J., Santomauro, D. F., Mantilla Herrera, A. M., Shadid, J., Ashbaugh, C., Erskine, H. E., Charlson, F. J., Degenhardt, L., Scott, J. G., McGrath, J. J., Allebeck, P., Benjet, C., Breitborde, N. J. K., Brugha, T., Dai, X., Dandona, L., Dandona, R., Fischer, F., Haagsma, J. A., … Whiteford, H. A. (2022). Global, regional, and national burden of 12 mental disorders in 204 countries and territories, 1990–2019: a systematic analysis for the Global Burden of Disease Study 2019. *The Lancet Psychiatry*, *9*(2), 137–150. https://doi.org/10.1016/S2215-0366(21)00395-3

Fingelkurts, A. A., Fingelkurts, A. A., Rytsälä, H., Suominen, K., Isometsä, E., & Kähkönen, S. (2007). Impaired functional connectivity at EEG alpha and theta frequency bands in major depression. *Human Brain Mapping*, *28*(3), 247–261. https://doi.org/10.1002/hbm.20275

Fraser, A. M., & Swinney, H. L. (1986). Independent coordinates for strange attractors from mutual information. *Physical Review A*, *33*(2), 1134–1140. https://doi.org/10.1103/PhysRevA.33.1134

Furlong, S., Cohen, J. R., Hopfinger, J., Snyder, J., Robertson, M. M., & Sheridan, M. A. (2021). Resting-state EEG connectivity in young children with ADHD. *Journal of Clinical Child & Adolescent Psychology*, *50*(6), 746–762. https://doi.org/10.1080/15374416.2020.1796680

Gasser, T., Bächer, P., & Steinberg, H. (1985). Test-retest reliability of spectral parameters of the EEG. *Electroencephalography and Clinical Neurophysiology*, *60*(4), 312–319. https://doi.org/10.1016/0013-4694(85)90005-7

Gevins, A., McEvoy, L. K., Smith, M. E., Chan, C. S., Sam-Vargas, L., Baum, C., & Ilan, A. B. (2012). Long-term and within-day variability of working memory performance and EEG in individuals. *Clinical Neurophysiology*, *123*(7), 1291–1299. https://doi.org/10.1016/j.clinph.2011.11.004

Gloss, D., Varma, J. K., Pringsheim, T., & Nuwer, M. R. (2016). Practice advisory: The utility of EEG theta/beta power ratio in ADHD diagnosis. *Neurology*, *87*(22), 2375–2379. https://doi.org/10.1212/WNL.0000000000003265

Greco, C., Matarazzo, O., Cordasco, G., Vinciarelli, A., Callejas, Z., & Esposito, A. (2021). Discriminative Power of EEG-Based Biomarkers in Major Depressive Disorder: A Systematic Review. *IEEE Access*, *9*, 112850–112870. https://doi.org/10.1109/ACCESS.2021.3103047

Gudmundsson, S., Runarsson, T. P., Sigurdsson, S., Eiriksdottir, G., & Johnsen, K. (2007). Reliability of quantitative EEG features. *Clinical Neurophysiology*, *118*(10), 2162–2171. https://doi.org/10.1016/j.clinph.2007.06.018

Hamilton, M. (1960). A rating scale for depression. *Journal of Neurology, Neurosurgery & Psychiatry*, *23*(1), 56–62. https://doi.org/10.1136/jnnp.23.1.56

Han, C., Wang, B., Peng, X., Li, M., Zhang, Z., Yao, C., Tu, M., Chen, X., Zhou, J., Wang, C., & Zhao, X. (2025). Distinct oscillatory mechanisms in low and high alpha-band activities for screening and potential treatment of schizophrenia. *Translational Psychiatry*, *15*(1), 210. https://doi.org/10.1038/s41398-025-03426-z

He, M., Liu, F., Nummenmaa, A., Hämäläinen, M., Dickerson, B. C., & Purdon, P. L. (2021). Age-related EEG power reductions cannot be explained by changes of the conductivity distribution in the head due to brain atrophy. *Frontiers in Aging Neuroscience*, *13*, 632310. https://doi.org/10.3389/fnagi.2021.632310

Higuchi, T. (1988). Approach to an irregular time series on the basis of the fractal theory. *Physica D: Nonlinear Phenomena*, *31*(2), 277–283. https://doi.org/10.1016/0167-2789(88)90081-4

Hinrikus, H., Suhhova, A., Bachmann, M., Aadamsoo, K., Võhma, Ü., Lass, J., & Tuulik, V. (2009). Electroencephalographic spectral asymmetry index for detection of depression. *Medical & Biological Engineering & Computing*, *47*(12), 1291–1299. https://doi.org/10.1007/s11517-009-0554-9

Hoffman, L. D., & Polich, J. (1998). EEG, ERPs and food consumption. *Biological Psychology*, *48*(2), 139–151. https://doi.org/10.1016/S0301-0511(98)00010-6

Höller, Y., Jónsdóttir, S. T., Hannesdóttir, A. H., & Ólafsson, R. P. (2022). EEG-responses to mood induction interact with seasonality and age. *Frontiers in Psychiatry*, *13*. https://doi.org/10.3389/fpsyt.2022.950328

Hosseini, Z., Delpazirian, R., Lanjanian, H., Salarifar, M., & Hassani-Abharian, P. (2021). Computer gaming and physiological changes in the brain: An insight from qEEG complexity analysis. *Applied Psychophysiology and Biofeedback*, *46*(3), 301–308. https://doi.org/10.1007/s10484-021-09518-y

Hosseinifard, B., Moradi, M. H., & Rostami, R. (2013). Classifying depression patients and normal subjects using machine learning techniques and nonlinear features from EEG signal. *Computer Methods and Programs in Biomedicine*, *109*(3), 339–345. https://doi.org/10.1016/j.cmpb.2012.10.008

Hu, S., Lai, Y., Valdes-Sosa, P. A., Bringas-Vega, M. L., & Yao, D. (2018). How do reference montage and electrodes setup affect the measured scalp EEG potentials? *Journal of Neural Engineering*, *15*(2), 026013. https://doi.org/10.1088/1741-2552/aaa13f

Ibáñez-Molina, A., Crespo Cobo, Y., Soriano Peña, M. F., Iglesias-Parro, S., & Ruiz de Miras, J. (2024). Mutual information of multiple rhythms in schizophrenia. *Brain Structure and Function*, *229*(2), 285–295. https://doi.org/10.1007/s00429-023-02744-6

Ibáñez-Molina, A. J., Soriano, M. F., & Iglesias-Parro, S. (2020). Mutual information of multiple rhythms for EEG signals. *Frontiers in Neuroscience*, *14*, 574796. https://doi.org/10.3389/fnins.2020.574796

Imperatori, L. S., Betta, M., Cecchetti, L., Canales-Johnson, A., Ricciardi, E., Siclari, F., Pietrini, P., Chennu, S., & Bernardi, G. (2019). EEG functional connectivity metrics wPLI and wSMI account for distinct types of brain functional interactions. *Scientific Reports*, *9*(1), 8894. https://doi.org/10.1038/s41598-019-45289-7

Ip, C.-T., Ganz, M., Ozenne, B., Sluth, L. B., Gram, M., Viardot, G., l'Hostis, P., Danjou, P., Knudsen, G. M., & Christensen, S. R. (2018). Pre-intervention test-retest reliability of EEG and ERP over four recording intervals. *International Journal of Psychophysiology*, *134*, 30–43. https://doi.org/10.1016/j.ijpsycho.2018.09.007

Kaiser, A. K., Doppelmayr, M., & Iglseder, B. (2018). Electroencephalogram alpha asymmetry in geriatric depression: Valid or vanished? *Zeitschrift Für Gerontologie Und Geriatrie*, *51*(2), 200–205. https://doi.org/10.1007/s00391-016-1108-z

Kam, J. W. Y., Bolbecker, A. R., O'Donnell, B. F., Hetrick, W. P., & Brenner, C. A. (2013). Resting state EEG power and coherence abnormalities in bipolar disorder and schizophrenia. *Journal of Psychiatric Research*, *47*(12), 1893–1901. https://doi.org/10.1016/j.jpsychires.2013.09.009

Kawe, T. N. J., Shadli, S. M., & McNaughton, N. (2019). Higuchi's fractal dimension, but not frontal or posterior alpha asymmetry, predicts PID-5 anxiousness more than depressivity. *Scientific Reports*, *9*(1), 19666. https://doi.org/10.1038/s41598-019-56229-w

Kesić, S., & Spasić, S. Z. (2016). Application of Higuchi's fractal dimension from basic to clinical neurophysiology: A review. *Computer Methods and Programs in Biomedicine*, *133*, 55–70. https://doi.org/10.1016/j.cmpb.2016.05.014

Khoa, T. Q. D., Ha, V. Q., & Toi, V. Van. (2012). Higuchi fractal properties of onset epilepsy electroencephalogram. *Computational and Mathematical Methods in Medicine*, 461426. https://doi.org/10.1155/2012/461426

Kim, D.-J., Bolbecker, A. R., Howell, J., Rass, O., Sporns, O., Hetrick, W. P., Breier, A., & O'Donnell, B. F. (2013). Disturbed resting state EEG synchronization in bipolar disorder: A graph-theoretic analysis. *NeuroImage: Clinical*, *2*, 414–423. https://doi.org/10.1016/j.nicl.2013.03.007

Knott, V., Mahoney, C., Kennedy, S., & Evans, K. (2001). EEG power, frequency, asymmetry and coherence in male depression. *Psychiatry Research: Neuroimaging*, *106*(2), 123–140. https://doi.org/10.1016/S0925-4927(00)00080-9

Kondacs, A., & Szabó, M. (1999). Long-term intra-individual variability of the background EEG in normals. *Clinical Neurophysiology*, *110*(10), 1708–1716. https://doi.org/10.1016/S1388-2457(99)00122-4

Koo, T. K., & Li, M. Y. (2016). A guideline of selecting and reporting intraclass correlation coefficients for reliability research. *Journal of Chiropractic Medicine*, *15*(2), 155–163. https://doi.org/10.1016/j.jcm.2016.02.012

Kruskal, W. H., & Wallis, W. A. (1952). Use of ranks in one-criterion variance analysis. *Journal of the American Statistical Association*, *47*(260), 583–621. https://doi.org/10.1080/01621459.1952.10483441

Langrová, J., Kremláček, J., Kuba, M., Kubová, Z., & Szanyi, J. (2012). Gender impact on electrophysiological activity of the brain. *Physiological Research*, *61(Suppl. 2)*, S119–S127. https://doi.org/10.33549/physiolres.932421

Lee, J. S., Yang, B. H., Lee, J. H., Choi, J. H., Choi, I. G., & Kim, S. B. (2007). Detrended fluctuation analysis of resting EEG in depressed outpatients and healthy controls. *Clinical Neurophysiology*, *118*(11), 2489–2496. https://doi.org/10.1016/j.clinph.2007.08.001

Lempel, A., & Ziv, J. (1976). On the complexity of finite sequences. *IEEE Transactions on Information Theory*, *22*(1), 75–81. https://doi.org/10.1109/TIT.1976.1055501

Leuchter, A. F., Cook, I. A., Hunter, A. M., Cai, C., & Horvath, S. (2012). Resting-state quantitative electroencephalography reveals increased neurophysiologic connectivity in depression. *PLoS ONE*, *7*(2), e32508. https://doi.org/10.1371/journal.pone.0032508

Li, Q., Coulson Theodorsen, M., Konvalinka, I., Eskelund, K., Karstoft, K.-I., Bo Andersen, S., & Andersen, T. S. (2022). Resting-state EEG functional connectivity predicts post-traumatic stress disorder subtypes in veterans. *Journal of Neural Engineering*, *19*(6), 066005. https://doi.org/10.1088/1741-2552/ac9aaf

Li, Y., Kang, C., Qu, X., Zhou, Y., Wang, W., & Hu, Y. (2016). Depression-related brain connectivity analyzed by EEG event-related phase synchrony measure. *Frontiers in Human Neuroscience*, *10*. https://doi.org/10.3389/fnhum.2016.00477

Li, Y., Tong, S., Liu, D., Gai, Y., Wang, X., Wang, J., Qiu, Y., & Zhu, Y. (2008). Abnormal EEG complexity in patients with schizophrenia and depression. *Clinical Neurophysiology*, *119*(6), 1232–1241. https://doi.org/10.1016/j.clinph.2008.01.104

Liu, W., Zhou, B., Li, G., & Luo, X. (2024). Enhanced diagnostics for generalized anxiety disorder: Leveraging differential channel and functional connectivity features based on frontal EEG signals. *Scientific Reports*, *14*(1), 22789. https://doi.org/10.1038/s41598-024-73615-1

Lopez, K. L., Monachino, A. D., Vincent, K. M., Peck, F. C., & Gabard-Durnam, L. J. (2023). Stability, change, and reliable individual differences in electroencephalography measures: A lifespan perspective on progress and opportunities. *NeuroImage*, *275*, 120116. https://doi.org/10.1016/j.neuroimage.2023.120116

Lord, B., & Allen, J. J. B. (2023). Evaluating EEG complexity metrics as biomarkers for depression. *Psychophysiology*, *60*(8), e14274. https://doi.org/10.1111/psyp.14274

Mahato, S., & Paul, S. (2019). Electroencephalogram (EEG) signal analysis for diagnosis of major depressive disorder (MDD): A review. In V. Nath & J. K. Mandal (Eds.), *Nanoelectronics, Circuits and Communication Systems* (Vol. 511, pp. 323–335). Springer. https://doi.org/10.1007/978-981-13-0776-8_30

McGraw, K. O., & Wong, S. P. (1996). Forming inferences about some intraclass correlation coefficients. *Psychological Methods*, *1*(1), 30–46. https://doi.org/10.1037/1082-989X.1.1.30

Minguillon, J., Lopez-Gordo, M. A., & Pelayo, F. (2016). Stress assessment by prefrontal relative gamma. *Frontiers in Computational Neuroscience*, *10*. https://doi.org/10.3389/fncom.2016.00101

Moran, J. K., Michail, G., Heinz, A., Keil, J., & Senkowski, D. (2019). Long-range temporal correlations in resting state beta oscillations are reduced in schizophrenia. *Frontiers in Psychiatry*, *10*. https://doi.org/10.3389/fpsyt.2019.00517

Mueen, A., Zhong, S., Zhu, Y., Yeh, M., Kamgar, K., Viswanathan, K., Gupta, C., & Keogh, E. (2022). *The fastest similarity search algorithm for time series subsequences under Euclidean distance*. http://www.cs.unm.edu/~mueen/FastestSimilaritySearch.html

Mumtaz, W., Malik, A. S., Ali, S. S. A., Yasin, M. A. M., & Amin, H. (2015). Detrended fluctuation analysis for major depressive disorder. *In 2015 37th Annual International Conference of the IEEE Engineering in Medicine and Biology Society (EMBC)*, 4162–4165. https://doi.org/10.1109/EMBC.2015.7319311

Na, S. H., Jin, S.-H., Kim, S. Y., & Ham, B.-J. (2002). EEG in schizophrenic patients: Mutual information analysis. *Clinical Neurophysiology*, *113*(12), 1954–1960. https://doi.org/10.1016/S1388-2457(02)00197-9

Newson, J. J., & Thiagarajan, T. C. (2019). EEG frequency bands in psychiatric disorders: A review of resting state studies. *Frontiers in Human Neuroscience*, *12*. https://doi.org/10.3389/fnhum.2018.00521

Niedermeyer, Ernst., & Lopes da Silva, F. H. (2005). *Electroencephalography: Basic principles, clinical applications, and related fields* (5th ed.). Lippincott Williams & Wilkins.

Nolte, G., Bai, O., Wheaton, L., Mari, Z., Vorbach, S., & Hallett, M. (2004). Identifying true brain interaction from EEG data using the imaginary part of coherency. *Clinical Neurophysiology*, *115*(10), 2292–2307. https://doi.org/10.1016/j.clinph.2004.04.029

Olbrich, S., Tränkner, A., Chittka, T., Hegerl, U., & Schönknecht, P. (2014). Functional connectivity in major depression: Increased phase synchronization between frontal cortical EEG-source estimates. *Psychiatry Research - Neuroimaging*, *222*(1–2), 91–99. https://doi.org/10.1016/j.pscychresns.2014.02.010

Olejarczyk, E., Gotman, J., & Frauscher, B. (2022). Region-specific complexity of the intracranial EEG in the sleeping human brain. *Scientific Reports*, *12*(1), 451. https://doi.org/10.1038/s41598-021-04213-8

Päeske, L., Bachmann, M., Põld, T., de Oliveira, S. P. M., Lass, J., Raik, J., & Hinrikus, H. (2018). Surrogate data method requires end-matched segmentation of electroencephalographic signals to estimate non-linearity. *Frontiers in Physiology*, *9*, 1350. https://doi.org/10.3389/fphys.2018.01350

Päeske, L., Hinrikus, H., Lass, J., Raik, J., & Bachmann, M. (2020). Negative correlation between functional connectivity and small-worldness in the alpha frequency band of a healthy brain. *Frontiers in Physiology*, *11*, 910. https://doi.org/10.3389/fphys.2020.00910

Parvizi, J., & Kastner, S. (2018). Promises and limitations of human intracranial electroencephalography. *Nature Neuroscience*, *21*(4), 474–483. https://doi.org/10.1038/s41593-018-0108-2

Patel, V., Saxena, S., Lund, C., Thornicroft, G., Baingana, F., Bolton, P., Chisholm, D., Collins, P. Y., Cooper, J. L., Eaton, J., Herrman, H., Herzallah, M. M., Huang, Y., Jordans, M. J. D., Kleinman, A., Medina-Mora, M. E., Morgan, E., Niaz, U., Omigbodun, O., … Unützer, J. (2018). The Lancet Commission on global mental health and sustainable development. *The Lancet*, *392*(10157), 1553–1598. https://doi.org/10.1016/S0140-6736(18)31612-X

Peng, C.-K., Buldyrev, S. V., Havlin, S., Simons, M., Stanley, H. E., & Goldberger, A. L. (1994). Mosaic organization of DNA nucleotides. *Physical Review E*, *49*(2), 1685–1689. https://doi.org/10.1103/PhysRevE.49.1685

Peng, C.-K., Havlin, S., Stanley, H. E., & Goldberger, A. L. (1995). Quantification of scaling exponents and crossover phenomena in nonstationary heartbeat time series. *Chaos: An Interdisciplinary Journal of Nonlinear Science*, *5*(1), 82–87. https://doi.org/10.1063/1.166141

Perera, M. P. N., Gotsis, E. S., Bailey, N. W., Fitzgibbon, B. M., & Fitzgerald, P. B. (2024). Exploring functional connectivity in large-scale brain networks in obsessive-compulsive disorder: A systematic review of EEG and fMRI studies. *Cerebral Cortex*, *34*(8), bhae327. https://doi.org/10.1093/cercor/bhae327

Põld, T., Bachman, M., Orgo, L., Kalev, K., Lass, J., & Hinrikus, H. (2018). EEG spectral asymmetry index detects differences between leaders and non-leaders. In H. Eskola, O. Väisänen, J. Viik, & J. Hyttinen (Eds.), *EMBEC & NBC 2017: Joint Conference of the European Medical and Biological Engineering Conference (EMBEC) and the Nordic-Baltic Conference on Biomedical Engineering and Medical Physics (NBC)* (pp. 17–20). Springer. https://doi.org/10.1007/978-981-10-5122-7_5

Põld, T., Päeske, L., Hinrikus, H., Lass, J., & Bachmann, M. (2021). Long-term stability of resting state EEG-based linear and nonlinear measures. *International Journal of Psychophysiology*, *159*, 83–87. https://doi.org/10.1016/j.ijpsycho.2020.11.013

Põld, T., Päeske, L., Hinrikus, H., Lass, J., & Bachmann, M. (2023). Temporal stability and correlation of EEG markers and depression questionnaires scores in healthy people. *Scientific Reports*, *13*(1), 21996. https://doi.org/10.1038/s41598-023-49237-4

Saifudinova, M., Bachmann, M., Lass, J., & Hinrikus, H. (2015). Effect of coffee on EEG spectral asymmetry. In D. A. Jaffray (Ed.), *World Congress on Medical Physics and Biomedical Engineering* (pp. 1030–1033). Springer. https://doi.org/10.1007/978-3-319-19387-8_251

Salinsky, M. C., Oken, B. S., & Morehead, L. (1991). Test-retest reliability in EEG frequency analysis. *Electroencephalography and Clinical Neurophysiology*, *79*(5), 382–392. https://doi.org/10.1016/0013-4694(91)90203-G

Santomauro, D. F., Mantilla Herrera, A. M., Shadid, J., Zheng, P., Ashbaugh, C., Pigott, D. M., Abbafati, C., Adolph, C., Amlag, J. O., Aravkin, A. Y., Bang-Jensen, B. L., Bertolacci, G. J., Bloom, S. S., Castellano, R., Castro, E., Chakrabarti, S., Chattopadhyay, J., Cogen, R. M., Collins, J. K., … Ferrari, A. J. (2021). Global prevalence and burden of depressive and anxiety disorders in 204 countries and territories in 2020 due to the COVID-19 pandemic. *The Lancet*, *398*(10312), 1700–1712. https://doi.org/10.1016/S0140-6736(21)02143-7

Schlink, B. R., Peterson, S. M., Hairston, W. D., König, P., Kerick, S. E., & Ferris, D. P. (2017). Independent component analysis and source localization on mobile EEG data can identify increased levels of acute stress. *Frontiers in Human Neuroscience*, *11*. https://doi.org/10.3389/fnhum.2017.00310

Seoni, S., Beeckman, S., Li, Y., Aasmul, S., Morbiducci, U., Baets, R., Boutouyrie, P., Molinari, F., Madhu, N., & Segers, P. (2022). Template matching and matrix profile for signal quality assessment of carotid and femoral laser doppler vibrometer signals. *Frontiers in Physiology*, *12*. https://doi.org/10.3389/fphys.2021.775052

Shrout, P. E., & Fleiss, J. L. (1979). Intraclass correlations: Uses in assessing rater reliability. *Psychological Bulletin*, *86*(2), 420–428. https://doi.org/10.1037/0033-2909.86.2.420

Šidák, Z. (1967). Rectangular confidence regions for the means of multivariate normal distributions. *Journal of the American Statistical Association*, *62*(318), 626–633. https://doi.org/10.1080/01621459.1967.10482935

Sörnmo, L., & Laguna, P. (2005). *Bioelectrical signal processing in cardiac and neurological applications*. Elsevier Academic Press.

Srinivasan, R., Winter, W. R., Ding, J., & Nunez, P. L. (2007). EEG and MEG coherence: Measures of functional connectivity at distinct spatial scales of neocortical dynamics. *Journal of Neuroscience Methods*, *166*(1), 41–52. https://doi.org/10.1016/j.jneumeth.2007.06.026

Stam, C. J., & van Dijk, B. W. (2002). Synchronization likelihood: An unbiased measure of generalized synchronization in multivariate data sets. *Physica D: Nonlinear Phenomena*, *163*(3–4), 236–251. https://doi.org/10.1016/S0167-2789(01)00386-4

Suhhova, A., Bachmann, M., Lass, J., Tuulik, V., & Hinrikus, H. (2011). EEG spectral asymmetry index reveals effect of microwave radiation. In Á. Jobbágy (Ed.), *5th European Conference of the International Federation for Medical and Biological Engineering* (pp. 1206–1209). Springer. https://doi.org/10.1007/978-3-642-23508-5_312

Sun, S., Li, X., Zhu, J., Wang, Y., La, R., Zhang, X., Wei, L., & Hu, B. (2019). Graph theory analysis of functional connectivity in major depression disorder with high-density resting state EEG data. *IEEE Transactions on Neural Systems and Rehabilitation Engineering*, *27*(3), 429–439. https://doi.org/10.1109/TNSRE.2019.2894423

Tatar, A. B. (2023). Biometric identification system using EEG signals. *Neural Computing and Applications*, *35*(1), 1009–1023. https://doi.org/10.1007/s00521-022-07795-0

Tenke, C. E., Kayser, J., Alvarenga, J. E., Abraham, K. S., Warner, V., Talati, A., Weissman, M. M., & Bruder, G. E. (2018). Temporal stability of posterior EEG alpha over twelve years. *Clinical Neurophysiology*, *129*(7), 1410–1417. https://doi.org/10.1016/j.clinph.2018.03.037

Thibodeau, R., Jorgensen, R. S., & Kim, S. (2006). Depression, anxiety, and resting frontal EEG asymmetry: A meta-analytic review. *Journal of Abnormal Psychology*, *115*(4), 715–729. https://doi.org/10.1037/0021-843X.115.4.715

Tsai, Y.-C., Li, C.-T., & Juan, C.-H. (2023). A review of critical brain oscillations in depression and the efficacy of transcranial magnetic stimulation treatment. *Frontiers in Psychiatry*, *14*, 1073984. https://doi.org/10.3389/fpsyt.2023.1073984

Uhlhaas, P. J., & Singer, W. (2006). Neural synchrony in brain disorders: Relevance for cognitive dysfunctions and pathophysiology. *Neuron*, *52*(1), 155–168. https://doi.org/10.1016/j.neuron.2006.09.020

Urigüen, J. A., & Garcia-Zapirain, B. (2015). EEG artifact removal—state-of-the-art and guidelines. *Journal of Neural Engineering*, *12*(3), 031001. https://doi.org/10.1088/1741-2560/12/3/031001

U.S. FDA. (2013). *De novo classification order for Neuropsychiatric EEG-Based Assessment Aid for ADHD (NEBA System) (K112711)*. U.S. Food and Drug Administration, Center for Devices and Radiological Health. https://www.accessdata.fda.gov/cdrh_docs/pdf11/k112711.pdf

van der Vinne, N., Vollebregt, M. A., van Putten, M. J. A. M., & Arns, M. (2017). Frontal alpha asymmetry as a diagnostic marker in depression: Fact or fiction? A meta-analysis. *NeuroImage: Clinical*, *16*, 79–87. https://doi.org/10.1016/j.nicl.2017.07.006

Walker, E. R., McGee, R. E., & Druss, B. G. (2015). Mortality in mental disorders and global disease burden implications: A systematic review and meta-analysis. *JAMA Psychiatry*, *72*(4), 334–341. https://doi.org/10.1001/jamapsychiatry.2014.2502

Wang, H., Mou, S., Pei, X., Zhang, X., Shen, S., Zhang, J., Shen, X., & Shen, Z. (2025). The power spectrum and functional connectivity characteristics of resting-state EEG in patients with generalized anxiety disorder. *Scientific Reports*, *15*(1), 5991. https://doi.org/10.1038/s41598-025-90362-z

Wankhedkar, R., & Jain, S. K. (2021). Motif discovery and anomaly detection in an ECG using matrix profile. In C. R. Panigrahi, B. Pati, P. Mohapatra, R. Buyya, & K.-C. Li (Eds.), *Progress in Advanced Computing and Intelligent Engineering* (pp. 88–95). Springer. https://doi.org/10.1007/978-981-15-6584-7_9

Wen, F., Su, Y., Liu, D., Wang, Y., & Liu, M. (2025). Automated sparse feature selection in high-dimensional proteomics data via 1-bit compressed sensing and K-Medoids clustering. *BMC Bioinformatics*, *26*(1), 165. https://doi.org/10.1186/s12859-025-06193-2

Whitham, E. M., Pope, K. J., Fitzgibbon, S. P., Lewis, T., Clark, C. R., Loveless, S., Broberg, M., Wallace, A., DeLosAngeles, D., Lillie, P., Hardy, A., Fronsko, R., Pulbrook, A., & Willoughby, J. O. (2007). Scalp electrical recording during paralysis: Quantitative evidence that EEG frequencies above 20 Hz are contaminated by EMG. *Clinical Neurophysiology*, *118*(8), 1877–1888. https://doi.org/10.1016/j.clinph.2007.04.027

WHO. (2022). *World mental health report: Transforming mental health for all*. https://iris.who.int/handle/10665/356115

WHO. (2024, September 2). *Mental health at work*. World Health Organization. https://www.who.int/news-room/fact-sheets/detail/mental-health-at-work

WHO. (2025, September 30). *Mental disorders*. World Health Organization. https://www.who.int/news-room/fact-sheets/detail/mental-disorders

Wolff, A., de la Salle, S., Sorgini, A., Lynn, E., Blier, P., Knott, V., & Northoff, G. (2019). Atypical temporal dynamics of resting state shapes stimulus-evoked activity in depression—An EEG study on rest–stimulus interaction. *Frontiers in Psychiatry*, *10*. https://doi.org/10.3389/fpsyt.2019.00719

Yao, D. (2001). A method to standardize a reference of scalp EEG recordings to a point at infinity. *Physiological Measurement*, *22*(4), 693–711. https://doi.org/10.1088/0967-3334/22/4/305

Yao, D., Qin, Y., Hu, S., Dong, L., Bringas Vega, M. L., & Valdés Sosa, P. A. (2019). Which reference should we use for EEG and ERP practice? *Brain Topography*, *32*(4), 530–549. https://doi.org/10.1007/s10548-019-00707-x

Yeh, C.-C. M., Zhu, Y., Ulanova, L., Begum, N., Ding, Y., Dau, H. A., Silva, D. F., Mueen, A., & Keogh, E. (2016). Matrix Profile I: All pairs similarity joins for time series: A unifying view that includes motifs, discords and shapelets. *In 2016 IEEE 16th International Conference on Data Mining (ICDM)*, 1317–1322. https://doi.org/10.1109/ICDM.2016.0179

Zhang, S., Sun, L., Mao, X., Hu, C., & Liu, P. (2021). Review on EEG-based authentication technology. *Computational Intelligence and Neuroscience*, 5229576. https://doi.org/10.1155/2021/5229576

Zhong, S., & Mueen, A. (2024). MASS: Distance profile of a query over a time series. *Data Mining and Knowledge Discovery*, *38*(3), 1466–1492. https://doi.org/10.1007/s10618-024-01005-2

Acknowledgements

I would like to express my sincere gratitude to my supervisor, Maie Bachmann, for her guidance, encouragement, and steady support throughout this PhD journey. Her expertise, thoughtful feedback, and high standards have shaped both this dissertation and my development as a researcher. I would also like to thank my co-supervisor, Juri Belikov, for his input and support at key moments along the way.

I am also profoundly thankful to all the members of the Brain Bioelectrical Signals Research Group for the stimulating discussions, shared knowledge, and generous help that have contributed significantly to my growth. Your collaboration and willingness to challenge ideas have strengthened this work and made the process far more rewarding. My appreciation extends to other colleagues and members of the Department of Health Technologies who have offered support in many forms—through practical assistance, constructive advice, and an encouraging academic environment.

Most of all, I am grateful to my family, who have been my most significant source of strength throughout this process. Marek, thank you for your exceptional patience and resilience during the many evenings and weekends when analyses and writing often kept me occupied—your steady support made this work possible. Marta, thank you for the ways you have challenged me to grow, and for teaching me patience and perspective beyond academia. Ragnar, thank you for your bright, playful nature—your joy made it easier to step away from work and be present.

This study was partly supported by the Estonian Centre of Excellence in IT (EXCITE) TAR16013 (funded by the European Regional Development Fund) and by the Estonian Centre of Excellence in IT (EstWell) TK 218 (funded by the Estonian Ministry of Education and Research).

Abstract

Sensitivity and Individual Temporal Stability of Electroencephalography-Based Measures

Mental health disorders affect over a billion people, yet routine care still lacks objective tools to monitor brain dynamics. Electroencephalography (EEG) is attractive for longitudinal monitoring because it is low-cost, noninvasive, and offers high temporal resolution. Despite extensive research, EEG measures have not been adopted in routine psychiatric practice, largely because reported effects are demonstrated at the group level and are not validated for individual-level tracking. Two practical obstacles stand out: the wide variety of EEG measures remains unorganized, with diverse ad hoc feature sets and limited clarity on how measures overlap or complement each other; and there is substantial dispersion across individuals, while the normative intra-individual range of EEG measures remains uncharacterized.

The thesis evaluates resting-state EEG measures to guide selection for individualized monitoring. It (1) maps interrelationships across commonly used EEG measures to support compact, interpretable sets; (2) introduces a mechanistically motivated single-channel measure of waveform stability, the in-phase matrix profile (pMP), implementable without user-tuned parameters; (3) quantifies long-term intra-individual stability, and (4) tests whether stable measures are sensitive to a controlled physiological perturbation.

Across a broad comparison of twelve widely used measures in healthy resting-state EEG data (n = 80), substantial overlap was observed, with 56% of pairwise relationships showing significant correlation. This structure revealed clear differences in reach: Higuchi's fractal dimension (HFD) acted as a broad-coverage descriptor, strongly connected to many other measures and thus suggested as a general-purpose indicator of diverse EEG alterations, whereas measures such as the spectral asymmetry index (SASI) and gamma band power (GBP) provided narrower, more specific information consistent with condition- or stressor-related spectral shifts. These insights motivate compact, interpretable panels that combine a broadly informative backbone measure with targeted, weakly correlated measures rather than maximal ad hoc feature sets.

To capture a dimension not directly quantified by standard measures, the thesis introduces pMP as a measure of waveform self-similarity after removing amplitude differences. In major depressive disorder (MDD; n = 66), both pMP and HFD differentiated patients from matched controls, but pMP yielded more spatially uniform group separation (significant across all channels after correction) and slightly higher single-channel classification accuracy than HFD, supporting the clinical relevance of altered waveform stability in resting-state MDD. Longitudinal monthly recordings over one year (n = 9) further showed that nonlinear single-channel measures, especially HFD and pMP, exhibit high intra-individual temporal stability. In contrast, baseline magnitudes and natural fluctuation ranges differ markedly between individuals, making global thresholds unreliable and motivating the use of individualized reference ranges. Finally, comparison of an individual's year-long baseline to measure values acquired after a controlled systemic stressor (mRNA vaccination; n = 1) demonstrated transient deviations in a subset of measures (HFD, SASI, and GBP) followed by return toward baseline, illustrating that long-term stability can coexist with responsiveness to physiologically meaningful perturbation.

Taken together, these findings outline a practical path toward individualized EEG monitoring: organize measures into compact panels that combine broad-coverage measures (e.g., HFD) with narrow-coverage, condition-sensitive measures (e.g., SASI and GBP), and anchor interpretation to person-specific baselines. Although pMP's relationships to the broader EEG measure selection and its responsiveness to immune-related perturbation were not examined here, its combination of group-level sensitivity in MDD and strong intra-individual stability provides a clear rationale to evaluate pMP further as a measure of individual-level deviation.

Lühikokkuvõte

Elektroentsefalograafial põhinevate mõõdikute tundlikkus ja individuaalne ajaline stabiilsus

Enam kui miljard inimest kannatab vaimse tervise häire all, samas on aju tervise jälgimiseks jätkuvalt vähe objektiivseid mõõdikuid. Elektroentsefalograafia (EEG) on selleks sobiv vahend olles suhteliselt odav, mitteinvasiivne ja hea ajalise lahutusvõimega. Hoolimata senisest mahukast teadustööst, ei ole EEG mõõdikud psühhiaatriliste haiguste hindamisel rutiinsesse kliinilisse kasutusse jõudnud. Peamiseks põhjuseks on enamasti ainult grupitasandil saadud tulemused, mis ei ole valideeritud individuaalseks jälgimiseks. Indiviiditasandil jälgimise rakendamisel on kaks olulist takistust. Esiteks, lai valik organiseerimata EEG mõõdikuid, millest kombineeritakse juhuslikke komplekte omamata teadmisi, kuidas mõõdikud üksteist informatsiooniliselt täiendavad või katavad. Teiseks, inimeste vahel on märkimisväärne erinevus ning puudub teadmine, mis vahemikus on EEG mõõdikute oodatav tavapärane kõikumine ning mil määral need vahemikud indiviiditi erinevad.

Väitekiri hindab puhkeoleku-EEG mõõdikuid, suunamaks tegema sobivaid mõõdikute valikuid individuaalseks jälgimiseks. Selleks (1) kaardistatakse tavapäraselt kasutatavate EEG mõõdikute omavahelisi seoseid toetamaks kompaktsete ja kergemini tõlgendatavate mõõdikukomplektide koostamist; (2) arendatakse ühe kanali andmetel rakendatav lainekuju stabiilsuse mõõdik, *in-phase matrix profile* (pMP), mis ei eelda kasutajapoolset parameetrite häälestamist; (3) kirjeldatakse mõõdikute pikaajalist stabiilsust indiviidi tasandil ning (4) testitakse, kas stabiilsed mõõdikud reageerivad kontrollitud füsioloogilisele häiringule.

Võrreldes 12 laialdaselt kasutatavat EEG mõõdikut, mida rakendati tervete inimeste puhkeolekusignaalidel (n = 80), tuvastati märkimisväärne informatsiooni ülekattuvus: 56% paarikaupa tehtud võrdlustest olid statistiliselt oluliselt korrelatsioonis. Selline struktuur tõi selgelt esile erinevused mõõdikute võimekuses püüda laiemat või kitsamat hulka informatsiooni. Higuchi fraktaaldimensioon (HFD) käitus laia katvusega mõõdikuna, olles tugevalt seotud paljude teistega ning sobides seetõttu mitmesuguste EEG signaalis asetleidvate muutuste üldiseks indikaatoriks. Seevastu näiteks spektraalne asümmeetriaindeks (SASI) ja gamma sagedusriba võimsus (GBP) kirjeldasid kitsamat ja spetsiifilisemat infot, mis on kooskõlas kindlate seisundite või stressoritega seotud spektraalsete nihetega. Need leiud toetavad kompaktsete ja kergemini tõlgendatavate mõõdikupaneelide kasutamist, kombineerides laiahaardelisi põhimõõdikuid spetsiifiliste, vähese informatsioonilise ülekattega mõõdikutega.

Käsitlemaks vaatenurka, mida tavapärased EEG mõõdikud ei võimalda, tutvustab väitekiri pMP-d kui lainekuju ajalise stabiilsuse mõõdikut, kus amplituudierinevuste mõju on minimeeritud. Kliinilise depressiooni (MDD; n = 66) korral eristasid nii pMP kui ka HFD kliinilist gruppi samasuguse vanuselise ja soolise koosseisuga kontrollgrupist. Samas pMP puhul oli grupieristus statistiliselt oluline kõigis EEG kanalites (HFD-l 43% kanalitest) ning veidi kõrgem klassifitseerimistäpsus võrreldes HFD-ga. Saadud tulemused toetavad lainekuju stabiilsuse kliinilist olulisust puhkeoleku EEG signaalis MDD puhul. Ühe aasta jooksul igakuiselt kogutud korduvsalvestused (n = 9) näitasid lisaks, et mittelineaarsed ühe kanali mõõdikud, eriti HFD ja pMP, on indiviidide lõikes ajas tugevalt stabiilsed. Samas tulid esile märkimisväärsed erinevused inimeste vahel nii mõõdikute baasväärtuste suurusjärkudes kui ka loomulike kõikumisvahemike ulatustes, muutes globaalsed lävendid

ebausaldusväärseks ja suunates kasutama individuaalseid referentsvahemikke. Olulise täiendusena näitas ühe isiku aastase baasväärtuste (referentsvahemik) võrdlus salvestustega pärast kontrollitud süsteemset stressorit (mRNA-vaktsineerimine; n = 1), et osa mõõdikuid (HFD, SASI ja GBP) kaldusid ajutiselt referentsvahemikust kõrvale, kuid naasid hiljem ootuspärasesse vahemikku tagasi. Saadud tulemused näitavad, et mõõdikud võivad olla üheaegselt pikaajaliselt stabiilsed ning tundlikud füsioloogiliselt tähenduslike häiringute suhtes.

Kokkuvõttes viitavad tulemused, et individuaalne EEG jälgimine on saavutatav järgnevalt: mõõdikud tuleks koondada kompaktsetesse paneelidesse, mis kombineerivad laia katvusega mõõdikuid (näiteks HFD) kitsama katvusega, seisunditundlike mõõdikutega (näiteks SASI ja GBP), ning saadud tulemusi tuleks tõlgendamisel siduda isikupõhiste referentsvahemikega. Kuigi pMP seoseid teiste EEG mõõdikutega ja selle tundlikkust immuunreaktsioonist tingitud häiringule käesolevas töös ei hinnatud, annab pMP grupitaseme tundlikkus MDD puhul ja tugev individuaalne ajaline stabiilsus selge ajendi pMP edasiseks hindamiseks indiviiditasandi kõrvalekallete mõõdikuna.

Appendix 1 – Publication I

Publication I

Päeske, L., **Uudeberg, T**., Hinrikus, H., Lass, J., & Bachmann, M. (2023). Correlation between electroencephalographic markers in the healthy brain. Scientific Reports, 13, 6307. https://doi.org/10.1038/s41598-023-33364-z

scientific reports

Check for updates

OPEN

Correlation between electroencephalographic markers in the healthy brain

Laura Päeske, Tuuli Uudeberg, Hiie Hinrikus✉, Jaanus Lass & Maie Bachmann

Mental disorders have an increasing tendency and represent the main burden of disease to society today. A wide variety of electroencephalographic (EEG) markers have been successfully used to assess different symptoms of mental disorders. Different EEG markers have demonstrated similar classification accuracy, raising a question of their independence. The current study is aimed to investigate the hypotheses that different EEG markers reveal partly the same EEG features reflecting brain functioning and therefore provide overlapping information. The assessment of the correlations between EEG signal frequency band power, dynamics, and functional connectivity markers demonstrates that a statistically significant correlation is evident in 37 of 66 (56%) comparisons performed between 12 markers of different natures. A significant correlation between the majority of the markers supports the similarity of information in the markers. The results of the performed study confirm the hypotheses that different EEG markers reflect partly the same features in brain functioning. Higuchi's fractal dimension has demonstrated a significant correlation with the 82% of other markers and is suggested to reveal a wide spectrum of various brain disorders. This marker is preferable in the early detection of symptoms of mental disorders.

Mental disorders have an increasing tendency and represent the main burden of disease to society today. According to WHO's recent report[1], nearly 15% of the world's working population is estimated to experience a mental disorder. There is a high demand for effective methods and markers for the early detection and treatment monitoring of mental disorders.

Electroencephalography (EEG) is a method for the registration of brain electrical activity using scalp electrodes. The EEG signal is complex, containing information about physiological, emotional, cognitive, and other processes occurring simultaneously in a person. The EEG has proved to be an effective tool in neurophysiology used in clinical practice[2]. EEG markers describe the physiological state of the brain and can reflect the changes in brain electrical activity related to mental disorders. EEG markers can detect the objective symptoms of mental disorders and contribute significantly to the assessment of stress, depression, anxiety, and others. EEG is a non-invasive, patient-friendly, and easy-to-apply method that can be implemented in portable and wearable devices for regular personal use.

Mental disorders cause only mild alterations in EEG which are difficult to detect. Therefore, parallel to the traditional quantitative EEG based on the comparison of powers in different frequency bands of the EEG spectrum, different advanced methods have been developed for EEG analyses to detect mental disorders.

EEG signal is complex, stochastic, nonstationary, and nonlinear. This is the reason why the field of possible EEG markers used in the detection of mental disorders is so diverse. Different EEG markers can describe various features of the signal[3,4]. All EEG markers can be divided into three categories depending on the phenomena they describe: the traditional EEG frequency band power, the dynamic pattern of the signal in a single-channel EEG, or the brain functional connectivity in a multichannel EEG.

The changes caused by mental disorders have been detected by traditional EEG markers based on the powers of EEG frequency bands[5–8]. The resting state EEG alpha and beta powers increase in depression groups[5–7]. The EEG alpha power is suggested associated with depression severity[7]. In addition to increased band powers, the altered inter-hemispheric alpha power asymmetry[5,6] and reduced coherence[5] have been discovered in the same depression groups. The review of 184 studies has demonstrated that differences in EEG frequency bands powers are evident for many psychiatric disorders including depression, attention deficit-hyperactivity disorder, autism, addiction, bipolar disorder, anxiety, panic disorder, post-traumatic stress disorder, obsessive compulsive disorder

Department of Health Technologies, School of Information Technology, Tallinn University of Technology, 5 Ehitajate Rd, 19086 Tallinn, Estonia. ✉email: hiie.hinrikus@gmail.com

and schizophrenia[8]. The power changes within specific frequency bands are not unique to one disorder but show overlap across disorders as well as variability within disorders[8].

The various nonlinear and dynamic features of the signal in depression and other disorders can be described using more advanced EEG markers such as fractality, complexity, and frequency balance[9–15]. Detrended fluctuation analysis (DFA) shows higher values for depressed patients[9] and also improves the diagnostic accuracy of Alzheimer's disease[10]. The Lempel–Ziv complexity (LZC) has indicated higher scores in both, schizophrenia and depression[11]. Higuchi's fractal dimension (HFD) has demonstrated good differentiation between the groups of depressive and healthy subjects[12–14]. The spectral asymmetry index (SASI) increases in the depressive group[14,15] and is correlated with Hamilton Depressive Rating Scale for indoor patients[15]. The combination of nonlinear markers HFD, DFA, correlation dimension, and Lyapunov exponent markers provides a classification accuracy of depression of 90% which is higher than the classification accuracy for the linear EEG band powers markers 76.6%[13]. Different combinations of EEG linear (SASI, alpha power variability, relative gamma power) and nonlinear markers (HFD, DFA, LZC) have demonstrated rather close accuracies of classification for both, 0.88% for linear and 0.85% for nonlinear markers[14].

The functionality of the brain, the coordination of neuronal activity in different brain areas, can be described by analyzing the connectivity between signals in different EEG channels[16–20]. Brain functional connectivity and EEG coherence increase in major depression[16–18]. The phase-sensitive markers, the imaginary part of coherence and synchronization, significantly contribute to the discrimination of depression[19,20].

Despite reflecting various features in brain physiology, different EEG markers have indicated similar results in detecting mental disorders. EEG band power, Higuchi's fractal dimension, Lempel–Ziv complexity, spectral asymmetry, and others have indicated quite a close accuracy in the evaluation of depression[13,14,21]. Based on these findings, two possible explanations can be proposed. First, the disorder causes different physiological changes reflected by the different features of the EEG signal and each marker detects a specific EEG feature. Second, the different EEG markers reveal the same EEG features and similar declinations in brain functioning.

Whereas the mild alterations in the EEG signal caused by mental disorders are hidden in the natural variability of the signal, the selection of appropriate markers revealing mental disorders is highly important. The selected EEG markers serve as the input data for classification algorithms. The classification accuracy depends strongly on the selection of the appropriate markers and not so much on the applied classification algorithms[22,23]. Therefore, the reasonable selection of EEG markers is especially important.

Only a few publications have been aimed to compare the effectiveness of different EEG markers[13,14,22]. The correlation between the EEG signals in different channels has been investigated[23,24]. To the best of our knowledge, the evaluation of the correlation between the markers and the independence between the information achieved from different markers has not been performed.

The current study is aimed to investigate the hypothesis that different EEG markers reveal partly the same EEG features and so provide overlapping information about the state of the brain.

To assess the hypothesis, the correlation between different EEG markers indicating various features of the signal is investigated. Some most frequently used EEG markers from band power, dynamics, and functional connectivity categories are selected for investigation, four from each category.

The band power markers describe the power of the signal inside the fixed EEG frequency bands and are not sensitive to the pattern of the signal. Theta band power (TBP), alpha band power (ABP), beta band power (BBP), and gamma band power (GBP) are selected for analyses in the first category.

The dynamics markers describe the pattern and the complexity of the signal. The four selected single-channel EEG dynamics markers describe various aspects of the complexity of the EEG signal. Higuchi's fractal dimension (HFD) describes the self-similarity of the signal[25]. Detrended fluctuations analysis (DFA) describes the self-correlation of the signal and determines the self-affinity of the EEG signal[26], while Lempel–Ziv complexity[27] (LZC) describes the randomness of the signal. The spectral asymmetry index[12] (SASI) describes the balance of low-frequency and high-frequency oscillations in the signal.

Functional connectivity markers describe the connectivity between different brain areas using multichannel data. Magnitude-squared coherence[28] (MSC) describes the intensity of coherence between two signals. The imaginary part of coherency[29] (ImC) characterizes phase relationships in the coherence between two complex signals[29]. Synchronization likelihood[30] (SL) describes dynamical interdependencies between two signals. Mutual information[31] (MI) describes the coherence of the information between two signals and can be considered a spatial analog of entropy.

The selection of markers considers linear (TBP, ABP, BBP, GBP, SASI, MSC, ImC) and nonlinear (HFD, DFA, LZC, SL, MI) EEG properties. The markers calculated in the time domain (HFD, DFA, LZC, SL, MI) and frequency domain (TBP, ABP, BBP, GBP, SASI, MSC, ImC) are included. The selection of functional connectivity markers is balanced between the phase-sensitive (ImC, SL) and phase-insensitive (MSC and MI) markers.

The study is planned in a way to minimize the impact of external factors and possible inter-subject variability due to the individual responses to a disorder on the EEG signals. The resting state eyes closed EEG of healthy people is analyzed in the study.

Methods

Subjects. The group of 80 volunteers, 38 (47.5%) female, and 42 (52.5%) male was selected for investigation. Their age varied from 19 to 75 years, with a mean age of 37 ± 15 years. They declared no mental or psychiatric disorders, epilepsy, brain injuries, or usage of narcotics or psychotropic medications. All the selected subjects were considered as healthy. The subjects were asked to abstain from alcohol for 24 h and from coffee two hours before the EEG recordings.

The study was conducted following the Declaration of Helsinki and was approved by the Tallinn Medical Research Ethics Committee. Before participating in the study, each subject signed informed consent.

EEG recordings. The Neuroscan Synamps2 acquisition system (Compumedics, NC, United States) was used for EEG recordings. Electrodes were placed according to the extended international 10–20 system. The signals were recorded from 30 electrodes (Fp1, Fp2, F7, F3, Fz, F4, F8, FT7, FC3, FCz, FC4, FT8, T7, C3, Cz, C4, T8, TP7, CP3, CPz, CP4, TP8, P7, P3, Pz, P4, P8, O1, Oz, O2) using linked mastoids as reference. During recordings, eye movements were monitored using horizontal and vertical electrooculograms. Electrodes impedances were lower than 10 kΩ.

All EEG recordings were performed in the morning before noon. The resting state eyes closed EEG was recorded for 6 min. During recordings, the subjects were in lying positions in a shielded and dimly lit room. Earplugs were used to minimize external sounds.

The raw EEG was recorded in the frequency band 0.5–200 Hz at the sampling frequency of 1000 Hz.

EEG preprocessing. The raw EEG signals were filtered into frequency band 1–45 Hz using a Butterworth filter.

To reduce the computing time, the signals were down-sampled to 200 Hz and recalculated to REST reference as preferable in EEG analyses[32,33]. The signals were divided into 20.48-s (4096 sample) segments. An experienced EEG specialist carefully inspected all segments and removed the segments with artifacts (ocular, muscular, or others). The first 10 artifact-free segments were used for further analysis. The signals were preprocessed using MATLAB (The Mathworks, Inc.).

EEG analyses. *Calculation of band power markers.* First, the power spectral density (PSD) of the recorded EEG signal was calculated using the Welsh's averaged periodogram method. The signal was divided into 50% overlapping sections and windowed by the Hanning window. Second, the markers were calculated as the mean of PSD over the frequencies within the fixed frequency bands TBP 4–7 Hz, ABP 8–12 Hz, BBP 13–30 Hz, and GBP 31–45 Hz.

Calculation of dynamics markers. The nonlinear dynamics markers (HFD, DFA, and LZC) were calculated in the time domain. Calculations were performed for ten 20.48-s segments. A nonlinear marker was determined as the mean value of the calculations' results over ten segments. The HFD was calculated according to Higuchi's original algorithm[25] at kmax = 8[14,34]. DFA was calculated according to the published by Peng et al. algorithms[26] applying the adaptation to EEG described by Bachmann et al.[14]. The calculation of LZC was performed based on the principles and algorithms published by Lempel and Ziv[27] and Zhang et al.[29] using the adjustment performed by Bachmann et al.[14]. SASI was calculated in the frequency domain summarizing PSD over the lower and higher EEG frequency bands and excluding the central alpha band from calculations[15].

Calculation of functional connectivity markers. SL was calculated in the time domain following the detailed explanation of the method by the authors Stam and Van Dijk[30], while the parameters were set as in Päeske et al.[34], as such parameters ensure that the time–frequency characteristics of the signals are fully considered. MI was calculated using the algorithm derived by Frazer and Swinney[31] following the method of the calculation for EEG signals published by Ibáñez-Molina and others[35]. MSC and ImC were calculated in the frequency domain, the algorithms were applied as described by Päeske et al.[36].

The calculations of markers were done in MATLAB (The Mathworks, Inc.).

Statistics. All EEG band power and dynamic markers were calculated for all EEG channels for each subject. All functional connectivity markers were calculated between 30 channels, in total 435 combinations were performed per marker for a subject. The averaged over all EEG channels values for a subject were used for statistical evaluation.

The null hypothesis for the difference between the values of markers was tested using the Wilkinson test. In total, $(12 \times 12-12)/2 = 66$ comparisons between the pairs of 12 markers were performed on the same EEG database. The adjustment to multiple comparisons was done using Bonferroni correction. The corrected confidence level $p < 0.05/66 = 0.00076$ was considered statistically significant.

The correlation between different EEG markers was assessed using the Spearman correlation coefficients. The null hypothesis for correlation coefficients was tested using t-test. The probability that the correlation between markers of two different categories is zero, decreases with the increase in the number of pairs n and the value of the correlation coefficient r. At the fixed number of pairs n = 80, the p score reaches the level of statistical significance $p < 0.00076$ at the value of the correlation coefficient $|r| > 0.37$.

Results

The nature of the EEG markers differs in different categories. Therefore, the results are presented separately in each of the markers' categories followed by inter-categories correlations results.

Band power markers. Wilkinson's test indicated that the calculated values of different band power markers are mutually statistically significant ($p < 0.00076$) in all combinations except TBP and BBP ($p = 0.03$).

The graphs in Fig. 1 present the correlations between the EEG band power markers. The calculated Spearman correlation coefficients and t-test p-values are indicated. The correlation is statistically significant between

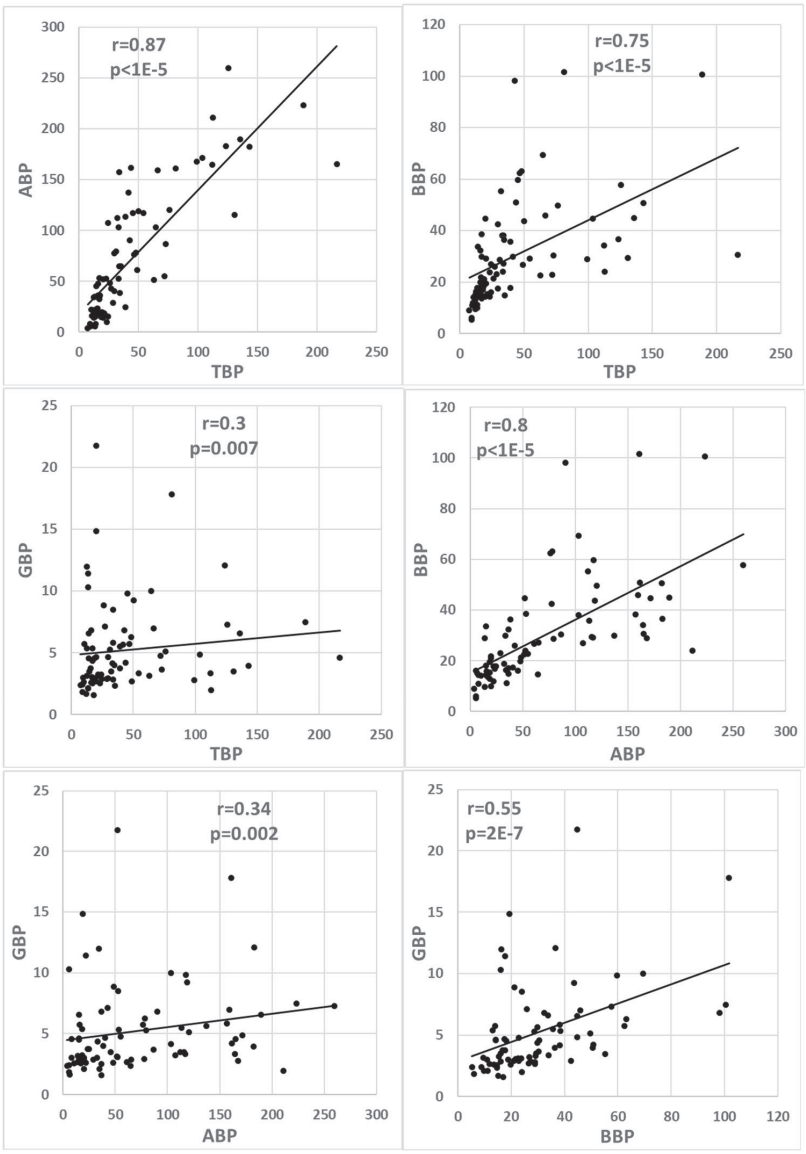

Figure 1. Correlation between various band power markers: TBP and ABP, TBP and BBP, TBP and GBP, ABP and BBP, ABP and GBP, BBP and GBP. The calculated Spearman correlation coefficients r between the markers and corresponding p-values are indicated ($n = 80$). The $p < 0.00076$ ($|r| > 0.37$) indicates statistical significance.

the markers of closer frequency bands TBP and ABP ($r = 0.87$), ABP and BBP ($r = 0.80$), whereas the correlation is somewhat less between TBP and BBP ($r = 0.75$) and insignificant between ABP and GBP ($r = 0.34$) as well as between TBP and GBP ($r = 0.3$). This finding may be related to the overlapping physiological processes in close frequency bands.

Four of six (66.7%) combinations between the band power markers indicate statistically significant correlations.

Dynamics markers. Wilkinson's test shows that the calculated values of all dynamics markers differ significantly in all combinations ($p < 0.00076$).

Figure 2 presents correlations between different dynamics markers. The calculated Spearman correlation coefficients and t-test *p*-values are indicated. HFD has a significant correlation with all other markers, maximal with DFA (r = 0.64), a little lower with SASI (r = 0.59), and with LZC (r = 0.52). The correlations between the other markers DFA, LZC, and SASI are not statistically significant. This finding supports the idea that HFD can incorporate partly the same EEG features as the DFA, LCZ, and SASI do. The other markers DFA, LZC, and SASI do not reveal mutually similar EEG features.

Three of six (50%) combinations between the dynamic markers indicate statistically significant correlations.

Functional connectivity markers. Wilkinson's test indicated that the calculated values of functional connectivity markers are statistically significant ($p < 0.00076$) in all combinations except SL and MI ($p = 0.297$).

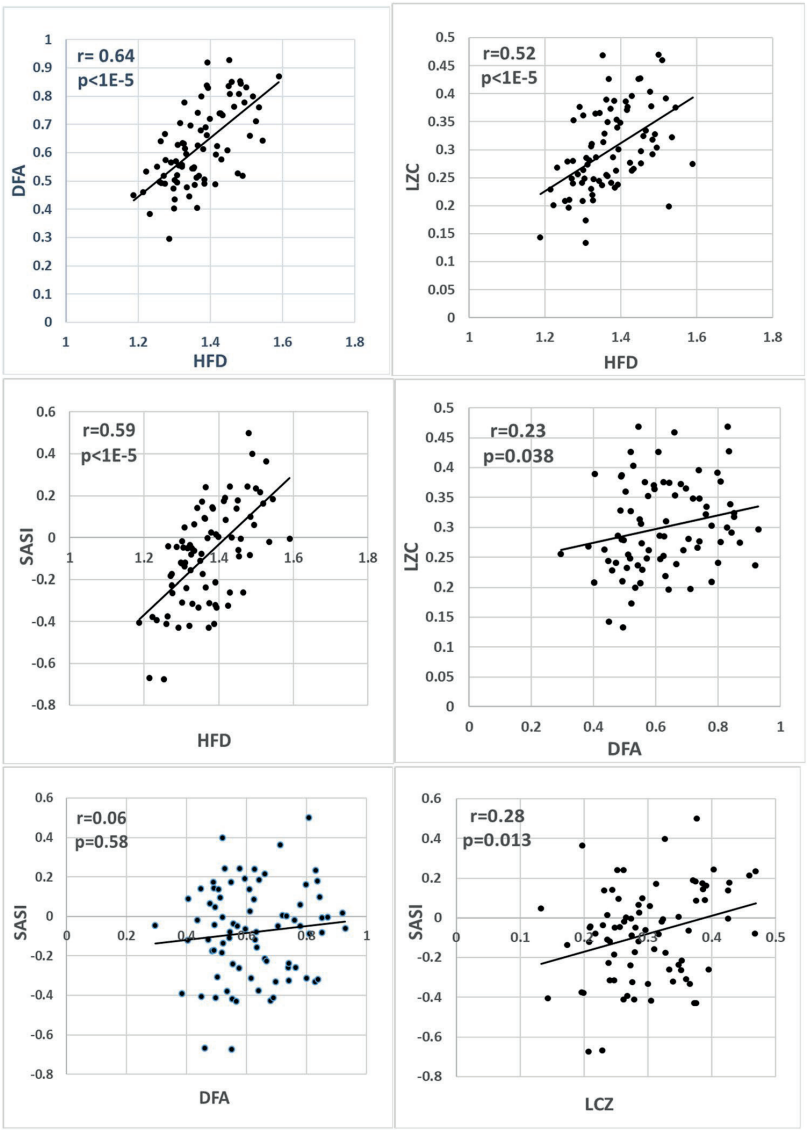

Figure 2. Correlation between various dynamics markers: HFD and DFA, HFD and LZC, HFD and SASI, DFA and LCZ, DFA and SASI, LZC and SASI. The calculated Spearman correlation coefficients *r* between the markers and corresponding *p*-values are indicated ($n = 80$). The $p < 0.00076$ ($|r| > 0.37$) indicates statistical significance.

Figure 3 presents the correlations between functional connectivity markers. The calculated Spearman correlation coefficients and t-test *p*-values are indicated. SL has a significant correlation with all other markers, the correlation coefficient between SL and MI is 0.77, between SL and ImC 0.7, and between SL and MSC 0.57. The expected correlation is between MSC and ImC (r = 0.64). Weaker but still significant is the correlation between ImC and MI (r = 0.41). This finding suggests that the various brain functional connectivity behaviors are mutually correlated and corresponding EEG features can be revealed by different markers.

Five of six (83.3%) combinations between the functional connectivity markers indicate a statistically significant correlation.

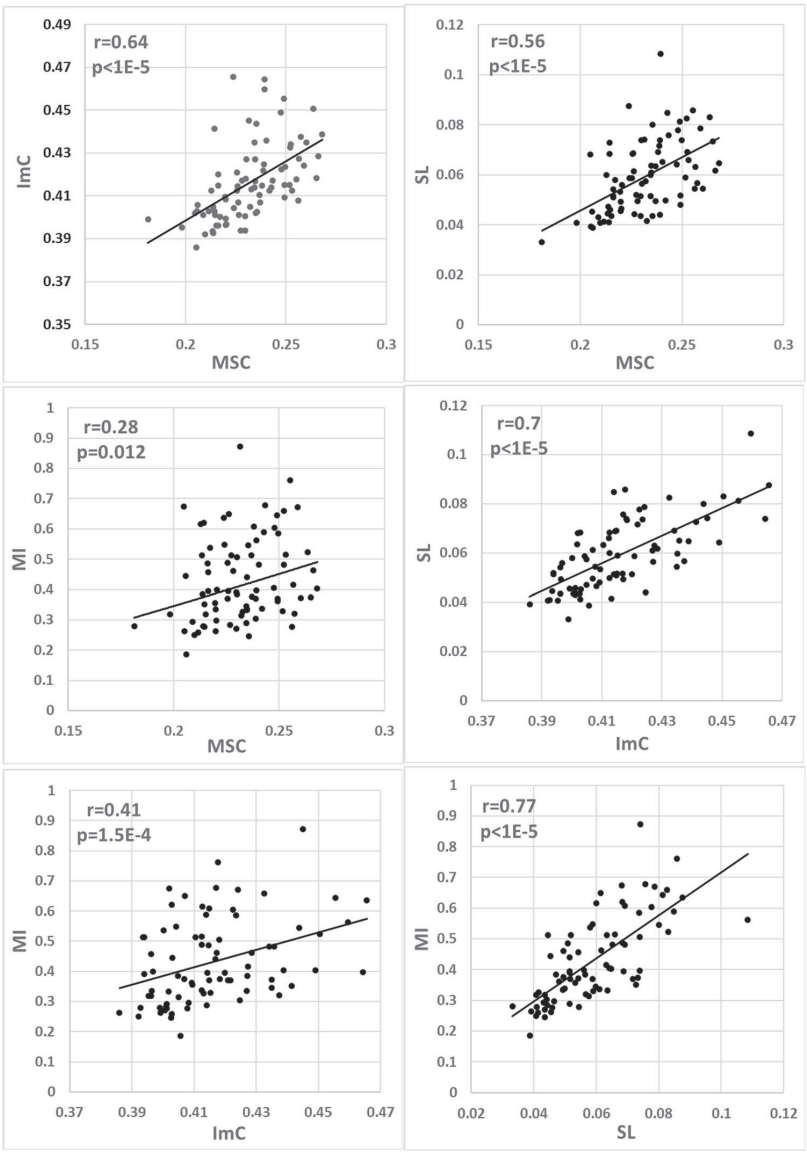

Figure 3. Correlation between various functional connectivity markers: MSC and ImC, MSC and SL, MSC and MI, ImC and SL, ImC and MI, SL and MI. The calculated Spearman correlation coefficients *r* between the markers and corresponding *p*-values are indicated ($n = 80$). The $p < 0.00076$ ($|r| > 0.37$) indicates statistical significance.

Markers of different categories. Table 1 presents the calculated Spearman correlation coefficients between the EEG band power markers, dynamic markers, and functional connectivity markers and corresponding t-test *p*-values. The data in the table show that the correlation between the markers of different categories is not weaker than between the markers of the same category. The dynamic markers are negatively correlated with the band power markers (except GBP) and functional connectivity markers.

The assessment of the correlations between EEG signal frequency band power, dynamics, and functional connectivity markers demonstrates that a statistically significant correlation is evident in 37 of 66 (56%) comparisons performed between 12 markers. HFD and SL are correlated with 9, MI and ABP with 8, TBP, BBP, and ImC with 7, DFA with 6, LZC and SASI with 4, and GBP and MSC only with 2 other markers. The level of correlation varies from 0.97 (between ABP and MI) to 0.38 (between LCZ and ImC, and GBP and SASI).

Discussion

The results of the performed study support the hypotheses that different EEG markers reveal partly the same EEG features. The assessment of the correlations between band power, dynamics, and functional connectivity markers demonstrates that despite the values of the markers being statistically different, a statistically significant correlation is evident in 56%, (in 37 from 66) of the combinations between 12 markers.

Mental disorders can cause very different unpredictable alterations in the EEG signal varying in individuals. For early detection of mental disorders, a marker is required to be able to reveal a wide scale of possible

Marker	HFD	DFA	LZC	SASI	TBP	ABP	BBP	GBP	MSC	ImC	SL	MI
HFD												
r		0.64	0.52	0.59	− 0.77	− 0.85	− 0.52	0.11	− 0.35	− 0.42	− 0.68	− 0.85
p		0.00E+00	1.10E-06	1.18E-08	0.00E+00	0.00E+00	1.10E-06	3.20E-01	1.77E-03	1.17E-04	0.00E+00	0.00E+00
DFA												
r	0.64		0.23	0.06	− 0.72	-0.83	− 0.77	− 0.35	− 0.23	− 0.38	− 0.67	− 0.82
p	0.00E+00		3.81E-02	5.84E-01	0.00E+00	0.00E+00	0.00E+00	1.44E-03	4.42E-02	5.83E-04	0.00E+00	0.00E+00
LZC												
r	0.52	0.23		0.28	− 0.29	− 0.39	− 0.02	0.10	− 0.21	− 0.38	− 0.42	− 0.34
p	1.10E-06	3.81E-02		1.33E-02	9.11E-03	4.58E-04	8.93E-01	3.63E-01	5.96E-02	5.97E-04	1.42E-04	2.25E-03
SASI												
r	0.59	0.06	0.28		− 0.51	− 0.29	− 0.08	0.38	− 0.06	− 0.05	− 0.09	− 0.36
p	1.18E-08	5.84E-01	1.33E-02		2.33E-06	9.08E-03	5.05E-01	5.86E-04	6.00E-01	6.83E-01	4.05E-01	1.02E-03
TBP												
r	− 0.77	− 0.72	-0.29	-0.51		0.87	0.75	0.30	0.11	0.24	0.56	0.91
p	0.00E+00	0.00E+00	9.11E-03	2.33E-06		0.00E+00	0.00E+00	7.37E-03	3.24E-01	2.90E-02	1.21E-07	0.00E+00
ABP												
r	− 0.85	− 0.83	-0.39	-0.29	0.87		0.80	0.34	0.23	0.39	0.75	0.97
p	0.00E+00	0.00E+00	4.58E-04	9.08E-03	0.00E+00		0.00E+00	2.15E-03	3.85E-02	4.05E-04	0.00E+00	0.00E+00
BBP												
r	− 0.52	− 0.77	-0.02	-0.06	0.75	0.80		0.55	0.12	0.18	0.49	0.81
p	1.10E-06	0.00E+00	8.93E-01	5.05E-01	0.00E+00	0.00E+00		1.96E-07	2.90E-01	1.07E-01	4.74E-06	0.00E+00
GBP												
r	0.11	− 0.35	0.10	0.38	0.30	0.34	0.55		-0.25	-0.04	0.19	0.30
p	3.20E-01	1.44E-03	3.63E-01	5.86E-04	7.37E-03	2.15E-03	1.96E-07		2.42E-02	7.18E-01	9.82E-02	7.83E-03
MSC												
r	− 0.35	− 0.23	− 0.21	− 0.06	0.11	0.23	0.12	− 0.25		0.64	0.57	0.28
p	1.77E-03	4.42E-02	5.96E-02	6.00E-01	3.24E-01	3.85E-02	2.90E-01	2.42E-02		0.00E+00	8.13E-08	1.15E-02
ImC												
r	− 0.42	-0.38	− 0.38	− 0.05	0.24	0.39	0.18	− 0.04	0.64		0.70	0.41
p	1.17E-04	5.83E-04	5.97E-04	6.83E-01	2.90E-02	4.05E-04	1.07E-01	7.18E-01	0.00E+00		0.00E+00	1.50E-04
SL												
r	− 0.68	− 0.67	− 0.42	− 0.09	0.56	0.75	0.49	0.19	0.57	0.70		0.77
p	0.00E+00	0.00E+00	1.42E-04	4.05E-01	1.21E-07	0.00E+00	4.74E-06	9.82E-02	8.13E-08	0.00E+00		0.00E+00
MI												
r	− 0.85	− 0.82	-0.34	− 0.36	0.91	0.97	0.81	0.30	0.28	0.41	0.77	
p	0.00E+00	0.00E+00	2.25E-03	1.02E-03	0.00E+00	0.00E+00	0.00E+00	7.83E-03	1.15E-02	1.50E-04	0.00E+00	

Table 1. The calculated Spearman correlation coefficients *r* between the pairs ($n = 80$) of different markers and corresponding *p*-values estimated by t-test. The $p < 0.00076$ ($|r| > 0.37$) indicates statistical significance.

symptoms. The ability of a marker to reveal disorders is based on both, the wide scale of EEG features incorporated by the markers determined by the number of correlated markers and the strengths of the correlations. A quantitative evaluation of different markers can be useful to compare their potential to reveal a wide scale of symptoms characteristic of various mental disorders. Therefore, an indicator describing the effectiveness of markers is used. The effectiveness of a marker E_i can be estimated as the product of the number of markers N_i correlated with marker i and the average value of the corresponding correlation coefficients R_i.

Figure 4 presents the effectiveness of each discussed in the current study markers. According to the graphs, the markers can be divided into three groups. The first group, HFD, SL, MI, and ABP, contains the markers expected to incorporate a wide scale of EEG features. The second group of markers DFA, TBP, BBP, and ImC covers a more specific part of EEG features. The markers GBP, MSC, LZC, and SASI from the third group can be useful for the detection of only a specific EEG feature. All the groups contain markers from all categories, band power, dynamics, and functional connectivity.

To provide a high-quality classification, the reasonable selection is an EEG marker from the first group correlated with many others and so incorporating very different features of the signal. The dynamic marker HFD is the marker of the highest effectiveness and is expected to incorporate a maximal part of the information from the EEG signal. This conclusion is supported by many studies where HFD has been successfully used for the detection of small alterations in EEG related to different factors such as depression, anxiety, or microwave radiation[22,37–40]. The traditional EEG band power marker ABP is the most commonly used band power marker which has shown good sensitivity in various applications[2,4,6,7].

Two functional connectivity markers in the first group SL and MI demonstrate that both, phase relations and power are important in brain functional connectivity.

The marker from the second group DFA has demonstrated high classification accuracy for depression[13,14]. DFA combined with alpha band improved the classification accuracy of Alzheimer's disease[10]. The combination of ImC and cluster-span threshold has been reported optimal in graph theory analyses of depression[20].

In addition, a second marker from the third group uncorrelated with the first one (e.g. GBP or LZC) can be useful, containing information about the features not incorporated in the first marker. This suggestion is supported by the analyses of depression EEG where the combinations of HFD and less correlated LZC lead to better classification accuracy compared to the combination of HFD and more correlated DFA[15].

The effectiveness of GBP is low due to a very low level of gamma-band power in the EEG signal (less than 4% of total EEG power according to the scales in Fig. 1). Gamma-band power is not able to affect much the main features of the signal and the other markers. However, the information in GBP is independent of that in other markers and can add a noticeable contribution to the quality of classification in combination with other markers when used as an additional marker in classification[15].

Table 1 shows that the correlation between the markers of different categories and different nature is not lower than the correlation between markers of the same category and similar nature. The correlation similar level of inter- and intra-categories correlations shows that the impact of the signal properties in the correlation between markers is not lower than the impact of the nature of the markers.

Today, no sufficient knowledge about brain functioning is available to explain the result of the study. Only some interesting trends in the relationships between the markers can be outlined.

There is a possibility that a high correlation of ABP with many other markers can be related to the higher power in the alpha band compared to other bands. The strength of the correlation of MI with band power markers follows the level of the power: 0.97 with ABP, 0.91 with TBP, 0.81 with BBP, and 0.30 with GBP. The strength of the correlation between SL and band powers shows the same trend. Such a trend agrees with the low effectiveness and correlation of GBP due to the low level of gamma band power. Despite that, gamma oscillations contain useful information and have been shown as a promising biomarker of depression[41].

Interestingly, the correlation between the real and imaginal parts of coherence MSC and ImC 0.64 is lower than the correlation between two phase-sensitive markers ImC and SL 0.7. Such a trend supports the idea that the markers of similar signal property, phase, are more strongly correlated than the markers of different properties,

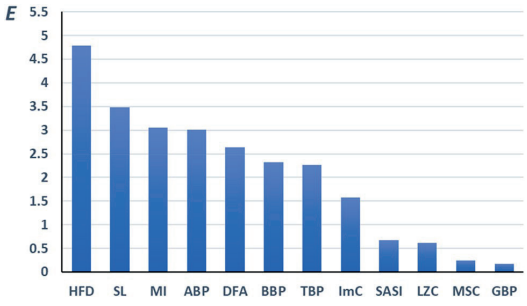

Figure 4. The effectiveness E of the EEG markers in detecting a wide spectrum of different EEG features. $E = NR$, where N is the number of markers correlated with the indicated marker and R is the average value of the corresponding correlation coefficients.

phase and power. However, no specific general trends between linear or nonlinear markers calculated in frequency or time domain become evident.

The dynamic markers indicate a negative correlation with all band power markers (except GBP) and all functional connectivity markers. Fractal dimensions and other dynamic markers are scale-invariant and, in principle, independent of signal level. Their correlation with band power markers should be explained by processes other than dependence on the level of the signal. The decreasing of dynamics with an increase in connectivity is possible, but the mechanisms behind that are unknown.

The presented in Figs. 1, 2 and 3 and Table 1 results demonstrate that the two-channel functional connectivity markers are more strongly correlated than the single-channel band power or dynamics markers. The stronger correlation between the two-channel markers is a rather unforeseen result because the possible chaotic instabilities in two channels are stronger than in one. For example, the temporal stability of two-channel markers has been reported lower compared to single-channel markers[42].

The results of the current study suggest that the HFD incorporating many various features of the signal is the best choice for EEG analysis to reveal signal features characteristic of early-stage mental disorders. The reported result may have a more general significance because the same markers can be used for signals other than EEG in several other applications.

The current study proves for the first time the correlation between different EEG markers. The difficulties in interpretation of the characteristic trends in the correlation between the markers underline the need for further investigations on the topic to get new knowledge about brain functioning and the relationship with EEG.

Limitations of the study

There are several limitations in the study. The limitations are partly related to the concentration of the study on the evaluation of raised hypotheses,

The number of participants is limited due to the limitations in the volume of the study. The number is sufficient to provide the reliability of statistical evaluation for the whole. But this is insufficient for splitting subjects into smaller subgroups (male–female, old-young, etc.) because statistical comparisons become unreliable.

The results can be affected by factors other than the mental state of the brain. The possible impacts of gender and age are not considered. The possible dependencies of correlation on gender and age need further investigation.

The possible variations of the correlation in different brain areas and EEG channels are not discussed. Depression, and most likely other mental disorders, affect EEG signal in all brain areas[9,43]. Despite that, the correlation between markers can differ in different brain areas and channels. This problem needs future investigations.

Not all markers used by various researchers for the detection of symptoms of mental disorders have been discussed in the study. The selection of markers has been limited by the volume of the study. The interpretable makers describing different features of the brain activity used in more than one study have been preferred. Additional investigations on the correlation for the markers of interest can be performed in the future.

Data availability

Data are available upon request from the corresponding author.

Received: 20 February 2023; Accepted: 12 April 2023
Published online: 18 April 2023

References

1. WHO. World mental health report: Transforming mental health for all. 16 June 2022. Report (2022). https://www.who.int/publications/i/item/9789240049338
2. Freeman, W. J., & Quian Quiroga, R. *Imaging brain function with EEG: Advanced temporal and spatial analysis of electroencephalographic signals*. New York: Springer, 265 p. (2013). https://dl.uswr.ac.ir/bitstream/Hannan/140344/1/9781461449836.pdf
3. Jaworska, N. & Protzner, A. Electrocortical features of depression and their clinical utility in assessing antidepressant treatment outcome. *Rev. Can J. Psychiatry.* **58**, 509–514 (2013).
4. de Aguiar Neto, F. S. & Rosa, J. L. G. Depression biomarkers using noninvasive EEG: A review. *Neurosci. Biobehav. Rev.* **105**, 83–93 (2019).
5. Knott, V., Mahoney, C., Kennedy, S. & Evans, K. EEG power, frequency, asymmetry and coherence in male depression. *Psychiatry Res.* **106**, 123–140 (2001).
6. Jaworska, N., Blier, P., Fusee, W. & Knott, V. Alpha power, alpha asymmetry and anterior cingulate cortex activity in depressed males and females. *J. Psychiatr. Res.* **46**, 1483–1491 (2012).
7. Zoon, H. F. *et al.* EEG alpha power as an intermediate measure between brain-derived neurotrophic factor Val66Met and depression severity in patients with major depressive disorder. *J. Clin. Neurophysiol.* **30**, 261–267 (2013).
8. Newson, J. J. & Thiagarajan, T. C. EEG frequency bands in psychiatric disorders: A review of resting state studies. *Front. Hum. Neurosci.* **12**, 521. https://doi.org/10.3389/fnhum.2018.00521 (2019).
9. Lee, J. S. *et al.* Detrended fluctuation analysis of resting EEG in depressed outpatients and healthy controls. *Clin. Neurophysiol.* **118**, 2489–2496 (2007).
10. Abásolo, D., Hornero, R., Escudero, J. & Espino, P. A study on the possible usefulness of detrended fluctuation analysis of the electroencephalogram background activity in Alzheimer's disease. *IEEE Trans. Biomed. Eng.* **55**(9), 2171–2179 (2008).
11. Li, Y. *et al.* Abnormal EEG complexity in patients with schizophrenia and depression. *Clin. Neurophysiol.* **119**, 1232–1241 (2008).
12. Ahmadlou, M., Adeli, H. & Adeli, A. Fractality analysis of frontal brain in major depressive disorder. *Int. J. Psychophysiol.* **85**, 206–211 (2012).
13. Hosseinifard, B., Moradi, M. H. & Rostami, R. Classifying depression patients and normal subjects using machine learning techniques and nonlinear features from EEG signal. *Comput. Methods Programs Biomed.* **109**, 339–345 (2013).
14. Bachmann, M. *et al.* Methods for classifying depression in single channel EEG using linear and nonlinear signal analysis. *Comput. Methods Programs Biomed.* **155**, 11–17 (2018).

15. Hinrikus, H. *et al.* Electroencephalographic spectral asymmetry index for detection of depression. *Med. Biol. Eng. Comput.* **47**, 1291–1299 (2009).
16. Fingelkurts, A. A. *et al.* Impaired functional connectivity at EEG alpha and theta frequency bands in major depression. *Hum. Brain. Mapp.* **28**, 247–261 (2007).
17. Leuchter, A. F., Cook, I. A., Hunter, A. M., Cai, C. & Horvath, S. Resting-state quantitative electroencephalography reveals increased neurophysiologic connectivity in depression. *PLoS ONE* **7**(2), e32508 (2012).
18. Li, X. *et al.* A resting-state brain functional network study in MDD based on minimum spanning tree analysis and the hierarchical clustering. *Complexity* **2017**, 9514369. https://doi.org/10.1155/2017/9514369 (2017).
19. Olbrich, S., Tränkner, A., Chittka, T., Hegerl, U. & Schönknecht, P. Functional connectivity in major depression: Increased phase synchronization between frontal cortical EEG-source estimates. *Psychiatr. Res. Neuroimaging* **222**, 91–99 (2014).
20. Sun, S. *et al.* Graph theory analysis of functional connectivity in major depression disorder with high-density resting state EEG data. *IEEE Trans. Neural Syst. Rehabil. Eng.* **27**, 429–439 (2019).
21. Mahato, S. & Paul, S. Electroencephalogram (EEG) signal analysis for diagnosis of major depressive disorder (MDD): A review. In *Nanoelectronics, Circuits and Communication Systems. Lecture Notes in Electrical Engineering* Vol. 511 (eds Nath, V. & Mandal, J.) (Springer, 2019). https://doi.org/10.1007/978-981-13-0776-8_30.
22. Čukić, M., Stokić, M., Simić, S. & Pokrajac, D. The successful discrimination of depression from EEG could be attributed to proper feature extraction and not to a particular classification method. *Cog Neurodyn.* **14**, 443–455 (2020).
23. Bonita, J. D. *et al.* Time domain measures of inter-channel EEG correlations: A comparison of linear, nonparametric and nonlinear measures. *Cogn Neurodyn.* **8**, 1–15 (2014).
24. Wang, B. *et al.* Depression signal correlation identification from different EEG channels based on CNN feature extraction. *Psychiatr. Res. Neuroimaging* **328**, 111582 (2023).
25. Higuchi, T. Approach to an irregular time series on the basis of the fractal theory. *Physica D* **31**, 277–283 (1988).
26. Peng, C. K., Havlin, S., Stanley, H. E. & Goldberger, A. L. Quantification of scaling exponents and crossover phenomena in non-stationary heartbeat time series. *Chaos* **5**, 82–87 (1995).
27. Lempel, A. & Ziv, J. On the complexity of finite sequences. *IEEE Trans. Inf. Theory.* **22**, 75–81 (1976).
28. Kay, S. M. *Modern Spectral Estimation* (Prentice-Hall, 1988).
29. Nolte, G. *et al.* Identifying true brain interaction from EEG data using the imaginary part of coherency. *Clin. Neurophysiol.* **115**, 2292–2307 (2004).
30. Stam, C. J. & Van Dijk, B. W. Synchronization likelihood: An unbiased measure of generalized synchronization in multivariate data sets. *Physica D* **163**, 236–251 (2002).
31. Fraser, A. M. & Swinney, H. L. Independent coordinates for strange attractors from mutual information. *Phys. Rev. A.* **33**, 1134–1140 (1986).
32. Yao, D. A method to standardize a reference of scalp EEG recordings to a point at infinity. *Physiol. Meas.* **22**, 693–711 (2001).
33. Qin, Y., Xu, P. & Yao, D. A comparative study of different references for EEG default mode network: The use of the infinity reference. *Clin. Neurophysiol.* **121**, 1981–1991 (2010).
34. Päeske, L. *et al.* Surrogate data method requires end-matched segmentation of electroencephalographic signals to estimate non-linearity. *Front. Physiol.* **9**, 1350. https://doi.org/10.3389/fphys.2018.01350 (2018).
35. Ibáñez-Molina, A. J., Soriano, M. F. & Iglesias-Parro, S. Mutual information of multiple rhythms for EEG signals. *Front. Neurosci.* **14**, 574796. https://doi.org/10.3389/fnins.2020.574796 (2020).
36. Päeske, L., Hinrikus, H., Lass, J., Raik, J. & Bachmann, M. Negative correlation between functional connectivity and small-worldness in the alpha frequency band of a healthy brain. *Front. Physiol.* **11**, 910. https://doi.org/10.3389/fphys.2020.00910 (2020).
37. Hinrikus, H. *et al.* Higuchi's fractal dimension for analysis of the effect of external periodic stressor on electrical oscillations in the brain. *Med. Biol. Eng. Comput.* **49**, 585–591 (2011).
38. Kawe, T. N. J., Shadli, S. M. & McNaughton, N. Higuchi's fractal dimension, but not frontal or posterior alpha asymmetry, predicts PID-5 anxiousness more than depressivity. *Sci. Rep.* **9**, 19666. https://doi.org/10.1038/s41598-019-56229-w (2019).
39. Hosseini, Z., Delpazirian, R., Lanjanian, H., Salarifar, M. & Hassani-Abharian, P. Computer gaming and physiological changes in the brain: An insight from QEEG complexity analysis. *Appl. Psychophysiol. Biofeedback* **46**, 301–308 (2021).
40. Olejarczyk, E., Gotman, J. & Frauscher, B. Region-specific complexity of the intracranial EEG in the sleeping human brain. *Sci. Rep.* **12**, 451. https://doi.org/10.1038/s41598-021-04213-8 (2022).
41. Fitzgerald, P. J. & Watson, B. O. Gamma oscillations as a biomarker for major depression: An emerging topic. *Transl. Psychiatry* **8**(1), 177. https://doi.org/10.1038/s41398-018-0239-y (2018).
42. Põld, T., Päeske, L., Hinrikus, H., Lass, J. & Bachmann, M. Long-term stability of resting state EEG-based linear and nonlinear measures. *Int. J. Psychophysiol.* **159**, 83–87 (2021).
43. Fingelkurts, A. A. Altered structure of dynamic electroencephalogram oscillatory pattern in major depression. *Biol. Psychiatry.* **77**, 1050–1060 (2015).

Acknowledgements

This study was financially supported by the Estonian Centre of Excellence in IT (EXCITE) TAR16013 funded by the European Regional Development Fund.

Author contributions

L.P. and M.B. performed E.E.G. recordings and signal processing, T.U., H.H. and J.L. performed the statistical evaluation, prepared figures and table. All authors contributed to the design of the study, discussion of results, and writing the manuscript. All authors have read and approved the manuscript.

Competing interests

The authors declare no competing interests.

Additional information

Correspondence and requests for materials should be addressed to H.H.

Reprints and permissions information is available at www.nature.com/reprints.

Publisher's note Springer Nature remains neutral with regard to jurisdictional claims in published maps and institutional affiliations.

Appendix 2 – Publication II

Publication II

Uudeberg, T., Belikov, J., Päeske, L., Hinrikus, H., Liiv, I., & Bachmann, M. (2024). In-phase matrix profile: A novel method for the detection of major depressive disorder. Biomedical Signal Processing and Control, 88, 105378. https://doi.org/10.1016/j.bspc.2023.105378d

Biomedical Signal Processing and Control 88 (2024) 105378

Contents lists available at ScienceDirect

Biomedical Signal Processing and Control

journal homepage: www.elsevier.com/locate/bspc

In-phase matrix profile: A novel method for the detection of major depressive disorder

Tuuli Uudeberg [a,*], Juri Belikov [b], Laura Päeske [a], Hiie Hinrikus [a], Innar Liiv [b], Maie Bachmann [a]

[a] Department of Health Technologies, School of Information Technologies, Tallinn University of Technology, Tallinn, Estonia
[b] Department of Software Science, School of Information Technologies, Tallinn University of Technology, Tallinn, Estonia

ARTICLE INFO

Keywords:
Electroencephalography
Euclidean distance
Higuchi's fractal dimension
In-phase matrix profile
Major depressive disorder
Similarity search

ABSTRACT

Background and Objective: Major depressive disorder (MDD) is the leading cause of disability worldwide. Reliable detection of MDD is the basis for early and successful intervention in treating the disorder and preventing disability. We introduce a novel feature extraction method, the in-phase matrix profile (pMP), which is specifically adapted for electroencephalographic (EEG) signals. Methods: The pMP characterizes general self-similarity of an EEG signal. The method extracts overlapping one-second-long subsegments from an EEG signal segment, calculates Euclidean distances between all possible subsegment pairs, and subsequently uses the distance values, where subsegments are most in phase, to calculate pMP. The method was applied to the resting-state eyes-closed EEG data of an MDD group and age- and gender-matched healthy controls (66 subjects). Higuchi's fractal dimension (HFD) values were calculated for the same groups for comparison. Results: Both pMP and HFD values were higher in MDD. The pMP successfully distinguished MDD and control group in all 30 EEG channels. In contrast, HFD resulted in statistically significant group distinguishability in 13 (43%) channels located mainly in the central region of the head. The highest classification accuracy for pMP was 73% and for HFD 67%. Conclusion: The present article shows that pMP outperforms HFD in detecting MDD and is a promising method for future MDD studies. Significance: The pMP is a sensitive parameter-free method for detecting MDD that can be used in future studies and is a potential method to reach clinical use for diagnosing MDD.

1. Introduction

Depression is a common disease that, depending on its severity, can strongly affect a person's daily ability to cope and even lead to suicide. Approximately 280 million people worldwide suffer from major depressive disorder (MDD, also referred to as clinical or unipolar depression), which makes it the leading cause of disability in the world [1], and the number has constantly been rising. Preliminary evidence indicates that the recent severe acute respiratory syndrome coronavirus 2 (SARS-CoV-2), which caused the COVID-19 pandemic, has also significantly increased the number of people suffering from MDD [2] and the extent of the full impact of the pandemic on mental health is yet to be seen.

There are different medications and treatment therapies available for MDD. However, many people do not get the help they need, especially in less developed countries [3]. Treatment availability is limited due to several factors, such as the small number of healthcare professionals, misdiagnosis, and the continuing social stigma associated with mental health problems. At present, MDD diagnosis and treatment monitoring are based on clinical interviews and questionnaires, which depend on the health professionals' experience and the answers given by the examinee. Therefore, the health assessment is based on subjective symptoms, and the conclusions may not be objective. No method, which provides an evaluation based on objective symptoms, is yet in use in clinical practice.

Neuronal activity in the brain is related to all physiological and emotional processes in a human. The brain's bioelectrical signals describe the state of the brain [4], and electroencephalography (EEG) can detect changes in the brain's bioelectric activity. In the case of mental disorders, including MDD, changes in the brain's electric activity occur [5–7], and EEG is a method suitable for detecting bioelectric changes related to mental disorders [7]. The alterations in EEG may appear even before the changes in well-being do, and the EEG features can be the input for an objective tool for assessing the state of the brain. EEG is also appropriate due to its portability and relatively low cost.

The EEG method has long been used to detect various mental

* Corresponding author at: Department of Health Technologies, School of Information Technologies, Tallinn University of Technology, Tallinn 19086, Estonia.
E-mail address: tuuli.uudeberg@taltech.ee (T. Uudeberg).

https://doi.org/10.1016/j.bspc.2023.105378
Received 1 March 2022; Received in revised form 12 July 2023; Accepted 14 August 2023
Available online 21 August 2023

disorders in research studies [4,7]. Several authors have used different linear EEG methods to detect various brain states/disorders [7–11]. Still, due to the complex nonlinear nature of the EEG signal [12], different nonlinear methods have been engaged to provide more information about mental health. In MDD studies, much attention has been paid to the alpha rhythm, and attempts have been made to find a possible indicator of MDD using only the alpha frequency. Initially, frontal alpha asymmetry [13] was promising, but today it has yielded unreliable results [10,14]. It has also been found that MDD can lower the alpha peak frequency, increase the coefficient of variation [15], and functional connectivity in the alpha frequency band [16].

Nonlinear methods such as fractal dimensions, detrended fluctuation analysis, and correlation dimensions are used to calculate EEG signal complexity measures that have been shown to be indicative of epilepsy [17,18], schizophrenia [19], Alzheimer's [20], and MDD [21–25]. It has been found that the values of features characterizing the complexity of EEG signals are higher in MDD, including fractal dimension estimate called Higuchi's fractal dimension (HFD). HFD is one of the most used nonlinear methods to study MDD and has shown some promising results in distinguishing between MDD and control subjects [9,23,24,26–28]. Although previous research has provided information in which direction EEG features' values in MDD typically change, the distinctiveness of independent groups has been insufficient. The results have not been consistent enough to reach clinical use. Therefore, there is a continuing need to find an even more sensitive method or combination of methods for evaluating the presence or the severity of MDD.

In this paper, we continue this line of research and propose a novel method to characterize the brain's state and help identify MDD. The hypothesis is that a method using a novel approach for considering the temporal complexity of the EEG signal can provide higher sensitivity in the detection of MDD than the previously used methods. We developed the method primarily for resting-state EEG signals, and it describes the complexity of EEG signals via general self-similarity. The proposed in-phase matrix profile (pMP) is a simple-to-use parameter-free method calculated directly in the time domain. The method is based on the Matrix Profile (MP) idea introduced by Yeh et al. [29], which divides a time signal into subsegments and compares the similarity between those subsegments, searching for the best matching subsegments. Unlike in the classic MP, in our method, the length of the subsegments is fixed, and all EEG subsegments that are in phase with each other are used in the calculations of pMP. We compare the proposed novel pMP with the widely used approach based on Higuchi's fractal dimension (HFD) [28].

The remainder of the paper is organized as follows: Section II introduces the classical methods and terminology on which pMP is based and explains the need to modify these methods for resting-state EEG signals. Section III describes the EEG data collection procedure, data preprocessing and explains the calculation procedure of our proposed method according to the preprocessed data. Section IV presents the MDD and control group results for pMP and HFD. Section V explains the nature and limitations of the results obtained and suggests the direction of future research. Finally, Section VI draws the conclusion.

2. Background and related work

2.1. Data mining

As the overall volume of data around us snowballs, different data mining algorithms are evolving in the same way. An essential part of data mining is similarity search, where large amounts of data are searched for patterns or trends in the data set. Popular methods include the distance range query (finds all elements in a data set where the distance from the query to set members is less than a given threshold) and the k-nearest neighbor query (retrieves k elements from a dataset with the lowest distances to query). Those methods have been used in many fields, such as marketing analysis [30], text and document mining [31], and multimedia analysis [32]. The input (query) can be an image, a word, a sound, a traffic sign, sales data, electricity consumption, etc., and the algorithm searches for a match that meets the specified requirements for that query in a given database.

The EEG signal can be viewed as a large amount of data, and thus data mining algorithms can also be used for EEG signals. Mining EEG signals have been used when working with evoked potentials or looking for a specific pattern, such as blinking [33], exploring the brain's pathways (synchronization likelihood) [34,35], or in sleep studies [36].

2.2. Matrix profile and its limitations in EEG data

In 2016, Yeh et al. [29] presented a new fast similarity search algorithm for data mining, Matrix Profile (MP), which can quickly find from a tremendous amount of data, e.g., electricity consumption over the years, accurate matches where consumption has been most similar or has changed from usual. The advantage of this method is that it is unnecessary to set a threshold below which comparable elements can be considered a match. That allows the MP to be used for time series without fear that some information might go unnoticed due to an unsuitable threshold set. MP is an effective way to find similarities and differences in time signals with a quasi-periodic pattern. The method detects a previously unknown (or known) repeating pattern, a motif, from the time signal. Recently, MP has been used to analyze physiological signals, e.g., electrocardiographic signals (ECG) [37]. In the case of ECG, the motif is a cardiac cycle, and the MP will be able to find anomalies, i.e., a discrepancy from the usual motif pattern, thereby detecting a change in the normal functioning of the heart. The key component for calculating similarity in MP is Mueen's Algorithm for Similarity Seach (MASS) [38].

The EEG is inherently a very periodic signal, being a combination of brain waves of different frequencies. In the eyes-closed relaxed state, the most outstanding frequency is the posteriorly dominant alpha rhythm. Thus, on the one hand, there are no repetitive-looking patterns in an average resting-state EEG signal. Still, on the other hand, it can become visibly very periodic with the dominance of the alpha wave. Therefore, EEG differs significantly from quasi-periodic physiological signals, such as an ECG signal, so the MP method described above cannot detect changes in EEG unless the EEG changes considerably over time, such as in epilepsy; there is no such pattern change in EEG for MDD. In the case of resting-state EEG, looking at signals' general self-similarity is more effective, which is what our new method does.

2.3. Definitions and notations

Here we define the principal terms and ideas common in related research and our proposed method. As our method is based on distance profiles, we explain how they can be calculated and the essence of distance profiles.

Segment is a time series $S = s_1, s_2, \ldots, s_n$ of length n.

Subsegment set $S_{i,m}$ is a continuous subset of subsegments extracted from S of the length m starting from position i, where $1 \le i \le n\text{-}m + 1$. $S_{i,m} = s_{1:m}, s_{2:m+1}, \ldots, s_{n\text{-}m+1:n}$.

Query q is one specific subsegment from the set $S_{i,m}$ from which the (Euclidean) distances to all subsegments in $S_{i,m}$ are calculated.

Euclidean distance (ED). Both MP and pMP are based on the idea of ED, which in this article shows the distance between two subsegments selected from $S_{i,m}$ in Euclidean space. The smaller the value for ED, the more similar the two subsegments are. By taking any two subsegments from $S_{i,m}$ (query q and a random subsegment s), the Euclidean distance between them can be calculated as in

$$\mathrm{ED}(q, s) = \sqrt{\sum_{j=1}^{m} (q_j - s_j)^2}. \quad (1)$$

For every ED calculation, the query and the subsegment are first z-normalized. The z-normalization is done as follows: the mean is

subtracted and divided by the standard deviation to get the zero mean and standard deviation of one for each subsegment.

Distance profile (DP). By taking the i-th subsegment from the set $S_{i,m}$ as a query q_i and calculating the distances between q_i and all subsegments in $S_{i,m}$, we get an array of distance values, e.g., the distance profile DP_i corresponding to the i-th subsegment [29] as in

$$DP_i = ED(q_i, s_{1:m}),\ ED(q_i, s_{2,m+1}),\ \ldots,\ ED(q_i,\ s_{n-m+1:n}) \quad (2)$$

As $S_{i,m}$ contains n-m + 1 subsegments, the same number of DP-s can be calculated. Fig. 1 illustrates graphically how the subsegments are selected between which the ED is calculated and how they form the DP-s.

The DP calculation using the conventional multilevel Euclidean distance calculation (also called the naïve method) described above (2) is computationally expensive. Another way to compute DP-s is like in MP

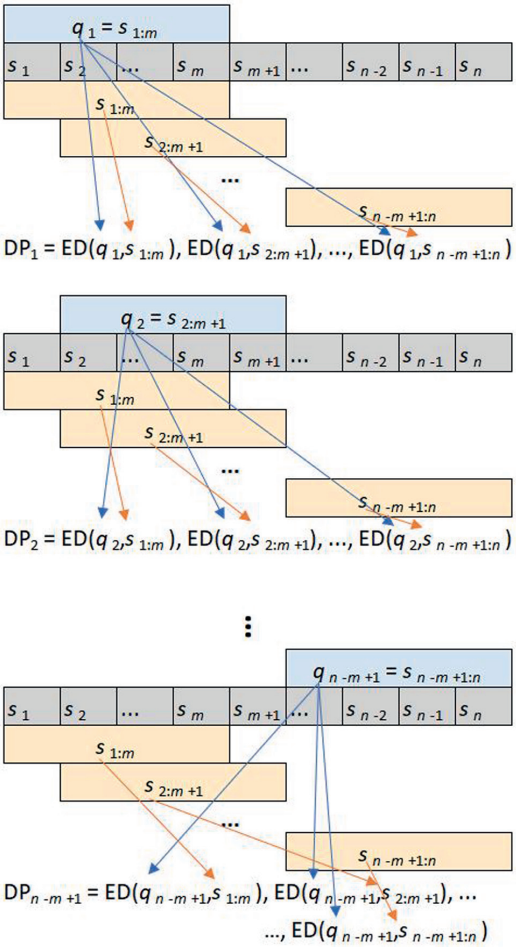

Fig. 1. Extraction and selection of subsegments for calculating distance profiles (DP-s) for an EEG signal segment $S = s_1, s_2, \ldots, s_n$. First, n-m + 1 subsegments ($s_{1:m}$, $s_{2:m+1}$, …, $s_{n\text{-}m+1:n}$) with the length m are extracted from S. Each subsegment is then used as query q, and Euclidean distances (ED-s) are calculated from each q to all subsegments extracted from S. By calculating the distance from a single query to all subsegments, we get the DP corresponding to that particular query. After all possible subsegments have been used as queries, n-m + 1 DP-s are obtained.

using the MASS algorithm (and other versions, e.g., MASS_V2) [38] to speed up the calculation but still get the same DP-s as using the naïve method. The MASS_V2 uses z-normalized Euclidean distance as a subroutine, exploiting the overlap between subsegments using the fast Fourier transform (FFT) algorithm to calculate dot products to retrieve all distances from a query to all subsegments in $S_{i,m}$ extracted from the time signal S. In that way, it is possible to get a full DP corresponding to one query significantly faster than with the naïve method, which is generally not used for large amounts of data due to time constraints. The code for MASS_V2 is presented in [39].

In the case of classic MP, only the minimum value of each DP is used, excluding trivial matches. The DP minimum value indicates how similar the query and the best matching subsegment from the rest of the segment are. The minimum values from each DP form a sequence called the MP. In our proposed method, we use several values from each DP. In the next chapter, we describe the EEG data on which we applied our proposed method and the specificity of our method.

3. Method

3.1. Subjects

We recorded EEG data from medication-free outpatients diagnosed with MDD and age- and gender-matched healthy controls. Both groups comprised 33 right-handed subjects (12 males and 21 females). The mean age and standard deviation for the control and MDD group were 34.7 ± 15.0 and 34.5 ± 14.9, respectively, and the age ranged from 18 to 75 years. All MDD group subjects underwent a clinical interview and were diagnosed with MDD by a psychiatrist based on ICD-10 criteria. Healthy controls completed the official Estonian self-report questionnaire (Emotional State Questionnaire – EST-Q) [40] for depressive disorder and anxiety, and the subjects without indication of these mental disorders were selected. The subjects were instructed to abstain from alcohol for 24 h and coffee for two hours before recording.

The study was conducted following the Declaration of Helsinki and was formally approved by the Tallinn Medical Research Ethics Committee. Participation in the study was voluntary, and all subjects signed written informed consent.

3.2. EEG data collection

All the recordings were conducted between 9 am and 12 pm using a Neuroscan Synamps2 acquisition system and a 32-channel Quick-Cap (Compumedics, NC, USA). The Quick-Cap employs electrode positioning according to the extended international 10/20 system. During the recording procedure, participants were lying in a relaxed supine position in a dimly lit laboratory room. Ten minutes of eyes-closed EEG data were acquired in 30 channels and electrooculograms in two channels (vertical and horizontal) to monitor eye movements. To achieve good conductivity between the skin and the electrode, the impedance of EEG electrodes was kept below 10 kΩ. The EEG data were recorded with a frequency band of 0.3 – 200 Hz at a sampling rate of 1000 Hz.

3.3. EEG data preprocessing

The data were processed using MATLAB software (The Mathworks, Inc.). EEG data were re-referenced using the reference electrode standardization technique (REST) [41]. REST relies on the idea that the EEG recordings are the brain activities generated by the neural current sources, which are attenuated and mixed due to volume conduction. It is a virtual reference that uses an equivalent source model to approximately re-reference EEG signals to a spatial location for a reference point at infinity to achieve roughly zero potential at the reference point, reflecting bioelectrical activity considerably only under the active electrode. Previous studies have shown that the REST reference is

suitable for low-density EEG montage and is a good reference technique for comparing the results across laboratories [42,43].

Parks-McClellan low and high-pass forward–backward filters were applied to the EEG signals to remove baseline fluctuations and high-frequency noise; a frequency bandwidth of 2 to 47 Hz remained for further processing. The calculations did not assume a high sampling rate, therefore, the EEG data were downsampled to 200 Hz. The first 6 min from each recording were used for the following processing and were divided into seventeen 20.48-second (4096 samples) long segments. EEG segments were visually inspected, and segments with muscle, ocular, or other artifacts were manually removed; each subject's first ten clean segments were used for further analysis (Fig. 2).

3.4. In-phase matrix profile

The proposed method, in-phase matrix profile (pMP), is specially adapted for EEG signals and considers the periodicity of alpha waves. The main idea is to calculate Euclidean distances between short subsegments extracted from an EEG signal segment and to use only those distance values where the subsegments are as well as possible in phase with each other and discard the distances where the subsegments are offset from each other.

First, we calculated DP-s using MASS_V2 for all queries in an EEG segment as in [39]. As DP calculation uses individually z-normalized subsections, it minimizes the effect of EEG electrode impedance variation during the EEG recording. Also, without z-normalization, EEG signal subsegments with higher absolute amplitude would have longer distances between them than lower amplitude signal subsegments even when more similar and z-normalization helps to reduce the chance of obtaining long distances incorrectly due to various amplitude effects. Our study used EEG signal segments of length 20.48 s ($n = 4096$ samples) as shown in Fig. 2 and subsegments of length one second ($m = 200$ samples). The graph in Fig. 3 illustrates one such EEG signal segment (S) and the red part represents the first query (q_1) extracted for DP_1 calculation. The DP of length n-$m + 1$ corresponding to the EEG signal segment and the extracted query presented in Fig. 3 is shown in Fig. 4. The DP in Fig. 4 has a sinusoidal appearance. When the query and comparable subsegments are more in phase, the distances are shorter and longer when the query and subsegments are out of phase.

Second, the ED values, where the query was most in phase with the EEG segment, were extracted from DP. Those ED values are seen as negative peaks marked with red circles (p_{neg}) in Fig. 4. As the method aims to find the similarity between EEG subsegments, ED values calculated between out-of-phase subsegments will be left aside.

Third, the median of the extracted ED values DP_{medi} (p_{neg}) was calculated for each DP forming a pMP vector (pMP_{vec}). As we pulled n-$m + 1$ different queries from S for the set $S_{i,m}$, we got n-$m + 1$ DP-s and consequently a pMP_{vec} with the length of n-$m + 1$.

Last, the mean of pMP_{vec} gave us the pMP value for the EEG segment. The calculation for this was as in

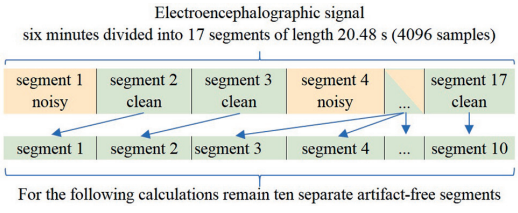

Fig. 2. EEG signal segments used for further calculations. Six minutes of recorded eyes-closed EEG signal was divided into 17 segments of length 20.48 s (4096 samples). After visually inspecting, the segments with muscular, ocular, or other artifacts were discarded. Ten separate clean segments remained for further calculations.

$$\mathrm{pMP} = \overline{\mathrm{pMP}_{\mathrm{vec}}} = \frac{1}{n-m+1} * \sum_{i=1}^{n-m+1} \mathrm{DP}_{\mathrm{med}_i}(p_{\mathrm{neg}}), \tag{3}$$

where DP_{medi} (p_{neg}) is the median value of all DP negative peaks p_{neg} for query i.

3.5. Higuchi's fractal dimension

Fractal dimensions are sensitive nonlinear methods to analyze waveform complexity of physiological signals and have been around for decades. Higuchi's fractal dimension [44] is one of the most used fractal dimension estimates considering EEG signals and is calculated in the time domain.

HFD is based on a measure of length (k) of the curve that represents the considered time series, whereas using a segment of k samples as a unit if $L(k)$ scales like $L(k) \sim k^{-\mathrm{FD}}$. The curve shows the fractal dimension (FD) and FD measures the complexity of the curve. In this study, the value of FD with a parameter $k_{max} = 8$ was calculated according to the algorithm described by Higuchi [44].

3.6. Statistics and classification

The present study aimed to examine the capability of the proposed new pMP parameter to differentiate between the MDD and the control group compared to HFD. The pMP and HFD values were calculated for all 30 EEG channels for all 66 subjects. Since we had ten signal segments for each subject's each channel, we used the median pMP and HFD values over these ten segments.

We used the Mann-Whitney U (MWU) test to compare the group differences. MWU test controls the hypothesis that two independent samples come from distributions with equal medians. Due to multiple comparisons, the modified Bonferroni correction was applied to the p values obtained from the MWU test, and the corrected p values p_{Bonf} were calculated as in

$$p_{\mathrm{Bonf}_j} = p_{\mathrm{sorted}_j} * (t + 1 - j) \tag{4}$$

where p_{sorted} are the p values obtained from the MWU test sorted in ascending order, t is the total number of tests performed ($t = 30$), and j is the index in descending order $j = t, t\text{-}1, t\text{-}2, \ldots, 1$. Channels up to the first p_{Bonf} value exceeding the significance level $\alpha = 0.05$ were considered statistically significant.

Support vector machine (SVM) with leave-one-out cross-validation was selected as a classifier. The classification accuracy was calculated for pMP and HFD separately using single-channel input.

4. Results

First, in this study, we used a novel pMP method to calculate EEG signals' complexity and examined how pMP distinguished between MDD and control group. Second, this study examined how well HFD differentiated between the two groups. Last, we compared the results obtained with both methods with each other. The group mean values for pMP and HFD in the healthy and MDD groups are presented in Table 1 and Fig. 5.

For both pMP and HFD, the mean values for the MDD group were higher than those for the control group. Both methods resulted in lower values in the occipital area and had higher values on the sides and prefrontal region. The differences in mean values between MDD and control group are shown in the last column of Fig. 5. The dots represent locations of the EEG channels, while extra-large dots represent channels, where the difference between the two groups was statistically significant based on the MWU test after modified Bonferroni correction ($p < 0.05$). The pMP method shows a statistically significant difference between the MDD and control group in all 30 EEG channels. In contrast, a statistically significant difference for HFD between the two groups was revealed in less than half of the channels (43%). Those channels are mainly located

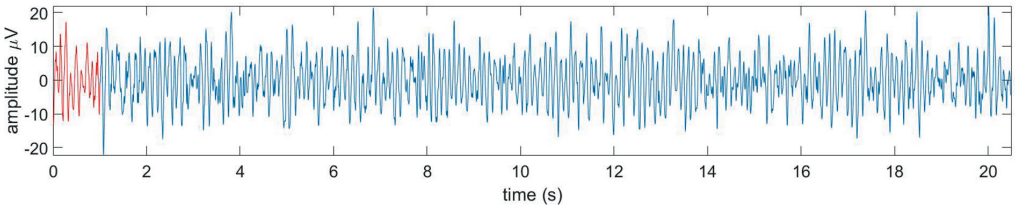

Fig. 3. EEG signal segment in channel FCz with the length of 20.48 s (4096 samples), red part represents the first query q_1 with the length of 1 s (200 samples) extracted from the EEG signal segment.

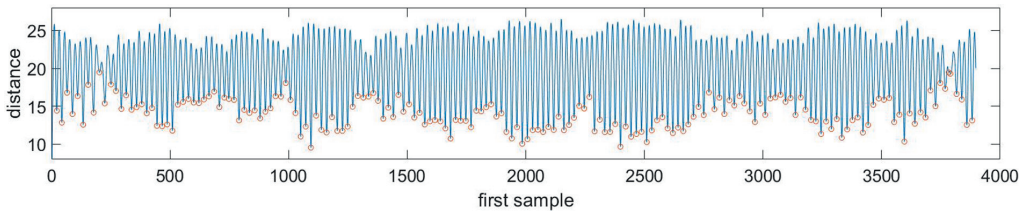

Fig. 4. An example of a Distance Profile (DP) corresponding to an EEG signal segment recorded in channel FCz of length 20.48 s (4096 samples) and a query of length 1 s (200 samples) extracted from the segment. The particular query and the segment are presented in Fig. 3. Red circles correspond to the distances, where the query is most in phase with the segment.

Table.1
The pMP and HFD mean values. Columns represent in-phase matrix profile (pMP) and Higuchi's fractal dimension (HFD) mean values across control and major depressive disorder (MDD) group; p_{Bonf} values are p values obtained from Mann-Whitney U Test with modified Bonferroni correction.

Channel	pMP			HFD		
	Control	MDD	p_{Bonf}	Control	MDD	p_{Bonf}
O2	16.098	17.166	**0.039**	1.263	1.310	**0.047**
O1	16.319	17.404	**0.039**	1.267	1.327	0.055
OZ	16.477	17.322	**0.032**	1.268	1.325	0.077
PZ	17.051	17.729	**0.038**	1.278	1.336	0.051
P4	16.929	17.697	**0.041**	1.280	1.340	0.058
CP4	17.631	18.247	**0.031**	1.323	1.386	**0.030**
P8	16.968	17.811	**0.038**	1.299	1.355	**0.034**
C4	17.700	18.400	**0.013**	1.340	1.408	**0.009**
TP8	18.075	18.636	**0.036**	1.377	1.438	0.051
T8	18.419	18.852	**0.036**	1.437	1.509	0.103
P7	17.336	18.291	**0.021**	1.318	1.388	**0.016**
P3	16.969	17.889	**0.036**	1.284	1.352	**0.026**
CP3	17.552	18.332	**0.011**	1.321	1.393	**0.005**
CPZ	17.409	18.212	**0.019**	1.302	1.373	**0.010**
CZ	17.496	18.329	**0.008**	1.325	1.398	**0.015**
FC4	17.477	18.200	**0.036**	1.332	1.398	0.052
FT8	18.079	18.624	**0.032**	1.393	1.457	0.093
TP7	18.274	18.772	**0.034**	1.400	1.453	0.085
C3	17.614	18.329	**0.005**	1.337	1.407	**0.007**
FCZ	17.322	18.150	**0.012**	1.307	1.376	**0.025**
FZ	17.123	17.975	**0.017**	1.291	1.358	**0.036**
F4	17.447	18.126	**0.026**	1.339	1.392	0.078
F8	17.950	18.611	**0.034**	1.384	1.466	0.077
T7	18.379	18.717	**0.031**	1.444	1.465	0.146
FT7	18.042	18.549	**0.032**	1.410	1.440	0.158
FC3	17.356	18.172	**0.015**	1.327	1.393	**0.035**
F3	17.300	18.093	**0.034**	1.326	1.393	0.071
FP2	18.064	18.611	**0.029**	1.429	1.489	0.155
F7	17.925	18.555	**0.035**	1.392	1.450	0.094
FP1	17.951	18.592	**0.033**	1.412	1.503	0.099

in the central region of the head (CP4, C4, P3, CP3, CPz, Cz, C3, FCz, Fz, FC3) and a few in the posterior region (O2, P7, P8).

The pMP appears to have greater symmetry in obtained values between the hemispheres, which is best illustrated by the difference between the MDD and control group in the third column of Fig. 5. In HFD, some asymmetry can be seen between the hemispheres while looking at the topoplot presenting the difference between the MDD and control group. Considering the channel locations indicating the statistically significant differences, the distinctiveness of the groups is somewhat better on the left side of the head. In pMP, the largest difference was observed in the occipital region, while in the case of HFD, the difference was smaller. Although HFD also provided a statistically significant distinction between the control and MDD group in 13 channels in the present study, the pMP result was considerably better, with significant group distinction in every channel.

We used SVM analysis to validate the obtained results. The highest classification accuracy using SVM was 73% in the case of pMP and 67% in the case of HFD.

5. Discussion

The results of the present study, which show higher HFD values for the MDD group compared to the control group, were expected. The results are consistent with previous studies [9,24,26,27], where the reported fractal dimension values were higher in the MDD group compared to the control group. In the present study, the lowest HFD values were in the occipital region regardless of the group. In contrast, HFD values obtained in [9], where the authors presented HFD values in eight channels, showed higher HFD values in the occipital area (O1, O2) and lower values in the prefrontal region (FP1, FP2) with the best MDD and control group distinguishability in parieto-occipital channels. The reason might be that in [9], the Cz channel was used as a reference, while in the current study, we used REST reference. The study by Zappasodi et al. [45] that also used REST reference like in this study, presented lower HFD values in the parieto-occipital area compared to fronto-central and side regions for the healthy control group, which is consistent with our results.

The pMP results have many similarities to those of HFD. Although pMP does not characterize fractality but is still a dimension of complexity, and similarly, the lower values are in the parieto-occipital region. Complexity measures, in general, tend to have higher values in MDD [9,24–27]. Therefore, pMP was also expected to have higher MDD values than the control group.

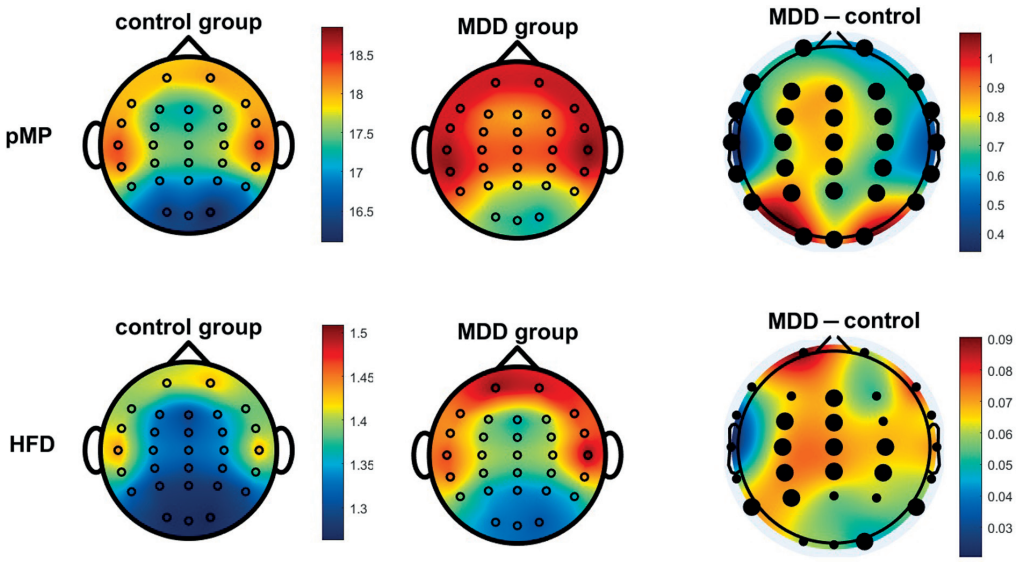

Fig. 5. Control and major depressive disorder (MDD) group mean values for in-phase matrix profile (pMP) in the first row and Higuchi's fractal dimension (HFD) in the second row for 30 EEG channels represented by dots. The MDD and control group differences (MDD – control) are shown in the last column. Extra-large dots represent channels where $p < 0.05$ according to the MWU test with modified Bonferroni correction.

Still, while looking at the pMP values for MDD and control subjects, both have lower values at the occipital region than other regions. The alpha frequency band dominates the occipital region, especially in eyes-closed conditions. This raises the question of whether pMP is strongly influenced by alpha frequencies. Fig. 4 presents a distance profile corresponding to an EEG signal subsegment and a query extracted from the segment for a random subject in the control group for channel FCz. This channel is located in the fronto-central region, so it has a relatively low alpha load. While looking at the negative peaks in Fig. 4, the mean interval between those peaks is 20 samples. Given that the sampling frequency is 200 Hz, this interval, 0.1 s, corresponds to a typical alpha wave duration illustrating that pMP is primarily influenced by the alpha rhythm even in the EEG channel FCz.

Considering that while calculating pMP, each one-second subsegment is individually z-normalized before calculating the ED, the effect of the amplitude of the EEG signal is minimized. Therefore, the pMP value is mainly affected not by the alpha amplitude but by the frequency fluctuations of the alpha frequency. In case the length of the alpha wave changes, the subsegments are no longer so well in phase with each other, resulting in a longer distance between the subsegments, which gives higher values for the DP negative peaks (Fig. 4). Wolff et al. [15] have demonstrated that the alpha peak frequency coefficient of variation is higher for MDD than controls. If the alpha rhythm's frequency variability is higher in the MDD group than in the control group, the higher pMP values for MDD subjects are justified. At the same time, as the most significant results do not appear in occipital channels - channels with the highest load of alpha frequency - other frequencies have a considerable impact, too. Still, the lowest pMP values at the occipital region can be explained by the high load of alpha frequencies, which are seemingly quite consistent in terms of frequency in the occipital region. The alpha frequency alone has been studied extensively in the assessment of MDD, and different levels of associations have been found [14–16], so it is plausible that the alpha frequency contains information about the presence of MDD.

It has been presented previously that the maximum classification accuracy for HFD was 77% when classifying depressive and control subjects in a single EEG channel [46]. At the same time, in the current study, it was 67%. Apart from different classification method, one has to take into account that in the previous study, the age range of subjects was more narrow and the number of subjects considerably smaller. Considering the results of the current study, pMP indicated somewhat better single-channel accuracy (73%) compared to HFD (67%).

There were some limitations to this study. First, the relatively small number of participants (n = 66) does not allow the results to be generalized. In the case of a small group, it is also not appropriate to divide it into subgroups based on gender, age, etc., and analyze the results of narrower groups separately, because there would be too few subjects in each group. Therefore, the method needs to be tested in larger groups. Second, the groups had large age variability. Still, at the same time, the subjects in MDD and control group were age- and gender-matched, which increases the comparability of the groups. However, with age, neurological changes occur in the human brain [47] and thus also changes in the bioelectrical signals measured using EEG. Therefore, it would be important to conduct a similar study to gain better knowledge, dividing the subjects into narrower age groups. It has been found that gender also significantly impacts EEG, and genders should also be analyzed separately [48]. Although the calculation of pMP using the MASS_V2 algorithm is very fast compared to the naïve method, the calculation of pMP is still more computationally intensive compared to HFD and therefore requires more resources. In the present study, we did not investigate the effect of noise on either method. Still, HFD has been shown to be sensitive to noise [49]. Low sensitivity to noise would be a relevant advantage of the measure used to assess MDD. However, as the effect of noise on pMP value and sensitivity has not been studied in the present work, it would be essential to perform a corresponding study. Since pMP values seem to be largely affected by alpha frequency fluctuations, it should be researched if the necessary information for MDD detection is hidden in the alpha frequency band alone. In addition, it could be investigated whether the method can also characterize the severity of MDD.

6. Conclusions

This article introduces a novel EEG-based nonlinear method, in-

phase matrix profile (pMP), for studying MDD. The pMP distinguished the MDD and control group in all 30 EEG channels studied, while HFD distinguished the two groups in 13 channels. As with other complexity measures, pMP values were higher for MDD. The method expresses the complexity of EEG signals and seems to be influenced by EEG alpha frequency. The peculiarity of the method is that it is not significantly affected by the amplitude of the signal.

CRediT authorship contribution statement

Tuuli Uudeberg: Writing – original draft, Methodology, Software, Conceptualization, Formal analysis, Visualization. **Juri Belikov:** Writing – review & editing, Methodology, Supervision. **Laura Päeske:** Writing – review & editing, Investigation, Software. **Hiie Hinrikus:** Writing – review & editing. **Innar Liiv:** Conceptualization. **Maie Bachmann:** Funding acquisition, Writing – review & editing, Supervision, Conceptualization, Investigation, Resources.

Declaration of Competing Interest

The authors declare that they have no known competing financial interests or personal relationships that could have appeared to influence the work reported in this paper.

Data availability

The authors do not have permission to share data.

Acknowledgments

This study was financially supported by the Estonian Centre of Excellence in IT (EXCITE), funded by the European Regional Development Fund.

References

[1] Institute of Health Metrics and Evaluation (IHME), Global Health Data Exchange (GHDx), 2019. Available: http://ghdx.healthdata.org/gbd-results-tool?params=gbd-api-2019-permalink/d780dffbe8a381b25e1416884959e88b. Last accessed 15.01.2022.

[2] Centers for Disease Control and Prevention (CDC), 2021. Household Pulse Survey. National Center for Health, U.S. Census Bureau. Available: https://www.cdc.gov/nchs/covid19/pulse/mental-health.htm. Last accessed 15.01.2022.

[3] P.S. Wang, S. Aguilar-Gaxiola, J. Alonso, M.C. Angermeyer, G. Borges, E.J. Bromet, R. Bruffaerts, G. de Girolamo, R. de Graaf, O. Gureje, J.M. Haro, E.G. Karam, R. C. Kessler, V. Kovess, M.C. Lane, S. Lee, D. Levinson, Y. Ono, M. Petukhova, J. Posada-Villa, S. Seedat, J.E. Wells, Use of mental health services for anxiety, mood, and substance disorders in 17 countries in the WHO world mental health surveys, Lancet 370 (2007) 841–850, https://doi.org/10.1016/S0140-6736(07)61414-7.

[4] A. Biasiucci, B. Franceschiello, M.M. Murray, Electroencephalography, Curr. Biol., 29(3) (2019) 80-85, https://doi.org/ 10.1016/j.cub.2018.11.052.

[5] D.C Van Essen, D.M. Barcht, The human connectome in healthy and psychopatology, World Psychiatry, 14(2) (2015) 154-157, https://doi.org/10.1002/wps.20228.

[6] P.J. Uhlhaas, Neural dynamics in mental disorders, World Psychiatry 14 (2) (2015) 116–118, https://doi.org/10.1002/wps.20203.

[7] J.J. Newson, T.C. Thiagarajan, EEG frequency bands in psychiatric disorders: a review of resting state studies, Front. Hum. Neurosci. 12 (2019) 521, https://doi.org/10.3389/fnhum.2018.00521.

[8] V. Knott, C. Mahoney, S. Kennedy, K. Evans, EEG power, frequency, asymmetry and coherence in male depression, Psychiatry Res. 106 (2) (2001) 123–140, https://doi.org/10.1016/s0925-4927(00)00080-9.

[9] M. Bachmann, J. Lass, A. Suhhova, H. Hinrikus, Spectral asymmetry and Higuchi's fractal dimension measures of depression electroencephalogram, Comput. Math. Methods Med. (2013), https://doi.org/10.1155/2013/251638.

[10] A. Kaiser, M. Gnjezda, S. Knasmüller, W. Aichhorn, Electroencephalogram alpha asymmetry in patients with depressive disorders: current perspectives, Neuropsychiatr. Dis. Treat. 14 (2018) 1493–1504, https://doi.org/10.2147/NDT.S137776.

[11] C.S. Musaeus, K. Engedal, P. Høgh, V. Jelic, M. Mørup, M. Naik, A.-R. Oeksengaard, J. Snaedal, L.-O. Wahlund, G. Waldemar, B.B. Andersen, EEG theta power is an early marker of cognitive decline in dementia due to Alzheimer's disease, J. Alzheimers Dis. 64 (4) (2018) 1359–1371, https://doi.org/10.3233/JAD-180300.

[12] K. Natarajan, U.R. Acharya, F. Alias, T. Tiboleng, S.K. Puthusserypady, Nonlinear analysis of EEG signals at different mental states, Biomed. Eng. Online 3 (1) (2004), https://doi.org/10.1186/1475-925X-3-7.

[13] R. Thibodeau, R.S. Jorgensen, S. Kim, Depression, anxiety, and resting frontal EEG asymmetry: a meta-analytic review, J. Abnorm. Psychol. 115 (2006) 715–729, https://doi.org/10.1037/0021-843x.115.4.715.

[14] N. van der Vinne, M.A. Vollebregt, M.J. van Putten, M. Arns, Frontal alpha asymmetry as a diagnostic marker in depression: fact or fiction? A meta-analysis, Neuroimage Clin. 16 (2017) 79–87, https://doi.org/10.1016/j.nicl.2017.07.006.

[15] A. Wolff, S. de la Salle, S. Sorgini, E. Lynn, P. Blier, V. Knott, G. Northoff, Atypical temporal dynamics of resting state shapes stimulus-evoked activity in depression — an EEG study on rest–stimulus interaction, Front. Psych. 10 (2019) 719, https://doi.org/10.3389/fpsyt.2019.00719.

[16] A.A. Fingelkurts, A.A. Fingelkurts, H. Rytsälä, K. Suominen, E. Isometsä, S. Kähkönen, Impaired functional connectivity at EEG alpha and theta frequency bands in major depression, Hum. Brain Mapp. 28 (3) (2007) 247–261, https://doi.org/10.1002/hbm.20275.

[17] S.A. Irimiciuc, A. Zala, D.-G. Dimitriu, L.M. Himiniuc, M. Agop, B.F. Toma, L. G. Gavril, D. Vasincu, L. Eva, Novel approach for EEG signal analysis in a multifractal paradigm of motions. Epileptic and eclamptic seizures as scale transitions, Symmetry 13 (6) (2021) 1024, https://doi.org/10.3390/sym13061024.

[18] T.Q. Khoa, V.Q. Ha, V.V. Toi, Higuchi fractal properties of onset epilepsy electroencephalogram, Comput. Math. Methods Med. (2012) 461–462, https://doi.org/10.1155/2012/461426.

[19] M. Koukkou, D. Lehmann, J. Wackermann, I. Dvorak, B. Henggeler, Dimensional complexity of EEG brain mechanisms in untreated schizophrenia, Biol. Psychiatry 33 (6) (1993) 397–407, https://doi.org/10.1016/0006-3223(93)90167-C.

[20] D. Abásolo, R. Hornero, J. Escudero, P. Espino, A study on the possible usefulness of detrended fluctuation analysis of the electroencephalogram background activity in Alzheimer's disease, I.E.E.E. Trans. Biomed. Eng. 55 (9) (2008) 2171–2179, https://doi.org/10.1109/TBME.2008.923145.

[21] T. Kawe, S. Shadli, N. McNaughton, Higuchi's fractal dimension, but not frontal or posterior alpha asymmetry, predicts PID-5 anxiousness more than depressivity, Sci. Rep. 9 (1) (2019), https://doi.org/10.1038/s41598-019-56229-w.

[22] W. Mumtaz, A.S. Malik, S.S. Ali, M.A. Yasin, H. Amin, Detrended fluctuation analysis for major depressive disorder, *Annu Int Conf IEEE Eng Med Biol Soc (EMBC)*, (2015) 4162-4165, https://doi.org/10.1109/EMBC.2015.7319311.

[23] B. Hosseinifard, M.H. Moradi, R. Rostami, Classifying depression patients and normal subjects using machine learning techniques and nonlinear features from EEG signal, Comput. Methods Programs Biomed. 109 (2013) 339–345, https://doi.org/10.1016/j.cmpb.2012.

[24] M. Ahmadlou, H. Adeli, A. Adeli, Fractality analysis of frontal brain in major depressive disorder, Int. J. Psychophysiol. 85 (2012) 206–211, https://doi.org/10.1016/j.ijpsycho.2012.05.001.

[25] J.S. Lee, B.H. Yang, J.H. Lee, J.H. Choi, I.G. Choi, S.B. Kim, Detrended fluctuation analysis of resting EEG in depressed outpatients and healthy controls, Clin. Neurophysiol. 118 (11) (2007) 2489–2496, https://doi.org/10.1016/j.clinph.2007.08.001.

[26] M. Čukić, M. Stokić, S. Simić, D. Pokrajac, D, The successful discrimination of depression from EEG could be attributed to proper feature extraction and not to a particular classification method, Cognitive Neurodynamics 14 (2020) 443–455, https://doi.org/10.1007/s11571-020-09581-x.

[27] S.A. Akar, S. Kara, S. Agambayev, V. Bilgiç, Nonlinear analysis of EEG in major depression with fractal dimensions, *Annu Int Conf IEEE Eng Med Biol Soc*, (EMBC) (2015), https://doi.org/10.1109/EMBC.2015.7320104.

[28] S. Kesić, S.Z. Spasić, Application of Higuchi's fractal dimension from basic to clinical neurophysiology: A review, Comput. Methods Programs Biomed. 133 (2016) 55–70, https://doi.org/10.1016/j.cmpb.2016.05.014.

[29] C.-C.-M. Yeh, Y. Zhu, L. Ulanova, N. Begum, Y. Ding, A. Dau, D.F. Silva, A. Mueen, E. Keogh, Matrix Profile I: all pairs similarity joins for time series: a unifying view that includes motifs, in: Discords and Shapelets, *IEEE 16th International Conference on Data Mining (ICDM)*, 2016, https://doi.org/10.1109/ICDM.2016.0179.

[30] M. Govindarajan, R.M. Chandrasekaran, Evaluation of k-Nearest Neighbor classifier performance for direct marketing, Expert Syst. Appl. 37 (1) (2010) 253–258, https://doi.org/10.1016/j.eswa.2009.04.055.

[31] V. Bijalwan, P. Kumari, J.P. Espada, V.B. Semwal, V. Kumar, Machine learning approach for text and document mining, Int. J. Database Theory Appl. 7 (1) (2014) 61–70, https://doi.org/10.14257/ijdta.2014.7.1.06.

[32] T. Seidl, Nearest neighbor search on multimedia indexing structures, *in Proc. First International Workshop on Computer Vision meets Databases (CVDB)*, (2004), https://doi.org/10.1145/1039470.1039474.

[33] M. Sovierzoski, F. Argoud, F. Azevedo, Identifying eye blinks in EEG signal analysis, *in Proc*, in: International Conference on Information Technology and Applications in Biomedicine (ITAB), 2008, https://doi.org/10.1109/ITAB.2008.4570605.

[34] C. Stam, B. Van Dijk, Synchronization likelihood: an unbiased measure of generalized synchronization in multivariate data sets, Physica D 163 (2002) 236–251, https://doi.org/10.1016/S0167-2789(01)00386-4.

[35] L. Päeske, M. Bachmann, T. Põld, S.P. de Oliveira, J. Lass, J. Raik, H. Hinrikus, Surrogate data method requires end-matched segmentation of electroencephalographic signals to estimate non-linearity, Front. Physiol. 9 (2018) 1350, https://doi.org/10.3389/fphys.2018.01350.

[36] M. Sharma, J. Tiwari, U. Acharya, Automatic sleep-stage scoring in healthy and sleep disorder patients using optimal wavelet filter bank technique with EEG

signals, Int. J. Environ. Res. Public Health 18 (6) (2021), https://doi.org/10.3390/ijerph18063087.
[37] R. Wankhedkar, S. Jain, Motif discovery and anomaly detection in an ECG using matrix profile, in: C.R. Panigrahi, B. Pati, P. Mohapatra, R. Buyya, K.C. Li (Eds.), Progress in Advanced Computing and Intelligent Engineering. Advances in Intelligent Systems and Computing, vol 1198, Springer, Singapore, 2009, https://doi.org/10.1007/978-981-15-6584-7_9.
[38] A. Mueen, Y. Zhu, M. Yeh, K. Kamgar, K. Viswanathan, C.K. Gupta, E. Keogh, The fastest similarity search algorithm for time series subsequences under Euclidean distance, Available: http://www.cs.unm.edu/~mueen/FastestSimilaritySearch.html. Last accessed 27 (2022) 02.
[39] A. Mueen, Y. Zhu, M. Yeh, K. Kamgar, K. Viswanathan, C.K. Gupta, E. Keogh, Algorithm for MASS_V2 (Version 2). Available: https://www.cs.unm.edu/~mueen/MASS_V2.m. Last accessed 27.02.2022.
[40] A. Aluoja, J. Shlik, V. Vasar, K. Luuk, M. Leinsalu, Development and psychometric properties of the Emotional State Questionnaire, a self-report questionnaire for depression and anxiety, Nord. J. Psychiatry 53 (6) (1999) 443–449, https://doi.org/10.1080/080394899427692.
[41] D. Yao, A method to standardize a reference of scalp EEG recordings to a point at infinity, Physiol. Meas. 22 (4) (2001) 693–711, https://doi.org/10.1088/0967-3334/22/4/305.
[42] Y. Qin, P. Xu, D. Yao, D, A comparative study of different references for EEG default mode network: the use of the infinity reference, Clin. Neurophysiol. 121 (12) (2010) 1981–1991, https://doi.org/10.1016/j.clinph.2010.03.056.
[43] Q. Liu, J. Balsters, M. Baechinger, O. van der Groen, N. Wenderoth, D. Mantini, Estimating a neutral reference for electroencephalographic recordings: the importance of using a high-density montage and a realistic head model, J. Neural Eng. 12 (5) (2015), https://doi.org/10.1088/1741-2560/12/5/056012.
[44] T. Higuchi, Approach to an irregular time series on the basis of the fractal theory, Phys. D: Nonlinear Phenom. 31 (2) (1988) 277–283, https://doi.org/10.1016/0167-2789(88)90081-4.
[45] F. Zappasodi, F. Tecchio, L. Marzetti, V. Pizzella, V. Di Lazzaro, G. Assenza, Longitudinal quantitative electroencephalographic study in mono-hemispheric stroke patients, Neural Regen. Res. 14 (7) (2019) 1237–1246, https://doi.org/10.4103/1673-5374.251331.
[46] M. Bachmann, L. Päeske, K. Kalev, K. Aarma, A. Lehtmets, P. Ööpik, J. Lass, H. Hinrikus, Methods for classifying depression in single channel EEG using linear and nonlinear signal analysis, Comput. Methods Programs Biomed. 155 (2018) 11–17, https://doi.org/10.1016/j.cmpb.2017.11.023.
[47] M. He, F. Liu, A. Nummenmaa, M. Hämäläinen, B.C. Dickerson, P.L. Purdon, Age-related EEG power reductions cannot be explained by changes of the conductivity distribution in the head due to brain atrophy, Front. Aging Neurosci., 13 (2021), https://doi.org/ 10.3389/fnagi.2021.632310.
[48] J. Langrova, J. Kremláček, M. Kuba, Z. Kubova, J. Szanyi, Gender impact on electrophysiological activity of the brain, Physiol. Res. 61 (2012) 119–127, https://doi.org/10.33549/physiolres.932421.
[49] R. Esteller, G. Vachtsevanos, J. Echauz, B. Litt, A comparison of waveform fractal dimension algorithms, IEEE Trans. Circ. Syst. I. Fundam. Theory Appl. 48 (2) (2001) 177–183, https://doi.org/10.1109/81.9048821.

Appendix 3 – Publication III

Publication III

Uudeberg, T., Päeske, L., Hinrikus, H., Lass, J., Põld, T., & Bachmann, M. (2025). Individual stability of single-channel EEG measures over one year in healthy adults. Scientific Reports, 15, 28426. https://doi.org/10.1038/s41598-025-13614-y

scientific reports

Check for updates

OPEN

Individual stability of single-channel EEG measures over one year in healthy adults

Tuuli Uudeberg[1]✉, Laura Päeske[1], Hiie Hinrikus[1], Jaanus Lass[1], Toomas Põld[1,2] & Maie Bachmann[1]

The clinical applicability of electroencephalography (EEG) relies on the reliability and temporal stability of its measures. While the reliability of linear EEG measures is well established, the long-term stability of both linear and nonlinear measures at the individual level, as well as interindividual variability, remains underexplored. This study evaluated the one-year stability of EEG absolute band powers (theta, alpha, beta, and gamma) and nonlinear measures (Higuchi's fractal dimension, Lempel–Ziv complexity, detrended fluctuation analysis, and in-phase Matrix Profile) across 12 monthly EEG recordings in nine healthy males aged 26–49. Intraclass correlation coefficients (ICCs) indicated excellent reliability across all measures, although beta power showed slightly reduced ICCs in temporal regions and gamma power demonstrated lower reliability in peripheral sites. At the individual level, nonlinear measures showed greater temporal stability than EEG band powers. Although a few individuals, particularly in band power measures, exhibited annual fluctuations comparable to or exceeding interindividual variability, most participants demonstrated consistent EEG profiles over time. These findings support the use of nonlinear EEG measures in longitudinal research and indicate their potential for developing personalized EEG-based neural biomarkers. They also highlight the importance of estimating expected individual variability when designing individualized monitoring approaches, as high reliability at the group level does not preclude substantial within-subject variability in some cases.

Mental health disorders affect nearly one billion individuals worldwide, with anxiety and unipolar depression being among the most prevalent conditions, impacting approximately 580 million people[1]. Mental health conditions constitute a leading cause of disability, and the COVID-19 pandemic further exacerbated their global burden, leading to a 25% increase in anxiety and depression cases due to social isolation, financial distress, and health-related concerns[1]. Despite their prevalence, mental disorders remain significantly undertreated, with 75% of individuals in low- and middle-income countries receiving no treatment due to resource limitations, stigma, and systemic barriers[1,2]. Furthermore, the diagnosis and treatment of mental health disorders remain largely subjective, relying on clinical interviews and self-report questionnaires. These methods introduce variability due to the respondents' willingness and ability to comprehend and answer questions, clinicians' expertise, and sociocultural factors, resulting in frequent misdiagnosis and inadequate treatment access[2].

Changes in mental health are reflected in alterations in brain activity. Electroencephalography (EEG) is an effective complementary method to traditional clinical assessments for evaluating mental health, offering an objective and cost-effective tool for capturing electrical activity generated by cortical neurons near the scalp. EEG provides quantifiable measures that can aid in early diagnosis, track disease progression, and evaluate treatment efficacy[3]. EEG's affordability, high temporal resolution, and non-invasive nature make it a valuable tool for investigating brain dynamics in both clinical and healthy populations. Over the decades, EEG has been widely utilized, leading to the development and adoption of various methods to compute different EEG measures for studying cognitive functions and neurological disorders[4–12].

EEG linear and nonlinear measures

Traditional EEG analysis relies on spectral band power measures, which provide essential insights into brain dynamics by quantifying neural oscillations across different frequency bands. EEG frequency bands are linked to distinct cognitive and physiological processes, with delta (0.5–4 Hz) associated with deep sleep, theta (4–8 Hz)

[1]Biosignal Processing Laboratory, Department of Health Technologies, School of Information Technologies, Tallinn University of Technology, Ehitajate tee 5, 19086 Tallinn, Estonia. [2]Meliva AS, Rävala pst 5, 10143 Tallinn, Estonia. ✉email: tuuli.uudeberg@taltech.ee

with memory and drowsiness, alpha (8–13 Hz) with relaxation and attentional control, beta (13–30 Hz) with active thinking and motor planning, and gamma (>30 Hz) with higher-order cognitive functions such as perception and consciousness[3]. While band power and other linear measures have been extensively studied, they do not fully account for the dynamic and complex nature of neural activity[3]. As the brain operates as a nonlinear system, nonlinear EEG measures have been developed or adapted from other domains to capture its self-organizing dynamics better. These methods provide additional information to linear measures by quantifying irregularity, complexity, and long-range temporal dependencies in neural signals. Probably the most used complexity measures are fractal dimensions. Higuchi's fractal dimension (HFD) estimates the self-similarity of EEG signals, reflecting neural complexity, and has been applied to many different areas of neurological and mental health research[6,8,12–16]. Detrended fluctuation analysis (DFA) measures long-range temporal correlations (LRTC)[17,18] and has also been successfully applied in EEG studies[4,7,10] as well as Lempel–Ziv complexity (LZC) that measures the number of new patterns in a time series[19,20]. A more recent method, the in-phase Matrix Profile (pMP), has been introduced to identify repeating patterns in EEG signals[12]. The in-phase Matrix Profile adapts the fast Matrix Profile similarity-search algorithm[21] to EEG by comparing fixed-length, phase-aligned subsegments by calculating Euclidean distances, yielding a parameter-free index of segment-to-segment self-similarity in the time domain. Its first EEG application outperformed HFD in distinguishing patients with major depressive disorder from healthy controls, underscoring the method's diagnostic potential[12]. Bachmann et al.[8] demonstrated that combining linear and nonlinear EEG measures improves classification accuracy when distinguishing depressed individuals from healthy controls, reinforcing the potential utility of these measures in clinical applications. Although some nonlinear EEG methods have been used for decades, their potential still remains underexplored compared to traditional spectral approaches. Given that nonlinear methods align more closely with the brain's intrinsic dynamics, richer information about neural function and dysfunction is expected.

For the present single-channel resting-state design, we restricted the nonlinear feature set to four time-domain measures (HFD, DFA, LZC, and pMP) because together they span scale-free complexity, long-range temporal correlations, algorithmic irregularity, and segment-to-segment in-phase self-similarity while requiring little or no parameter tuning. Entropy-based alternatives (e.g., sample or permutation entropy) were not included, as their reliability depends strongly on embedding and tolerance parameters and on longer stationary epochs, which can hamper longitudinal comparability[22–24].

Reliability of EEG measures

For EEG measures to be effectively utilized in clinical and research applications, they must demonstrate high reliability and temporal stability. Establishing temporal stability in EEG measures is essential to distinguish genuine brain-state-related neural changes from intrinsic EEG variability. Stable EEG measures enhance the validity and interpretability of findings, thereby improving clinical decision-making and advancing scientific understanding of brain function and disorders.

The reliability of linear EEG measures, particularly power in standard frequency bands, has been well studied, with early studies confirming the reliability and stability of power across different frequency bands[25–27]. More recent investigations have expanded on these findings by examining the reliability of additional linear measures[28–31]. However, considerably less research has focused on the reliability and stability of nonlinear EEG measures. Only a few studies have included them in their analyses[15,16,32,33]. The available evidence suggests that nonlinear measures exhibit either lower reliability than traditional EEG band power measures[32,33] or a level of reliability comparable to linear measures[15], indicating that these measures may capture aspects of EEG dynamics not reflected in the power of traditional frequency bands.

Gudmundsson et al.[33] investigated the stability of quantitative EEG measures in 15 healthy elderly individuals over two months (19 EEG recordings per participant). Their findings indicated that band power measures demonstrated the highest reliability, with mean ICCs of 0.77 for absolute power and 0.80 for relative power across eight channels and all frequency bands. Complexity-based measures such as LZC exhibited lower reliability (ICC = 0.70), while coherence measures were the least stable, with their reliability strongly dependent on channel location.

Põld et al.[15] conducted a three-year test–retest study on 17 healthy participants, reporting that relative power measures exhibited reliability comparable to nonlinear measures such as HFD and DFA. The highest reliability was observed for relative alpha power (mean ICC = 0.87 across 18 channels). Although ICCs for EEG frequency bands and nonlinear measures were comparable, the nonlinear measures demonstrated greater temporal stability at the group level, as reflected by smaller relative differences between the two recordings. Lord & Allen[16] studied 306 subjects, including controls and individuals with a history or current episode of depression, and found high internal consistency for HFD and sample entropy within single sessions, as well as high reliability across multiple days (ICCs for HFD ranging between 0.64 and 0.86 across different channels in eight recording sessions conducted over four days within two weeks).

Despite these contributions, existing studies provide limited understanding of EEG temporal stability at the individual level. Many studies employ test–retest designs with only a few EEG recordings per participant[15,26–28,30–32], while others cover short observation periods of up to two months[16,33]. While these studies offer valuable insights into EEG stability, they do not consider the characteristics of individual participants.

Person-specific EEG patterns

Numerous studies have successfully distinguished between a control group and a group with mental disorders using both linear and nonlinear EEG measures[8–12]. However, although these group-level results are promising, a measure that separates diagnostic groups may still reveal little about within-person EEG variability and thus may not capture clinically meaningful deviations in an individual over time.

Brain activity patterns are expected to exhibit strong individual specificity[34], and EEG signals have been suggested to function as a unique neural fingerprint[35,36]. However, for EEG measures to be effective in detecting neural changes within individuals, it is essential first to establish their normal variability in a healthy state, as this variability is expected to differ from individual to individual. Without a clear understanding of this baseline variability, it remains difficult to determine whether a new measurement reflects normal fluctuations or a deviation indicative of altered brain function. Detecting such deviations assumes that EEG measures remain relatively stable within an individual under normal conditions. At the same time, excessive fluctuations may either lead to misinterpreting normal variability as pathological or cause true pathological changes to go unnoticed, thereby undermining the applicability of an EEG measure.

Although interest in individualized EEG analysis is increasing, longitudinal studies examining EEG stability at the individual level over extended periods remain limited. Previously, we conducted a single-participant case study evaluating EEG-based individual measures over 15 sessions spanning 14 months[37]. While this study provided valuable insights into the long-term stability of linear and nonlinear measures, inter-individual differences cannot be assessed based on a single subject. More extensive studies are needed to establish individual variability in the healthy state by determining the extent to which EEG measures remain stable within individuals over months or years.

The lack of longitudinal research at the individual level is a significant barrier to the clinical application of EEG. While EEG measures may exhibit high test–retest reliability and temporal stability, their long-term stability at the individual level remains largely unexamined. A dependable clinical measure should achieve an optimal balance between long-term stability, ensuring consistency across repeated measurements under similar conditions, and sensitivity to meaningful physiological changes over time. Understanding these dynamics of EEG variability is critical for both clinical and research applications, ensuring that EEG-based measures are applicable, interpretable, and reliable for individual-level diagnostics and monitoring.

Study objectives

The aim of this study is to examine the temporal stability of single-channel EEG measures at the individual level over one year, based on repeated monthly recordings. While previous research has primarily addressed short-term test–retest reliability or group-level comparisons, this study focuses on individual consistency and variation over time in healthy adults. We assess both linear EEG measures (absolute power in theta, alpha, beta, and gamma frequency bands) and nonlinear measures (HFD, LZC, DFA, and pMP), evaluating their person-specific variability. Based on this framework, we formulate two hypotheses: (1) Although EEG measures differ between individuals, they remain temporally stable within the same person over one year. (2) Nonlinear EEG measures exhibit greater temporal stability at the individual level compared to absolute band powers.

By characterizing stable, person-specific EEG patterns and describing the typical range of variation observed for each individual, this study aims to support the development of individualized EEG biomarkers and contribute to future personalized monitoring approaches in mental health research.

Methods

Subjects

Nine healthy male subjects participated in the study. We restricted the sample to males to avoid menstrual-cycle–related variability, as resting-state neural oscillations have been shown to fluctuate across cycle phases in EEG[38] and magnetoencephalography[39]. At the time of the first recording, participants had a mean age of 37.2 ± 8.1 years, with an age range of 26 to 49 years. All participants self-reported as right-handed, nonsmokers, and free of any history of concussions involving loss of consciousness, narcotic or psychotropic substance use, alcohol abuse, or mental or psychiatric disorders.

To ensure consistency, participants were instructed to maintain their usual daily routines and refrain from consuming alcohol or caffeinated beverages for 24 h before each recording. The study was conducted following the Declaration of Helsinki and received formal approval from the Tallinn Medical Research Ethics Committee and the Estonian Institute for Health Development's Human Research Ethics Committee. All participants signed written informed consent before the study.

Collection of EEG data

For each participant, EEG recordings were scheduled every four weeks (with flexibility for five to six weeks in exceptional cases, such as illness or travel), resulting in a total of 12 recordings over the course of one year. Recordings were conducted on a consistent day of the week and at the same time of day, ensuring homogeneity. To minimize dietary influences on EEG activity, all recordings took place in the morning, with participants instructed to abstain from eating or drinking (except water) beforehand[40].

EEG data were collected using the Neuroscan Synamps2 acquisition system and a 32-channel (30 EEG + 2 EOG) Quick-Cap (Compumedics, NC, USA). Electrodes were positioned according to the extended international 10/20 system, with linked mastoids as reference. The placement of the 30 EEG electrodes is shown in Fig. 1.

During recordings, participants were lying in a relaxed supine position in a dimly lit laboratory room. EEG was recorded for 10 min with eyes closed and 5 min with eyes open across 30 EEG channels. Electrode impedance was maintained below 10 kΩ. EEG data were recorded at a sampling rate of 1 kHz, within a frequency range of 0.3–200 Hz.

EEG data preprocessing

All calculations were performed using MATLAB software (The MathWorks, Inc.). Initially, the eyes-closed EEG recordings were divided into 20.48-second segments, and segments with apparent artifacts were identified through visual inspection. Next, the full eyes closed EEG data were re-referenced using the Reference Electrode

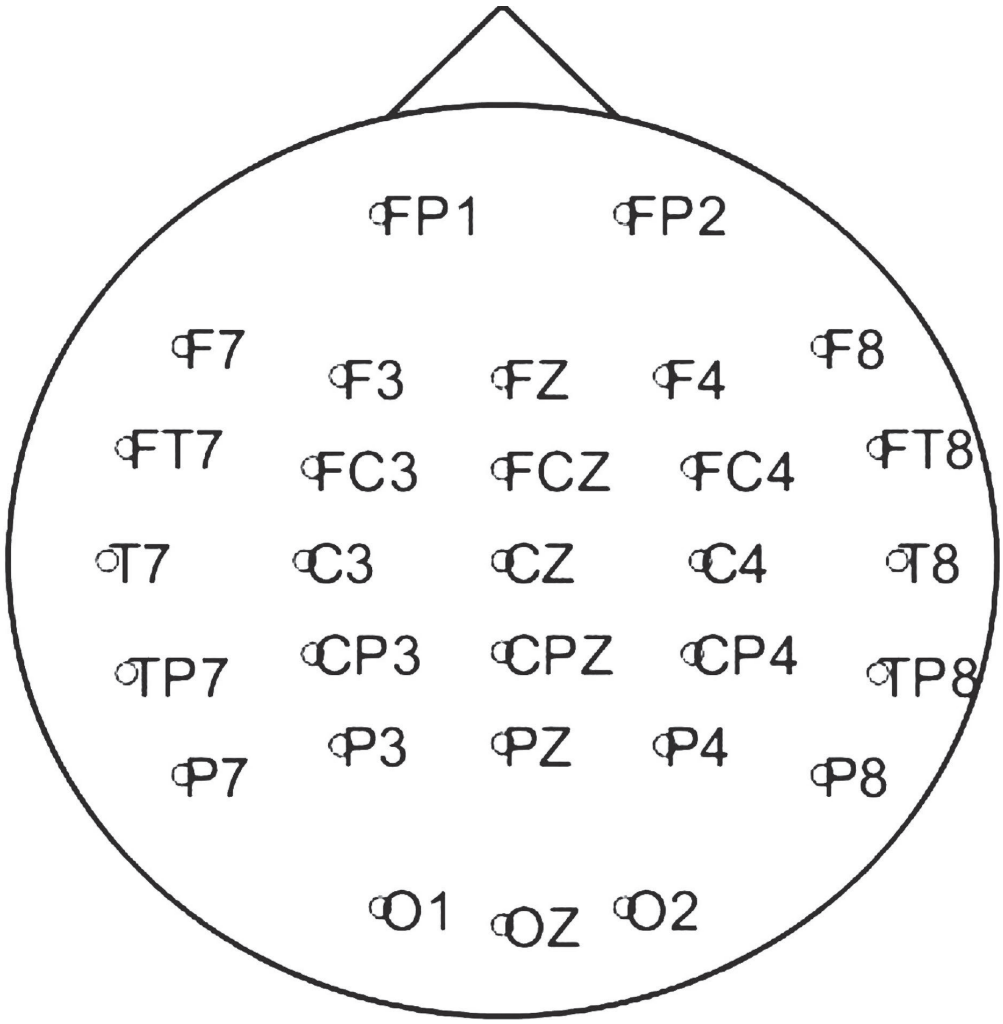

Fig. 1. Locations of the 30 EEG electrodes corresponding to the channels used in this study, positioned according to the extended international 10/20 system.

Standardization Technique (REST), which is a reliable method for low-density EEG montages and facilitates comparability across laboratories[41–43]. To remove baseline fluctuations and high-frequency noise, Parks–McClellan forward-backward filters were applied, yielding a frequency bandwidth of 2–47 Hz for further analysis. Absolute power in each frequency band was computed using the original sampling rate of 1 kHz, while EEG data were downsampled to 200 Hz for nonlinear measure calculations. After filtering (and downsampling), the EEG signals were divided into 20.48-second non-overlapping segments again, with segment lengths defined as 20,480 samples (for absolute power calculations) and 4096 samples (for nonlinear measures). The first 12 clean segments were selected for the computation of the following EEG measures, resulting in 12 values for each measure per subject and per recording session.

Calculation of EEG measures

Absolute power of EEG frequency bands

The absolute power P for each frequency band was calculated directly from a filtered EEG signal using a time-domain approach. Each frequency band was first extracted using a Parks–McClellan forward-backward bandpass filter. In this study, the absolute powers of the traditional theta (4–8 Hz), alpha (8–13 Hz), beta (13–30 Hz), and gamma (30–47 Hz) frequency bands were calculated for each subject according to

$$P = \frac{1}{n}\sum {}^{n}_{i=1}x^{2}(i), \tag{1}$$

where *x(i)* was the filtered EEG signal segment with the length *n* (20,480 samples) at sample *i*.

Higuchi's fractal dimension

HFD is used to quantify the complexity of EEG signals, providing a measure of scale invariance or self-similarity across multiple temporal scales. The method, originally proposed by Higuchi[14], estimates the fractal dimension within the interval [1,2] of a time series by analyzing its length at different scales. A higher HFD value indicates greater signal complexity, while a lower value reflects more regular and predictable neural activity. The HFD was calculated with the parameter k_{max} = 8 according to the algorithm presented in[14]. For the calculation of HFD for an EEG signal segment with the length *n* (4096 samples), a time series X_k^m is formed for each scale factor *k* as in

$$X_k^m = \{x(m),\ x(m+k),\ x(m+2k),\ \ldots\}, \quad m = 1,\ 2,\ \ldots,\ k, \tag{2}$$

where *k* represents the step size and *m* is the starting index of each subseries. The length of each subseries $L_k(m)$ is calculated as in

$$L_k(m) = \frac{1}{k}\sum {}^{\lfloor\frac{n-m}{k}\rfloor}_{i=1} |x(m+ik) - x(m+(i-1)k)| \cdot \frac{n-1}{k\lfloor\frac{n-m}{k}\rfloor}, \tag{3}$$

The $\lfloor\frac{n-m}{k}\rfloor$ term $\frac{n-1}{k\lfloor\frac{n-m}{k}\rfloor}$ normalizes the subseries length and ensures that the length $L_k(m)$ is expressed by the average number of points in the subseries and therefore comparable across all scale factors *k* (see[44] for a step-by-step illustration). $L_k(m)$ The mean length for each *k* is obtained by averaging across all subseries as in

$$L(k) = \frac{1}{k}\sum {}^{k}_{m=1}L_k(m). \tag{4}$$

The fractal dimension is estimated by fitting a linear regression line to the logarithmic plot of $L(k)$ versus 1/*k*, where the slope of this resulting log–log line corresponds to Higuchi's fractal dimension.

Lempel–Ziv complexity

LZC is a measure of sequence complexity, quantifying the rate at which new patterns emerge as a sequence progresses[19]. It is used to assess signal randomness and complexity, with higher LZC values indicating more irregular and complex signals, while lower values suggest more repetitive or structured patterns. To calculate LZC, first, EEG signal segment *x(i)* of length 4096 samples is binarized into B_i using threshold *T*, which in this study was the median of the EEG signal segment to minimize the impact of outliers. Samples below the median get a new value of zero, others one as in

$$B_i = \begin{cases} 1, & if\ S_i \geq T \\ 0, & if\ S_i < T \end{cases}. \tag{5}$$

Second, the binary sequence is scanned from left to right to find new patterns. A new pattern is detected whenever a substring is encountered that has not appeared previously in the sequence during left-to-right parsing. The complexity counter $C(n)$ increases each time a new pattern is encountered. Finally, LZC is normalized to avoid variations due to segment length as in

$$LZC_{norm} = \frac{C(n)}{C_{max}(n)}, \tag{6}$$

where $C_{max}(n)$ is the theoretical maximum complexity for a completely random sequence of length *n*, approximated as $n/\log_2(n)$. This normalization ensures that LZC values range between 0 (completely regular signal) and 1 (maximally complex, random signal).

Detrended fluctuation analysis

DFA was calculated according to the method described by Peng et al.[17,18]. First, the cumulative sum of the mean-centered EEG signal segment *x(i)*, with the length of *N* (4096 samples) was calculated to generate an integrated time series as in

$$y(k) = \sum {}^{k}_{i=1}[x(i) - \bar{x}], \tag{7}$$

where *k* gets a value from 1 to *N* and $\bar{x}$ is the arithmetic mean of the signal segment *x(i)*. Second, the integrated signal *y(k)* is divided into *n* equal nonoverlapping windows of a length ranging from 4 to 200 samples. In each window *n*, the local trend is estimated using a least-squares linear fit $\widehat{y}_n(k)$, which fits the data *y(k)*, and the local trend is subtracted from the data. Average fluctuations are given by

$$F(n) = \sqrt{\frac{1}{K}\sum_{k=1}^{K}[y(k) - \widehat{y}_n(k)]^2}. \quad (8)$$

Here, K is the number of nonoverlapping windows of length n. These average fluctuations are calculated for all window lengths. A log-log plot of $F(n)$ versus n, reveals a linear scaling, characterized by the slope of the line, which represents the scaling exponent α. This exponent reflects the presence and strength of long-range temporal correlations in the signal: $\alpha = 0.5$ indicates white noise (no correlation), while $\alpha > 0.5$ suggests persistent correlations.

In-phase matrix profile

The pMP method captures the self-similarity of the EEG signal by considering only the in-phase subsegments, making it sensitive to the periodicity of alpha waves and other frequency fluctuations in the EEG signal. First, a one-second subsegment (200 samples) was extracted from a 4096-sample EEG segment, and its Euclidean distance to all other subsegments within the same segment was calculated, generating a distance profile (DP). This process was then repeated for the next subsegment, continuing in a sliding window manner until a DP was obtained for each subsegment.

From each DP, the smallest Euclidean distances corresponding to the most in-phase subsegments were extracted. In-phase subsegments are defined as those with minimal phase shift and the highest waveform similarity to the reference window, based on time-domain Euclidean distance. The median of these in-phase distance values was then calculated for each DP, forming a pMP vector (pMPvec). The median was used to ensure robustness against outliers in the signal.

Finally, the mean of the pMPvec is computed to obtain the overall pMP value for the EEG segment. This value reflects the degree of temporal regularity and self-similarity in the signal, where lower values indicate more consistent recurring patterns. The calculation process is explained in detail in[12].

Statistical analysis

Since we calculated 12 values for each measure for every EEG channel in each recording of each participant, we subsequently used the median of these 12 values.

With 12 monthly recordings for nine subjects, we utilized the intraclass correlation coefficient (ICC)[45,46] to assess the reliability of repeated EEG measurements. ICC quantifies the proportion of total variance attributable to differences between subjects, providing a measure of the stability and consistency of EEG measures over time. When applied to datasets with multiple measurements per subject, ICC evaluates the degree of agreement among repeated observations within individuals relative to overall variability. A high ICC indicates that an EEG measure is relatively consistent within individuals across repeated sessions and shows greater variability between individuals than within individuals. We employed a two-way mixed-effects model (average measures, absolute agreement)[45,47] for all 30 channels, ensuring that both systematic subject differences and measurement error were accounted for in assessing temporal stability.

ICC was calculated as in

$$ICC = \frac{MS_R - MS_E}{MS_R + \frac{MS_C - MS_E}{n}}, \quad (9)$$

where MS_R is the mean square for subjects (i.e., between-subject variance), MS_C is the mean square for repeated measurements (i.e., between-measurement variance), MS_E is the mean square error, and n is the number of subjects.

We employed the Kruskal–Wallis test (α = 0.05) for data analysis[48]. The Kruskal–Wallis test is a nonparametric alternative to ANOVA to determine whether there are significant differences between three or more groups (in this case, subjects). Unlike ANOVA, the Kruskal–Wallis test does not assume a normal distribution of the data and is not sensitive to unequal variances. If a significant difference is detected between any of the subjects, a post-hoc test can be conducted to determine which subjects are different from each other. In this study, we employed the Dunn test (α = 0.05) to determine how many subject pairs were statistically different from each other[49]. As with 9 subjects, we had 9(9 – 1)/2 = 36 unique pairwise comparisons, we used the Šidák correction[50] of the probability (p) values as in

$$p^* = 1 - (1 - p)^m, \quad (10)$$

where m is the number of comparisons and p^* is the corrected p-value.

For each participant, we calculated the annual mean and standard deviation for each measure, as well as the maximum relative difference ($rDif$), which indicates the largest deviation from the annual mean as in

$$rDif = \left|\frac{v_{max} - \bar{v}}{\bar{v}}\right| * 100, \quad (11)$$

where v_{max} is the most extreme monthly measurement across the year for a given subject, and $\bar{v}$ is that subject's annual average.

Results

Intraclass correlation coefficients for EEG measures

Figure 2 presents the intraclass correlation coefficients (ICCs) for EEG band powers and nonlinear measures, while detailed ICCs for all EEG measures across all 30 channels are provided in Supplementary Table S1. Based on the classification proposed by Koo and Li[47], we considered ICCs to indicate excellent reliability when the lower bound (LB) of the 95% confidence interval (CI) exceeded 0.9.

Band power measures

The data in Fig. 2 demonstrate that lower-frequency EEG bands, theta and alpha, exhibited reliability classified as excellent over one year across all 30 EEG channels. The lowest ICCs were 0.979, 95% CI [0.952, 0.994] in P4 for theta power and 0.964, 95% CI [0.917, 0.990] in O2 for alpha power, indicating high reliability over time. Beta power demonstrated excellent ICCs across 27 channels, with slightly lower values in three temporal channels (TP7, T8, TP8). The lowest ICC was observed at TP8 (0.908, 95% CI [0.786, 0.975]), still indicative of good reliability. For gamma power, ICCs were excellent in 17 channels in the center of the head but lower in 13 peripheral channels, including the prefrontal area, with the lowest ICC at FT8 (0.756, 95% CI [0.424, 0.935]).

A slight reduction in ICCs observed in a few temporal channels in the beta band, and more notably lower ICCs across several peripheral channels in the gamma band, may be influenced by the presence of electromyographic (EMG) activity. EMG signals, resulting from muscle contractions, are commonly associated with movements such as swallowing, chewing, or speaking, but can also be present at a low level during resting state without overt motion[51]. Although relaxation can help minimize such activity, the spectral overlap between EMG and the beta and gamma frequency bands complicates the effective removal of these artifacts. EMG activity typically spans the 15–300 Hz range, with most power concentrated at the lower end[52,53].

In this study, muscle artifacts related to conscious movement were excluded from the EEG recordings. However, some low-level muscle tension, which is difficult to detect through visual inspection, may have remained in channels positioned over the temporalis and frontalis muscles. Tonic muscle activity, referring to the continuous low-level contraction of muscles even in a relaxed state, can contribute to subtle EEG interference. Unlike phasic muscle activity, which is associated with voluntary movements, tonic muscle activity persists at a baseline level and can be influenced by factors such as posture, alertness, and individual muscle tone[51]. In EEG recordings, this may appear as low-amplitude, high-frequency activity, particularly in frontal and temporal regions where muscles like the frontalis and temporalis are located.

Nonlinear measures

All nonlinear EEG measures (HFD, LZC, DFA, and pMP) exhibited excellent reliability (ICC 95% CI LB > 0.9) across all EEG channels (Fig. 2). The lowest ICC among these measures was observed for pMP, with a value of 0.960, 95% CI [0.908, 0.989] in the occipital channel Oz. LZC demonstrated a slightly higher ICC of 0.967, 95% CI [0.922, 0.991] in T7, while DFA and HFD showed the highest reliability with the lowest ICC of 0.986, 95% CI [0.967, 0.996] in O2 and 0.978, 95% CI [0.949, 0.994] in T7, respectively. Although pMP had slightly lower ICCs in the occipital region, they remained within the excellent reliability range. Given that pMP is influenced by alpha oscillations[12] and alpha power is strongest in occipital areas, variability in alpha activity may have contributed to this observation.

While beta power showed slightly reduced ICCs in only a few temporal channels, gamma power exhibited more widespread reductions (ICC 95% CI LBs ≤ 0.9 in 13 channels), particularly in peripheral temporal, frontotemporal, and prefrontal areas. These reductions may, at least in part, reflect the potential influence of residual EMG activity. Nevertheless, given the overall excellent reliability across measures, any channel may be used for further analysis, while it may be advisable to avoid regions that are more prone to muscle-related influences.

Individual variability of EEG measures

To investigate person-specific EEG dynamics over time, we examined the individual temporal variability of EEG measures across one year, as presented in Fig. 3; Tables 1 and 2. The figure displays the EEG measure values recorded throughout the year, along with the annual mean and standard deviation for the parietal channel P3. This channel was selected as an example due to its consistent reliability in resting-state EEG, low susceptibility to muscle artifacts, and its well-established role in reflecting stable, individual differences in neural activity, particularly within parietal regions involved in cognitive processing[54,55].

As illustrated in Fig. 3, EEG measure values for each subject fluctuate around a distinct annual mean, with variability ranges that are specific to the individual. These subject-specific patterns give rise to clearly separable clusters in the data, with the extent of variability differing across individuals. A Kruskal–Wallis test confirmed that at least one of the clusters was statistically different from the others for each measure ($p \leq 1.1 \times 10^{-15}$).

Statistically significant differences were observed between 14 and 16 subject pairs out of 36 pairwise comparisons, depending on the measure, using Dunn's test with Šidák p-value correction. There was no considerable difference in statistical significance between EEG band power and nonlinear measures. Specifically, theta power differed significantly in 15 pairs, alpha power in 16 pairs, and beta and gamma power in 14 pairs. Among nonlinear measures, significant differences were observed in 14 pairs for HFD and LZC, and in 15 pairs for DFA and pMP, out of 36 comparisons. These results indicate that, regardless of the type of measure, individual EEG profiles are characterized by distinct annual means and specific fluctuation ranges, supporting the idea of temporally stable neural individuality.

Compared to EEG frequency band powers, nonlinear EEG measures show relatively higher temporal stability on the individual scale (Tables 1 and 2). Among the band power measures, theta power shows the greatest individual fluctuation, with a single recording maximally differing from the annual mean by an average across

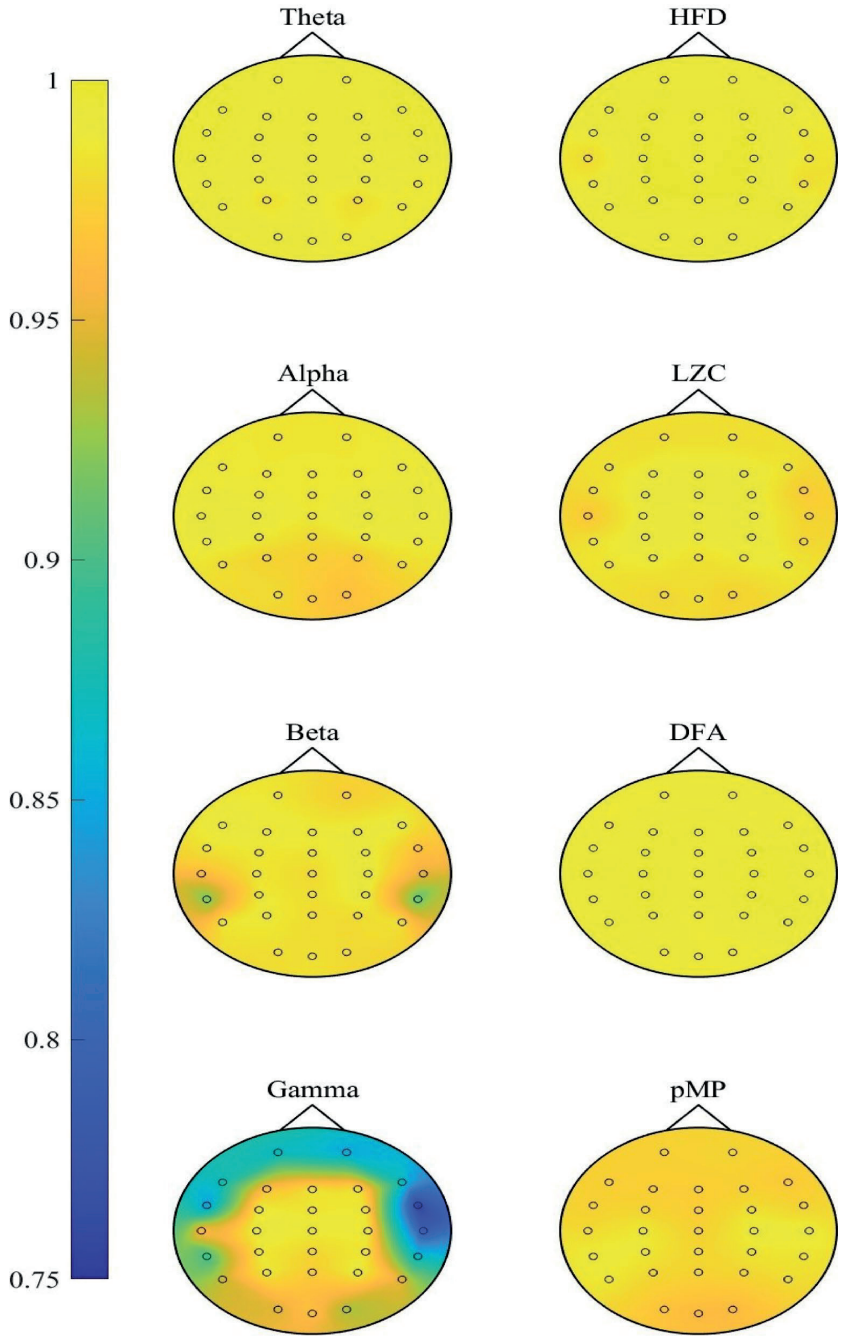

Fig. 2. Intraclass correlation coefficients for EEG measures across all 30 EEG channels ($n = 9$), including theta, alpha, beta, and gamma absolute powers, as well as nonlinear measures: Higuchi's fractal dimension (HFD), Lempel–Ziv complexity (LZC), detrended fluctuation analysis (DFA), and in-phase Matrix Profile (pMP).

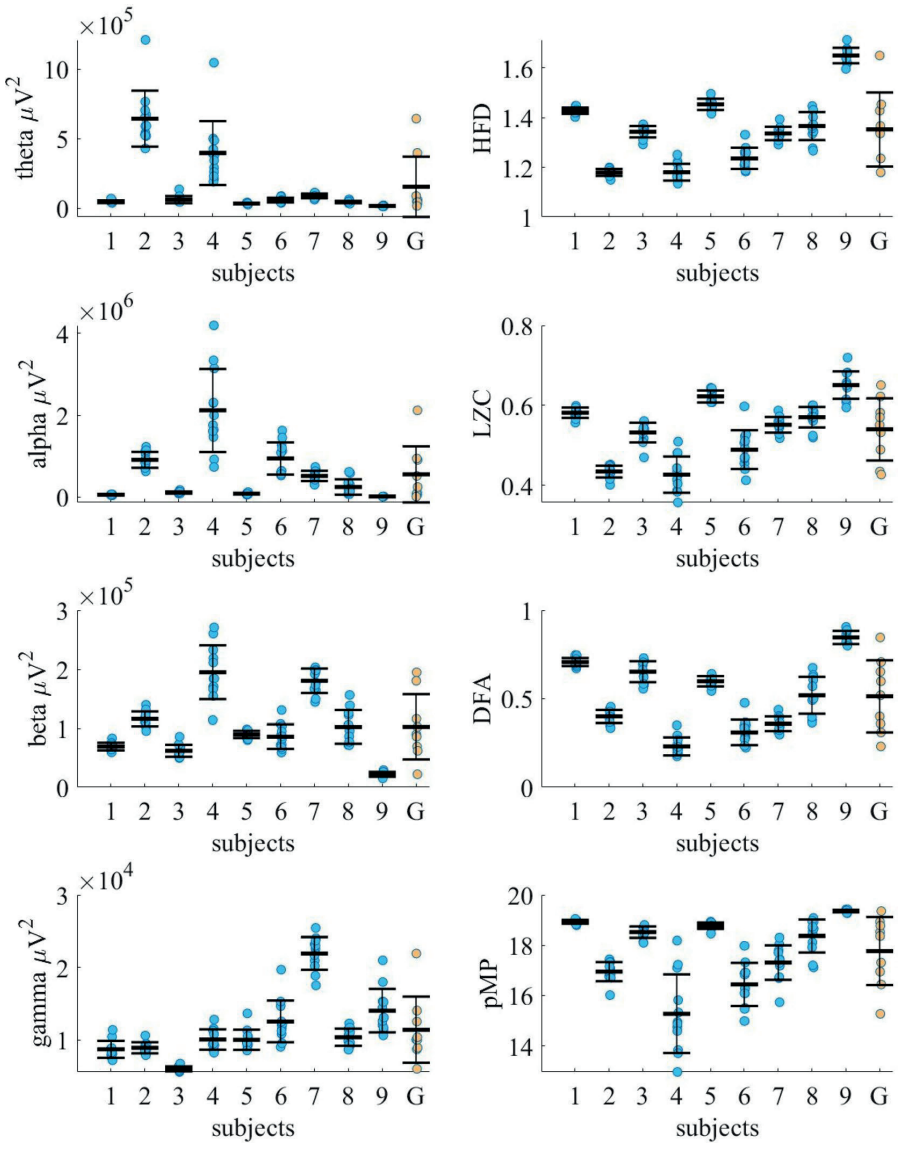

Fig. 3. Interindividual and intraindividual variability in EEG measures across one year for each subject 1–9 and the group G ($n = 9$). Blue dots represent 12 individual monthly values; black dashes show subject-specific annual means. Error bars for subjects 1–9 represent within-subject standard deviations. For group G, yellow dots represent the annual mean of each subject, the black dash shows the group-level mean, and error bars indicate the standard deviation.

all subjects of 66% (ranging from 24 to 163%, depending on the subject). This is followed by alpha power, which maximally fluctuates by an average of 64%, with individual variation ranging from 27 to 152%. Beta and gamma power exhibit lower variability, with average maximal deviations of 32% and 30%, respectively. Individual maximal fluctuations range from 11 to 53% for beta power and 12–57% for gamma power.

Among nonlinear measures, DFA and LZC show the largest individual fluctuations, with average maximal deviations of 23% and 10%, respectively (ranging from 5 to 54% for DFA and 4–22% for LZC, depending on the subject). HFD and pMP exhibit the lowest variability, with average maximal deviations of 4% and 6%, respectively. Individual maximal variation ranges from 2 to 8% for HFD and 0–19% for pMP.

	Theta			Alpha			Beta			Gamma		
	Mean[a]	SD[a]	rDif	Mean[a]	SD[a]	rDif	Mean[a]	SD[a]	rDif	Mean[a]	SD[a]	rDif
Subject 1	46.93	9.48	48	55.73	9.19	27	68.97	6.48	20	8.69	1.18	31
Subject 2	643.66	201.24	88	912.09	196.03	35	115.89	12.61	21	8.91	0.76	19
Subject 3	62.10	25.90	120	110.14	26.05	58	61.86	10.15	39	5.98	0.35	12
Subject 4	396.86	228.87	163	2119.96	1015.02	98	194.81	45.43	42	10.05	1.41	27
Subject 5	34.29	4.90	24	80.81	18.97	50	89.63	6.07	11	10.00	1.39	37
Subject 6	58.90	16.73	50	945.82	395.22	72	85.79	20.80	52	12.54	2.87	57
Subject 7	88.54	16.45	30	517.02	124.77	43	180.43	20.73	20	21.92	2.26	20
Subject 8	44.60	8.49	43	245.04	189.06	152	102.30	28.56	53	10.36	1.19	18
Subject 9	16.96	2.94	27	11.26	2.41	43	21.92	4.16	32	14.03	2.99	49
Group	154.76	217.10	316	555.32	688.71	282	102.40	55.33	90	11.39	4.56	92

Table 1. Annual mean values, standard deviations, and relative maximal differences from the annual mean (rDif, %) of theta, alpha, beta, and gamma absolute power calculated for nine subjects in channel P3 and for the group ($n = 9$). [a] Values must be multiplied by 10^3 to obtain the correct magnitude in μV^2.

	HFD			LZC			DFA			pMP		
	Mean	SD	rDif	Mean	SD	rDif	Mean	SD	rDif	Mean	SD	rDif
Subject 1	1.43	0.01	2	0.58	0.01	4	0.71	0.02	5	18.93	0.08	1
Subject 2	1.18	0.01	3	0.43	0.01	8	0.40	0.04	16	16.95	0.38	6
Subject 3	1.34	0.02	4	0.53	0.02	12	0.65	0.06	15	18.52	0.22	2
Subject 4	1.18	0.03	6	0.43	0.05	19	0.23	0.05	52	15.28	1.56	19
Subject 5	1.45	0.02	3	0.62	0.02	4	0.60	0.03	9	18.77	0.13	2
Subject 6	1.24	0.04	8	0.49	0.05	22	0.31	0.07	54	16.44	0.86	9
Subject 7	1.34	0.03	4	0.55	0.02	7	0.36	0.04	22	17.31	0.69	9
Subject 8	1.37	0.06	7	0.57	0.03	9	0.52	0.10	30	18.37	0.65	7
Subject 9	1.65	0.03	4	0.65	0.03	11	0.85	0.04	7	19.36	0.05	0
Group	1.35	0.15	22	0.54	0.08	21	0.51	0.20	65	17.77	1.35	14

Table 2. Annual mean values, standard deviations, and relative maximal differences from the annual mean (rDif, %) of Higuchi's fractal dimension (HFD), Lempel–Ziv complexity (LZC), detrended fluctuation analysis (DFA), and in-phase matrix profile (pMP) calculated for nine subjects in channel P3 and for the group ($n = 9$).

When examining individual subjects separately, it is evident that subject S4 shows significantly greater variability, with an average maximal fluctuation of 53% across all measures. In contrast, subjects S1 and S5 exhibit considerably lower variability, with an average maximal fluctuation of 17%. This further emphasizes the strong individuality in EEG measures.

As shown in Fig. 3; Tables 1 and 2, intra-individual annual variation is generally smaller than inter-individual variation, apart from a few exceptions. Notably, in the theta frequency band, subjects S2 and S4 exhibit annual variability comparable in magnitude to that observed between individuals. In subject S4, the variability within the alpha band markedly exceeds inter-individual differences, while in the beta band, it is again of comparable magnitude. For most nonlinear measures (HFD, LZC, DFA), intra-individual variation remains lower than the variation across subjects, with no exceptions. However, in the case of pMP, subject S4 again exhibits greater variability than the group.

Discussion

In this study, we tested whether EEG measures, while differing between individuals, remain temporally stable within the same person across one year, and if nonlinear measures are temporally more stable at the individual level compared to absolute band powers. For this, we investigated the reliability and long-term temporal stability of EEG band powers and nonlinear EEG measures across 12 months in healthy individuals. Our findings largely support the hypothesis of individual temporal stability, though some nuances remain.

A key finding of this study is the strong individual specificity of EEG measures, with each subject's values remaining tightly grouped within their own subject-specific range. This largely supports the concept that EEG measures may serve as neural fingerprints — remaining principally stable within individuals while differing significantly between them[34–36] — although some individuals exhibited fluctuations that challenge the assumption of consistent intra-individual stability.

Regarding the reliability of EEG measures, our findings align with previous research[15,33], showing that lower-frequency bands (theta and alpha) are the most reliable across sessions. Beta power shows only slightly reduced ICCs in a few temporal channels. Gamma power, in turn, shows a more pronounced decrease in reliability in

several channels. Nevertheless, reliability remained high overall, with our lowest observed mean ICC being 0.935 (in the gamma band), which is substantially higher than the ICC of 0.77 for absolute power reported by Gudmundsson et al.[33]. Põld et al.[15] similarly reported ICCs of 0.80 for gamma and 0.87 for alpha relative power, which is consistent with our results. The reduced reliability in the peripheral channels in gamma and beta bands may be explained by low-level tonic EMG activity that spectrally overlaps with these frequency ranges and is not fully removed by standard preprocessing[51–53]. Although we aimed to obtain EEG recordings free of visible artefacts, the potential influence of subtle tonic EMG activity, particularly in high-frequency bands, was not directly investigated in this study. Nevertheless, it should be kept in mind when interpreting gamma and beta activity in longitudinal analyses, especially in muscle-prone regions.

For nonlinear measures, our results also indicate higher reliability than previously reported. Gudmundsson et al.[33] found an ICC of 0.70 for LZC, and Põld et al.[15] reported ICCs of 0.81 for HFD and 0.84 for DFA. In contrast, we observed consistently excellent ICCs above 0.96 (95% CI LBs ≥ 0.908) across all EEG channels for all nonlinear measures. Notably, these measures showed minimal differences between channels, suggesting reduced sensitivity to possible slight EMG input and highlighting their robustness across the spatial domain. Although the study by Põld et al.[15] assessed long-term stability over three years, the use of only two recordings per subject may have contributed to slightly lower ICCs. Gudmundsson et al.[33] included 19 recordings over two months, but the older age of participants could have increased intra-individual variability. Our study, using monthly recordings over one year in a younger cohort, showed that nonlinear measures remained highly reliable across all sessions, reinforcing their potential for individualized longitudinal monitoring.

While all EEG measures demonstrated excellent test–retest reliability in all or most channels, high reliability does not necessarily equate to high temporal stability. Therefore, we separately quantified intra-individual variation by calculating the maximum relative differences from each subject's mean across 12 monthly recordings. This allowed us to directly assess how much a person's EEG measure fluctuated over time, regardless of between-subject differences. These analyses revealed that although many participants demonstrated stable EEG patterns, a few (most notably participant S4) exhibited fluctuations over time that were comparable to or greater than the variability observed between individuals. Thus, EEG measures cannot universally be assumed to be temporally stable at the individual level, even if group-level reliability appears excellent.

While methodological aspects, such as recording conditions and electrode placement, were carefully controlled, intrinsic physiological factors still contribute to variability. Individual differences in hormonal levels, neuroanatomy, and overall brain physiology may result in varying degrees of natural fluctuation in EEG measures. Additionally, lifestyle factors such as sleep patterns, diet, and physical activity can subtly modulate EEG signals, affecting their stability over time[40].

Although subject S4 was considered healthy by self-report at the time of the study, such variability may still reflect transient changes in mental state or the early signs of psychological shifts that were not yet subjectively perceived. Psychological states and mental health conditions are known to affect EEG patterns, as shown in previous group studies[4–13]. High levels of stress, anxiety, depression, and other mental states or psychiatric disorders are known to alter brain activity patterns, potentially leading to deviations from typical EEG signatures. Identifying the sources of EEG variability — whether due to intrinsic traits, temporary states, or early pathological changes — will be critical for tailoring analysis strategies.

Equally important is the ability to estimate, in advance, the expected range of normal variability for a given individual. Achieving this requires identifying the key individual factors that contribute to greater variability in EEG measures in the healthy state. Such person-specific variability profiles could help distinguish between brain disorder-related fluctuations and those indicative of normal neuropsychological changes. In future applications, developing heuristics to detect high-variability profiles without the need for long-term tracking will enhance efficiency and individualization. In high variability cases, alternative EEG measures or a combination of measures for individualized baseline approaches may be required.

The second hypothesis proposed that nonlinear EEG measures would exhibit better intra-individual temporal stability than traditional band power measures. Our results strongly support this hypothesis.

While all EEG measures demonstrated excellent test–retest reliability in channel P3, intra-individual temporal stability in the same channel, assessed as maximum relative difference from the individual's mean, was substantially smaller for nonlinear measures. For instance, mean deviations across subjects for theta and alpha power were 66% and 64%, respectively, compared to only 4% for HFD and 6% pMP.

These results are further supported by findings from Põld et al.[15], who observed very low relative changes in nonlinear measures at a group level in a test-retest study over three years: 0.18% for HFD and 0.49% for DFA. In comparison, their relative band power measures showed relative changes from 0.72% up to 2.28%. The fact that nonlinear measures in our study showed such small variability even across 12 sessions strengthens the conclusion that they are temporally more stable than traditional band power measures. Põld et al.[15] demonstrated that nonlinear measures are not only reliable but also temporally more stable at the group level. The present study confirms that these measures are likewise both reliable and highly temporally stable at the individual level. In contrast, band power measures appear more vulnerable to transient fluctuations and may not provide reliable baselines for individual monitoring.

Current findings highlight the importance of an individualized approach to EEG interpretation, moving beyond reliance on fixed population-level norms. Rather than comparing individuals to group averages, establishing person-specific baselines under stable conditions allows for more accurate identification of meaningful neural changes versus natural fluctuations[56]. Our results emphasize that such individualized baselining is essential for reliable longitudinal monitoring. Notably, nonlinear EEG measures provide a particularly strong foundation for this approach, as they exhibit greater resistance to temporal variability than traditional band power measures. This stability makes them promising candidates for biomarkers intended to track brain function over extended periods.

Despite the strong temporal stability observed, the small sample size (nine male participants) limits the generalizability of our findings. Future studies should validate these results in larger, more diverse populations and assess how EEG stability is affected by factors such as age, sex, and individual differences in cognitive functioning. Additionally, a clinically applicable EEG measure must balance long-term stability with sensitivity to dynamic physiological states. Future research should explore this balance to determine which EEG measures are most suitable for clinical applications. Since various biological and lifestyle-related factors can influence natural variability in EEG measures, it is essential to account for individual-specific differences, even in the absence of overt psychological stress or neurological conditions. Deviations from a healthy psychological state and overall mental well-being are precisely the types of changes that are intended to be detected through the establishment of a baseline for EEG variability. Even when working with self-reported healthy subjects, future protocols should include a clinician-led screening to confirm the absence of neurological or psychiatric conditions. Future work should also establish how segment length influences stability and sensitivity of single-channel EEG measures. Varying window sizes will clarify the minimum duration that still yields stable resting-state estimates, and whether longer windows narrow or widen the normative range. Finally, as all recordings were conducted in controlled laboratory conditions, it remains unclear how real-world factors (e.g., time of day, environmental stressors, or diet) influence EEG stability. Future studies should assess EEG reliability in naturalistic settings to improve its applicability for longitudinal monitoring.

Conclusion

This study confirmed that EEG band power measures are highly reliable over long-term recordings and that nonlinear measures demonstrate comparable levels of reliability. However, nonlinear measures showed greater temporal stability across sessions, making them potentially more suitable for assessing brain state over time, provided they also demonstrate sufficient sensitivity to meaningful neural changes. These findings support the use of nonlinear EEG measures in individualized, longitudinal monitoring frameworks. Furthermore, establishing personalized baselines, rather than relying on normative population averages, appears essential for accurate interpretation of EEG data. Given the overall high reliability across EEG channels, researchers have flexibility in channel selection, although peripheral channels may be best avoided to minimize the influence of artifacts.

Data availability

The raw EEG data generated and analyzed during the current study are not publicly available due to data protection and ethical restrictions. However, derived data supporting the findings of this study (including computed measures) are available from the corresponding author upon reasonable request.

Received: 16 May 2025; Accepted: 25 July 2025
Published online: 04 August 2025

References

1. World Health Organization (WHO). *World mental health report: Transforming mental health for all*. World Health Organization. (2022). https://iris.who.int/handle/10665/356115
2. Patel, V. et al. The lancet commission on global mental health and sustainable development. *Lancet* **392**, 1553–1598 (2018).
3. Buzsáki, G. *Rhythms of the Brain* (Oxford University Press, 2006).
4. Abásolo, D., Hornero, R., Escudero, J. & Espino, P. A study on the possible usefulness of detrended fluctuation analysis of the electroencephalogram background activity in alzheimer's disease. *IEEE Trans. Biomed. Eng.* **55**, 2171–2179 (2008).
5. Hinrikus, H. et al. Electroencephalographic spectral asymmetry index for detection of depression. *Med. Biol. Eng. Comput.* **47**, 1291–1299 (2009).
6. Ahmadlou, M., Adeli, H. & Adeli, A. Fractality analysis of frontal brain signals in major depressive disorder. *Int. J. Psychophysiol.* **85**, 206–211 (2012).
7. Mumtaz, W., Malik, A. S., Yasin, M. A. M. & Xia, L. Review on EEG and ERP predictive biomarkers for major depressive disorder. *Biomed. Signal. Process. Control.* **22**, 85–98 (2015).
8. Bachmann, M. et al. Methods for classifying depression in single-channel EEG using linear and nonlinear signal analysis. *Comput. Methods Progr. Biomed.* **155**, 11–17 (2018).
9. Musaeus, C. S. et al. EEG theta power is an early marker of cognitive decline in dementia due to alzheimer's disease. *J. Alzheimers Dis.* **64**, 1359–1371 (2018).
10. Thiery, T. et al. Long-range Temporal correlations in the brain distinguish conscious wakefulness from induced unconsciousness. *Neuroimage* **179**, 30–39 (2018).
11. Newson, J. J. & Thiagarajan, T. C. EEG frequency bands in psychiatric disorders: A review of resting state studies. *Front. Hum. Neurosci.* **12**, 521. https://doi.org/10.3389/fnhum.2018.00521 (2019).
12. Uudeberg, T. et al. In-phase matrix profile: A novel method for the detection of major depressive disorder. *Biomed. Signal. Process. Control.* **88**, 105378. https://doi.org/10.1016/j.bspc.2023.105378 (2024).
13. Accardo, A., Affinito, M., Carrozzi, M. & Bouquet, F. Use of the fractal dimension for the analysis of electroencephalographic time series. *Biol. Cybern.* **77**, 339–350 (1997).
14. Higuchi, T. Approach to an irregular time series on the basis of fractal theory. *Phys. D.* **31**, 277–283 (1988).
15. Põld, J., Päeske, L., Hinrikus, H., Lass, J. & Bachmann, M. Long-term stability of resting state EEG-based linear and nonlinear measures. *Int. J. Psychophysiol.* **159**, 83–87 (2021).
16. Lord, B. & Allen, J. J. B. Evaluating EEG complexity metrics as biomarkers for depression. *Psychophysiology* **60**, 14274. https://doi.org/10.1111/psyp.14274 (2023).
17. Peng, C. K. et al. Mosaic organization of DNA nucleotides. *Phys. Rev. E.* **49**, 1685–1689 (1994).
18. Peng, C. K., Havlin, S., Stanley, H. E. & Goldberger, A. L. Quantification of scaling exponents and crossover phenomena in nonstationary heartbeat time series. *Chaos* **5**, 82–87 (1995).
19. Lempel, A. & Ziv, J. On the complexity of finite sequences. *IEEE Trans. Inf. Theory.* **22**, 75–81 (1976).
20. Wolff, A. et al. Atypical Temporal dynamics of resting state shapes stimulus-evoked activity in depression—an EEG study on rest-stimulus interaction. *Front. Psychiatry.* **10**, 719. https://doi.org/10.3389/fpsyt.2019.00719 (2019).

21. Yeh, C. C. M. et al. Matrix Profile I: all-pairs similarity joins for time series: A unifying view that includes motifs, discords and shapelets. *Proc. IEEE Int. Conf. Data Mining (ICDM)* 1317–1322 (2016).
22. Richman, J. S. & Moorman, J. R. Physiological time-series analysis using approximate entropy and sample entropy. *Am. J. Physiol. Heart Circ. Physiol.* **278**, 2039–2049 (2000).
23. Bosl, W. J., Tager-Flusberg, H. & Nelson, C. A. EEG analytics for early detection of autism spectrum disorder: A data-driven approach. *Sci. Rep.* **8**, 6828. https://doi.org/10.1038/s41598-018-24318-x (2018).
24. Päeske, L., Uudeberg, T., Hinrikus, H., Lass, J. & Bachmann, M. Correlation between electroencephalographic markers in the healthy brain. *Sci. Rep.* **13**, 6307. https://doi.org/10.1038/s41598-023-33364-z (2023).
25. Gasser, T., Bächer, P. & Steinberg, H. Test–retest reliability of spectral parameters of the EEG. *Electroencephalogr. Clin. Neurophysiol.* **60**, 312–319 (1985).
26. Salinsky, M. C., Oken, B. S. & Morehead, L. Test–retest reliability in EEG frequency analysis. *Electroencephalogr. Clin. Neurophysiol.* **79**, 382–392 (1991).
27. Kondacs, A. & Szabó, M. Long-term intra-individual variability of the background EEG in normals. *Clin. Neurophysiol.* **110**, 1708–1716 (1999).
28. Cannon, R. L. et al. Reliability of quantitative EEG (qEEG) measures and LORETA current source density at 30 days. *Neurosci. Lett.* **14**, 27–31 (2012).
29. Gevins, A. et al. Long-term and within-day variability of working memory performance and EEG in individuals. *Clin. Neurophysiol.* **123**, 1291–1299 (2012).
30. Ip, C. T. et al. Pre-intervention test–retest reliability of EEG and ERP over four recording intervals. *Int. J. Psychophysiol.* **134**, 30–43 (2012).
31. Tenke, C. E. et al. Temporal stability of posterior EEG alpha over twelve years. *Clin. Neurophysiol.* **129**, 1410–1417 (2018).
32. Dünki, R. M., Schmid, G. B. & Stassen, H. H. Intraindividual specificity and stability of human EEG: Comparing a linear vs a nonlinear approach. *Methods Inf. Med.* **39**, 78–82 (2000).
33. Gudmundsson, S., Runarsson, T. P., Sigurdsson, S., Eiriksdottir, G. & Johnsen, K. Reliability of quantitative EEG markers. *Clin. Neurophysiol.* **118**, 2162–2171 (2007).
34. Lopez, K. L., Monachino, A. D., Vincent, K. M., Peck, F. C. & Gabard–Durnam, L. J. Stability, change, and reliable individual differences in electroencephalography measures: A lifespan perspective on progress and opportunities. *Neuroimage* **275**, 120116. https://doi.org/10.1016/j.neuroimage.2023.120116 (2023).
35. Zhang, S., Sun, L., Mao, X., Hu, C. & Liu, P. Review on EEG-based authentication technology. *Comput. Intell. Neurosci.* **2021** (5229576). https://doi.org/10.1155/2021/5229576 (2021).
36. Tatar, A. B. Biometric identification system using EEG signals. *Neural Comput. Appl.* **35**, 1009–1023 (2023).
37. Uudeberg, T., Päeske, L., Hinrikus, H., Lass, J. & Bachmann, M. Reliability of electroencephalogram-based individual markers—case study. *Proc. Annu. Int. Conf. IEEE Eng. Med. Biol. Soc.* **2020**, 276–279 (2020).
38. Brötzner, C. P., Klimesch, W., Doppelmayr, M., Zauner, A. & Kerschbaum, H. H. Resting state alpha frequency is associated with menstrual cycle phase, estradiol and use of oral contraceptives. *Brain Res.* **1577**, 36–44 (2014).
39. Haraguchi, R. et al. The menstrual cycle alters resting-state cortical activity: A magnetoencephalography study. *Front. Hum. Neurosci.* **15**, 652789. https://doi.org/10.3389/fnhum.2021.652789 (2021).
40. Hoffman, L. D. & Polich, J. E. E. G. ERPs and food consumption. *Biol. Psychol.* **48**, 139–151 (1998).
41. Yao, D. A method to standardize a reference of scalp EEG recordings to a point at infinity. *Physiol. Meas.* **22**, 693–711 (2001).
42. Yao, D. et al. Which reference should we use for EEG and ERP practice? *Brain Topogr.* **32**, 530–549 (2019).
43. Hu, S., Lai, Y., Valdés Sosa, P. A., Vega, B. & Yao, D. M. L. How do reference montage and electrodes setup affect the measured scalp EEG potentials? *J. Neural Eng.* **15**, (2018).
44. Moaveninejad, S., Cauzzo, S. & Porcaro, C. Fractal dimension and clinical neurophysiology fusion to gain a deeper brain signal understanding: A systematic review. *Inf. Fusion*. **118**, 102936. https://doi.org/10.1016/j.inffus.2025.102936 (2025).
45. McGraw, K. O. & Wong, S. P. Forming inferences about some intraclass correlation coefficients. *Psychol. Methods*. **1**, 30–46 (1996).
46. Shrout, P. E. & Fleiss, J. L. Intraclass correlations: Uses in assessing rater reliability. *Psychol. Bull.* **86**, 420–428 (1979).
47. Koo, T. K. & Li, M. Y. A guideline of selecting and reporting intraclass correlation coefficients for reliability research. *J. Chiropr. Med.* **15**, 155–163 (2016).
48. Kruskal, W. H. & Wallis, W. A. Use of ranks in one-criterion variance analysis. *J. Am. Stat. Assoc.* **47**, 583–621 (1952).
49. Dunn, O. J. Multiple comparisons using rank sums. *Technometrics* **6**, 241–252 (1964).
50. Šidák, Z. Rectangular confidence regions for the means of multivariate normal distributions. *J. Am. Stat. Assoc*. **62**, 626–633 (1967).
51. Whitham, E. M. et al. Scalp electrical recording during paralysis: Quantitative evidence that EEG frequencies above 20 hz are contaminated by EMG. *Clin. Neurophysiol.* **118**, 1877–1888 (2007).
52. Sörnmo, L. & Laguna, P. *Bioelectrical Signal Processing in Cardiac and Neurological Applications* (Academic, 2005).
53. Urigüen, J. A. García zapirain, B. EEG artifact removal—state-of-the-art and guidelines. *J. Neural Eng.* **12** https://doi.org/10.1088/1741-2560/12/3/031001 (2015).
54. Polich, J. Updating P300: An integrative theory of P3a and P3b. *Clin. Neurophysiol.* **118**, 2128–2148 (2007).
55. Jann, K., Kottlow, M., Dierks, T., Boesch, C. & Koenig, T. Topographic electrophysiological signatures of fMRI resting state networks. *PLoS ONE*. **5**, e12945. https://doi.org/10.1371/journal.pone.0012945 (2010).
56. Päeske, L., Hinrikus, H., Lass, J., Põld, T. & Bachmann, M. The impact of the natural level of blood biochemicals on electroencephalographic markers in healthy people. *Sensors* **24**, 7438. https://doi.org/10.3390/s24237438 (2024).

Acknowledgements

This research was supported by Estonian Center of Excellence for Well-Being Sciences (EstWell), funded by grant TK218 from the Estonian Ministry of Education and Research.

Author contributions

T.U. and M.B. conceptualized the study, designed the methodology, and conducted EEG data collection. T.U. performed data analysis, wrote custom analysis scripts, and prepared all visualizations and the initial manuscript. L.P. contributed to software development and methodological design. M.B. secured project funding and edited the manuscript. T.P. provided medical input by clarifying the clinical significance of EEG-related findings. H.H. and J.L. contributed to the manuscript revision and provided feedback. All authors reviewed and approved the final manuscript.

Declarations

Competing interests

The authors declare no competing interests.

Additional information

Supplementary Information The online version contains supplementary material available at https://doi.org/10.1038/s41598-025-13614-y.

Correspondence and requests for materials should be addressed to T.U.

Reprints and permissions information is available at www.nature.com/reprints.

Publisher's note Springer Nature remains neutral with regard to jurisdictional claims in published maps and institutional affiliations.

Appendix 4 – Publication IV

Publication IV

Uudeberg, T., Hinrikus, H., Päeske, L., Lass, J., & Bachmann, M. (2022). Changes in EEG measures of a recipient of the mRNA COVID-19 vaccine—A case study. In 2022 44th Annual International Conference of the IEEE Engineering in Medicine and Biology Society (EMBC), 3702–3705. IEEE. https://doi.org/10.1109/EMBC48229.2022.9871524

Changes in EEG Measures of a Recipient of the mRNA COVID-19 Vaccine – A Case Study *

Tuuli Uudeberg, *Student Member, IEEE*, Hiie Hinrikus, Laura Päeske, Jaanus Lass, and Maie Bachmann, *Member, IEEE*

***Abstract:*— The current study is aimed to evaluate the effect of COVID-19 vaccine on human EEG and the persistence of the effect. Within a one-year-long resting EEG study period, the healthy male subject was administered two Comirnaty doses three weeks apart to prevent COVID-19. Fourteen recordings were acquired from the subject in one year: twelve reference and two post-vaccination recordings after administrating the second dose of Comirnaty. The changes in absolute powers of EEG frequency bands, EEG spectral asymmetry index (SASI), and Higuchi's fractal dimension (HFD) were analyzed. The results indicated a statistically significant increase in absolute gamma power, SASI and HFD values on the fifth day after the vaccination, while the EEG had restored its normal character on the twelfth day after vaccination. These measures seem to have higher sensitivity for the detection of the effects of the vaccine**

***Clinical Relevance* – This is the first study evaluating COVID-19 vaccine effect on healthy human EEG. The study indicated that the vaccine disturbs EEG, but the impact is not long-lasting.**

I. Introduction

COVID-19, caused by a severe acute respiratory syndrome coronavirus 2 (SARS-CoV-2), has become a worldwide pandemic illness. In addition to respiratory system disorders, a significant part (36.4%) of COVID-19 patients had acute neurological expressions [1]. Acute neurological syndromes can be caused by a viral infection of the brain or by disease-related hypoxia and inflammation.

Today, the potential effects of COVID-19 on the central nervous system are put forward, but we do not have the information if and how COVID-19 vaccines affect the brain. Some studies have been conducted to analyze neurological complications by COVID-19 vaccines [2], [3]. However, the complications are rare and not always directly associated with vaccination. Still, to the best of our knowledge, the before-and-after study of the effects of COVID-19 vaccines on the healthy brain has not been performed.

Vaccines introduce antigens to our immune system, followed by our body's immune response that later helps to identify the pathogens when infected and counteract the invaders more effectively. COVID-19 vaccines have mild side effects similar to those seen with COVID-19, including neurological symptoms such as headaches and fatigue [1], [4], [5]. On the other hand, the brain can also be affected by stress caused by the vaccines' side effects. Stress can also affect the central nervous system and cause alterations in the brain's physiology.

Brain bioelectrical activity can be measured by electroencephalography (EEG) – a non-invasive and cost-effective method used to detect changes in brain function. Several EEG measures have shown changes during stressful situations. Studies using different tests of stress, theta and alpha band power indicated a decrease [6], [7], while in higher frequency rhythms, like beta and gamma, an increase was detected [7], [8]. The spectral asymmetry index (SASI), characterizing the balance between EEG higher and lower band powers, has been shown effective to detect the effect of different stressors: a physical stressor, microwave radiation [9], a chemical stressor, coffee intake [10], and occupational stress [8]. In addition, SASI distinguished between major depressive disorder and healthy groups [11], [12]. Still, not all information can be collected by linear methods; the nonlinear Higuchi's fractal dimension (HFD) describes the EEG signal's self-similarity and characterizes the signal's complexity. It has been shown that the complexity of the EEG signal raises in the case of depression and under stress conditions [8], [11].

Although the EEG measures can be considered as stable markers [13], [14], each EEG measure has a normal variability which is in turn individual [15] and usually unknown. We hypothesize that in the conditions of the impact by vaccine or increased stress due to the immunization, the EEG will be disturbed compared to the normal state. Thus, to evaluate the effects of a stressor, we need to know the subject's normal variability of the EEG measures of interest. The EEG and the sensitivity to vaccination are individual; therefore, a more detailed study on a single subject would provide clearer preliminary results on the effects of the vaccine.

The present study aims to investigate the effects of the COVID-19 vaccine on the central nervous system and the durability of the effect. For this purpose, the normal variability of the EEG measures, including spectral band power, SASI, and HFD, for a selected subject were evaluated over a year. The alterations in the measures after administration of Comirnaty (BioNTech Manufacturing GmbH) second dose were compared to the average levels of variability of the measures in normal conditions.

*This study was financially supported by the Estonian Centre of Excellence in IT (EXCITE) funded by the European Regional Development Fund.

T. Uudeberg is with the Department of Health Technologies, School of Information Technologies, Tallinn University of Technology, Ehitajate Road 5, Tallinn, 19086 Estonia (phone: +372-620-2207 e-mail: tuuli.uudeberg@taltech.ee).

H. Hinrikus, L. Päeske, J. Lass, and M. Bachmann are with the Department of Health Technologies, School of Information Technologies, Tallinn University of Technology, Tallinn, 19086 Estonia (e-mail: hiie.hinrikus@taltech.ee; laura.paeske@taltech.ee; jaanus.lass@taltech.ee; maie.bachmann@taltech.ee).

II. METHODS

A. Subject

The EEG data were repeatedly recorded from a healthy right-handed 49(50)-year-old male. The subject had no history of mental disorders or head traumas. He was a nonsmoker, did not consume narcotic or psychotropic substances. The study was conducted following the Declaration of Helsinki and was formally approved by the Research Ethics Committee of the National Institute for Health Development. Participation in the study was voluntary and the subject signed written informed consent.

B. Comirnaty Administration and Side Effects

During the one-year-long study period, the subject got two Comirnaty injections three weeks apart. Comirnaty contains a molecule called messenger RNA (mRNA) with instructions for producing a spike protein from SARS-CoV-2, the virus that causes COVID-19. After the first Comirnaty injection, the side effects were limited to pain at the injection site and left upper limb where the injection was administered and lasted for a few days. After the second injection, the side effects were pain in the left upper limb, headache, muscle aches, tiredness, fever, and fogginess. Fogginess lasted for about a week, with other side effects resolved by the fourth day after vaccination.

C. Collection of EEG Data

Fourteen recordings were acquired from the subject in one year: twelve reference (r1-r12) and two post-vaccination recordings after the second Comirnaty administration (p1, p2). The intervals between recordings were usually four weeks, except for post-vaccination recordings (5 and 12 days after vaccination), which were deliberately shorter. The interval between the first dose of vaccine and the subsequent EEG recording was 19 days. Due to the extensive time interval, we treated the corresponding recording (r7) as a reference recording.

To minimize the impact of the environment and the impact of the subject's activities on the EEG data, we used a routine where all recordings were acquired on the same day of the week and at the same time (Wednesday 7:30). The subject was instructed to abstain from alcohol and simulating drinks (coffee, tea, energy drinks, etc.) 24 hours before recording. The subject came to the recording without eating or drinking (excluding water) to avoid the effect of different breakfasts on the EEG. After arriving at the research laboratory, the subject completed the health data form and mental health questionnaires before each recording. The EEG data were recorded using Neuroscan Synamps2 acquisition system and a 32 channel Quick-Cap (Compumedics, NC, USA) with a sampling rate of 1000 Hz. EEG electrodes were positioned according to the extended international 10/20 system with linked mastoids as reference. The subject was lying in a relaxed supine position in a dimly lit laboratory room during the recording procedure. Ten minutes of eyes-closed and five minutes of eyes-open EEG data were acquired in 30 channels and vertical and horizontal electrooculograms to monitor eye movements in two channels. The impedance of EEG electrodes was kept below ten kΩ to achieve good conductivity between the skin and the electrode.

D. EEG Data Preprocessing

The data were processed using MATLAB software (The Mathworks, Inc.). EEG data were re-referenced using the reference electrode standardization technique (REST) [16]. Previous studies have shown that the REST reference is suitable for low-density EEG montage and is a good reference technique for comparing the results across laboratories [17], [18]. Parks-McClellan low and high-pass forward-backward filters were applied to the EEG signals to remove baseline fluctuations and high-frequency noise; frequency bandwidth of 2 to 47 Hz remained for further processing. The first 3 minutes from each recording were used for the following processing and were divided into nine nonoverlapping 20.48-second long segments. According to [19], stress affects the brain's (pre)frontal region the most; therefore, channel Fz was chosen for further processing and analysis. Next, theta, alpha, beta, gamma frequency band powers, SASI, and HFD values were calculated for all nine segments and a median value over those segments was found.

E. Frequency Band Power

We decomposed EEG data into classical frequency bands, such as theta (4-8 Hz), alpha (8-12 Hz), beta (12-30 Hz), and gamma (30-47 Hz) frequency bands. Each frequency band was first obtained using high and low pass Parks-McClellan forward-backward filter. The bandwidth power P for the filtered signal S with the length N was calculated as in

$$P = \sum_{i=1}^{N} S(i)^2. \quad (1)$$

F. Spectral Asymmetry Index

First, power spectrum density was estimated by means of Welch's averaged periodogram method (Hanning window with the length of 1024 samples, 50% overlap). Next, powers for predefined lower frequency band P_{low} (4 to 7 Hz) and higher P_{high} frequency band (14 to 38 Hz) were calculated as described in [11], [12] and SASI was calculated as in

$$SASI = \frac{P_{high} - P_{low}}{P_{high} + P_{low}}. \quad (2)$$

G. Higuchi's Fractal Dimension

Fractal dimension is a very sensitive nonlinear method for finding information about the physiological signal. Fractal dimension estimate HFD is a fast method calculated in the time domain, which does not need long signal segments. HFD is based on a measure of length *(k)* of the curve that represents the considered time series while using a segment of *k* samples as a unit if *L(k)* scales like $L(k) \sim k^{-FD}$. To calculate HFD, the EEG data were first downsampled to 200 Hz and the value of fractal dimension FD with a parameter k_{max}=8 was calculated according to the algorithm presented by Higuchi [20].

H. Statistics

We used two-sample t-test to control the hypothesis that EEG measures' values from post-vaccination recordings come from the same distribution as the reference recordings. The initial significance level was chosen $\alpha = 0.05$. As we had six different measures, we conducted statistical tests multiple times (6), therefore p-values were adjusted applying modified Bonferroni correction.

III. Results

The main results of this study are presented in Fig. 1 and Table I. Theta, alpha, beta, and gamma frequency band absolute powers, SASI, and HFD values for each recording in channel Fz are presented in Fig.1. The mean and standard deviation values over 12 reference recordings, i.e., regular variation, are presented in Table I and shown with straight and dashed lines, respectively, in Fig.1. There is more or less change in all frequency bands except beta in the first post-vaccine recording. The absolute power in the theta and alpha frequency band are somewhat lower after vaccination, being more noticeable in the alpha band. After vaccination, a statistically significant change can be seen in the gamma band power (Bonferroni corrected $p<0.0084$). SASI measure value also reveals a statistically significant change after vaccination being noticeably higher than in reference recordings (Bonferroni corrected $p<0.0125$). HFD also shows a statistically significant increase in complexity (Bonferroni corrected $p<0.01$). Five days after vaccination, there is a significant change in spectral power/ power asymmetry (gamma band, SASI) and in the signal complexity. However, it can be seen that a week later, on the twelfth day after vaccination, there is no longer any significant deviation in the bands' powers, asymmetry, or fractal dimension, and the values are again in the normal range.

IV. Discussion

Deviation of EEG measure values outside the usual range could characterize an effect of a prominent stressor. After the vaccination, the subject in this study experienced mild but still disturbing side effects from Comirnaty, such as fever, headache, and fogginess. Although fogginess had almost entirely resolved by day five, the changes in EEG measures were still strongly evident. Therefore, the alterations in EEG were related rather to the effect of vaccine than to the stress related to side effects.

TABLE I. Subject's Usual EEG Measure values and values after Administrating Comirnaty (BioNTech Manufacturing GmbH) vaccine in Channel Fz

Measure	*Mean*[a]	*SD*	*5 days post-vac.*	*12 days post-vac.*
Theta power[b] (10^5)	3.03	0,86	1.63	3.79
Alpha power (10^6)	1.00	0.20	0.47	1.14
Beta power (10^5)	1.38	0.15	1.32	1.29
Gamma power (10^3)	7.32	0.75	10.81*	6.27
SASI	0.034	0.055	0.214*	0.041
HFD	1.194	0.027	1.288*	1.170

a. Mean and standard deviation are calculated over 12 EEG reference recordings, excluding post-vaccination recordings.

b. Power values are presented in μV^2.

* Statistically significant difference after applying modified Bonferroni correction

The subject had somewhat decreased theta and alpha rhythm powers, which is consistent with the results of [6], [7], where responses to acute stress had a similar effect. However, the difference was not statistically significant after Bonferroni correction. There was no change from the usual absolute power deviation in the beta band. Still, it is possible that if lower and higher frequency beta bands had been used separately, a significant change would have been revealed. The relative power of the gamma band is often used to assess stress [8], an increase in the absolute gamma power is also evident in this study. SASI, combining besides beta and theta, also a

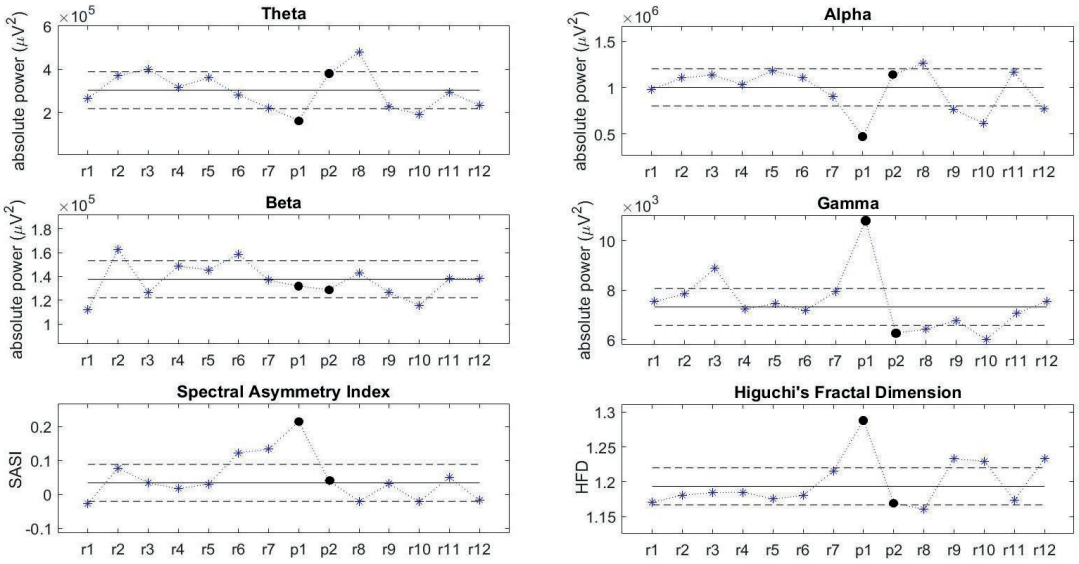

Figure 1. Results of the absolute powers of the EEG theta, alpha, beta, gamma frequency band, spectral asymmetry index, and Higuchi's fractal dimension during one year for one subject. Asterisks indicate reference recordings (r1-r12) that were acquired four weeks apart on regular basis. The dots (p1, p2) show the values on the fifth and twelfth days after vaccination with Comirnaty COVID-19 vaccine. Straight and dashed lines represent the mean and standard deviation values of the twelve reference recordings.

part of gamma band, noteworthy highlighted the increase in its value. In the previous studies, SASI has been shown to be able to highlight the effects of different stressors [8], [9], [10], [11], [12]. The current results are consistent with the results reported in the studies cited above. Therefore, vaccines might be considered a biological stressor to the central nervous system.

Twelve days after vaccination, all EEG measure values have returned to their normal range, indicating a temporary effect. Unfortunately, this study does not answer whether the impact on the EEG is directly due to the reaction caused by the vaccine or the discomfort caused by the symptoms.

The present study illustrates that EEG absolute gamma power, SASI, and HFD are the methods of sufficient sensitivity to detect the changes in brain physiology related to vaccination.

Although the study presents changes in only one person, those are consistent with the results of previous studies on stress and stressors. Thus, temporary abnormalities in EEG signals after vaccination may occur to a greater or lesser extent also in other persons.

V. Conclusion

The results of this preliminary study performed on a single subject indicated clearly that the COVID-19 vaccine caused a response in the brain detectable by the EEG measures. The statistically significant increases in the EEG absolute gamma power, spectral asymmetry index, and Higuchi's fractal dimension illustrated the high sensitivity of these measures to detect the effects caused by the vaccine. The impact of the vaccine was short-term; by the twelfth day after the vaccination, the brain had restored normal activity and the EEG measures were back to their normal levels. Further investigation on larger numbers of subjects is needed to support the conclusions.

References

[1] L. Mao, M. Wang, S. Chen, Q. He, J. Chang, C. Hong, Y. Zhou, D. Wang, Y. Li, H. Jin, and B. Hu, "Neurological Manifestations of Hospitalized Patients with COVID-19 in Wuhan, China: a retrospective case series study," *medRxiv,* 2020.

[2] M. Patone, L. Handunnetthi, D. Saatci, J. Pan, S. V. Katikireddi, S. Razvi, D. Hunt, X. W. Mei, S. Dixon, F. Zaccardi, K. Khunti, P. Watkinson, C. A. C. Coupland, J. Doidge, D. A. Harrison, R. Ravanan, A. Sheikh, C. Robertson, and J. Hippisley-Cox, "Neurological complications after first dose of COVID-19 vaccines and SARS-CoV-2 infection," *Nat. Med.,* vol. 27, p. 2144–2153, 2021.

[3] L. Lu, W. Xiong, J. Mu, Q. Zhang, H. Zhang, L. Zou, W. Li, L. He, J. Sander, and D. Zhou, "The potential neurological effect of the COVID-19 vaccines: A review," *Acta Neurol. Scand.,* vol. 144, no. 1, pp. 3-12, 2021.

[4] European Medicines Agency, "Product Information - Comirnaty," [Online]. Available: https://www.ema.europa.eu/en/documents/product-information/comirnaty-epar-product-information_en.pdf. [Accessed January 2022].

[5] European Medicines Agency, "Product Information - Spikevax," [Online]. Available: https://www.ema.europa.eu/en/documents/product-information/spikevax-previously-covid-19-vaccine-moderna-epar-product-information_en.pdf. [Accessed January 2022].

[6] B. R. Schlink, S. M. Peterson, W. D. Hairston, P. König, S. E. Kerick and, D. P. Ferris, "Independent component analysis and source localization on mobile EEG data can identify increased levels of acute stress," *Front. Hum. Neurosci.,* vol. 11, no. 310, 2017.

[7] F. Al-Shargie, M. Kiguchi, N. Badruddin, S. Dass, A. Hani, and T. Tang, "Mental stress assessment using simultaneous measurement of EEG and fNIRS," *Biomed. Opt. Express.,* vol. 7, p. 3882–3898, 2016.

[8] T. Põld, M. Bachman, L. Orgo, K. Kalev, J. Lass, and H. Hinrikus, "EEG Spectral Asymmetry Index Detects Differences Between Leaders and Non-leaders," in *IFMBE Proc.*, 2018.

[9] A. Suhhova, M. Bachmann, J. Lass, and H. Hinrikus, "EEG Spectral Asymmetry Index Reveals Effect of Microwave Radiation," in *IFMBE Proc.*, 2011.

[10] M. Saifudinova, M. Bachmann, J. Lass, and H. Hinrikus., "Effect of Coffee on EEG Spectral Asymmetry," in *IFMBE Proc.*, 2015.

[11] M. Bachmann, J. Lass, A. Suhhova and H. Hinrikus, "Spectral asymmetry and Higuchi's fractal dimension measures of depression electroencephalogram," *Comput Math Methods Med,* 2013.

[12] H. Hinrikus, A. Suhhova, M. Bachmann, K. Adamsoo, Ü. Võhma, J. Lass, and V. Tuulik, "Electroencephalographic spectral asymmetry index for detection of depression," *Med. Biol. Eng. Comp.,* vol. 47, no. 12, pp. 1291-1299, 2009.

[13] T. Põld, L. Päeske, H. Hinrikus, J. Lass, and M. Bachmann, "Long-term stability of resting state EEG-based linear and nonlinear measures," *Int J Psychophysiol,* vol. 159, pp. 83-87, 2021.

[14] M. DelPozo-Bano, C. Travieso, C. Weidemann, and J. Alonso, "EEG biometric identification: a thorough exploration of the time-frequency domain," *J. Neural Eng.,* vol. 12, no. 5, 2015.

[15] T. Uudeberg, L. Paeske, H. Hinrikus, J. Lass and M. Bachmann, "Reliability of Electroencephalogram-Based Individual Markers - Case Study.," in Proc. *42nd Annu. Int. Conf. IEEE EMBS*, Montreal, 2020.

[16] D. Yao, "A method to standardize a reference of scalp EEG recordings to a point at infinity," *Physiol Meas,* vol. 22, no. 4, pp. 693-711, 2001.

[17] Q. Liu, J. Balsters, M. Baechinger, O. van der Groen, N. Wenderoth, and D. Mantini, "Estimating a neutral reference for electroencephalographic recordings: the importance of using a high-density montage and a realistic head model," *J Neural Eng,* vol. 12, no. 5, 2015.

[18] Y. Qin, P. Xu and D. Yao, "A comparative study of different references for EEG default mode network: the use of the infinity reference," *Clin Neurophysiol,* vol. 121, no. 12, pp. 1981-1991, 2010.

[19] A. Arnsten, M. Raskind, F. Taylor and D. Daniel F. Connor, "The effects of stress exposure on prefrontal cortex: Translating basic research into successful treatments for post-traumatic stress disorder," *Neurobiology of Stress,* vol. 1, pp. 89-99, 2015.

[20] T. Higuchi, "Approach to an irregular time series on the basis of the fractal theory," *Phys. D: Nonlinear Phenom,* vol. 31, no. 2, pp. 277-283, June 1988.

Curriculum vitae

Personal data

Name:	Tuuli Uudeberg
Date of birth:	01.07.1986
Place of birth:	Estonia
Citizenship:	Estonian

Contact data

E-mail:	tuuliuudeberg@gmail.com

Education

2019–present	Tallinn University of Technology, PhD Programme in Physical Sciences, specialization in Biomedicine and Health Technologies
2016–2019	Tallinn University of Technology / University of Tartu, MSc in Engineering (Biomedical Engineering and Medical Physics)
2010–2012	Tallinn University, MA in Social Sciences (Government and Administration)
2005–2008	University of Tartu, BSc in Health Sciences (Physiotherapy)
2002–2005	Hugo Treffner Gymnasium (Hugo Treffneri Gümnaasium)

Language competence

Estonian	Native
English	Fluent
German	Basic
Spanish	Basic

Professional employment

2019–present	Tallinn University of Technology, Early Stage Researcher
2019–present	West Tallinn Central Hospital, Radiology Engineer
2012–2018	Porkuni School, Physical Therapist, Head of Rehabilitation Team
2008–2012	Rakvere Hospital, Physical Therapist

Elulookirjeldus

Isikuandmed

Nimi:	Tuuli Uudeberg
Sünniaeg:	01.07.1986
Sünnikoht:	Eesti
Kodakondsus:	Eesti

Kontaktandmed

E-post:	tuuliuudeberg@gmail.com

Hariduskäik

2019–…	Tallinna Tehnikaülikool, doktoriõpe spetsialiseerumisega biomeditsiinile ja tervisetehnoloogiatele
2016–2019	Tallinna Tehnikaülikool / Tartu Ülikool, tehnikateaduste magister (biomeditsiinitehnika ja meditsiinifüüsika)
2010–2012	Tallinna Ülikool, sotsiaalteaduste magister (riigiteadused)
2005–2008	Tartu Ülikool, terviseteaduste bakalaureusekraad (füsioteraapia)
2002–2005	Hugo Treffneri Gümnaasium

Keelteoskus

Eesti keel	emakeel
Inglise keel	kõrgtase
Saksa keel	algtase
Hispaania keel	algtase

Teenistuskäik

2019–…	Tallinna Tehnikaülikool, doktorant-nooremteadur
2019–…	AS Lääne-Tallinna Keskhaigla, radioloogiainsener
2012–2018	Porkuni Kool, füsioterapeut, rehabilitatsioonimeeskonna juht
2008–2012	Rakvere Haigla, füsioterapeut

ISSN 2585-6901 (PDF)
ISBN 978-9916-80-467-4 (PDF)